A MODIFIED HIGH PRESSURE APPROACH TO INVESTIGATE THE SEALING INTEGRITY OF LOST CIRCULATION MATERIALS IN COMBINATION WITH NANOPARTICLES

By

SETH MICHAEL JAMES LOGGINS

Bachelor of Science in Petroleum Engineering

New Mexico Institute of Mining and Technology

Socorro, New Mexico

2014

Submitted to the Faculty of the
Graduate College of the
Oklahoma State University
in partial fulfillment of
the requirements for
the Degree of
MASTER OF SCIENCE
December, 2017

A MODIFIED HIGH PRESSURE APPROACH TO INVESTIGATE THE SEALING INTEGRITY OF LOST CIRCULATION MATERIALS IN COMBINATION WITH NANOPARTICLES

Thesis Approved:

Thesis Adviser – Dr. Geir Hareland

Dr. Prem Bikkina

Dr. Runar Nygaard

ACKNOWLEDGEMENTS

With great appreciation I would like to thank my advisor, Dr. Geir Hareland, for allowing me to pursue an opportunity that will benefit me for years to come. It was his venture he took on with me that allowed me to continue my education in a field that I have a true passion for and deeply value. His free-reign leadership and supportive guidance, as well as the occasional putting lesson, has influenced me both academically and professionally.

I would like to recognize my committee members and professors for all the guidance and instruction throughout my time at Oklahoma State University. Being part of an up-and-coming graduate program and having the opportunity to study under such motivating leadership has truly clarified my future goals and aspirations. It is my hope that one day I can inspire others the way these mentors and professors have inspired me.

Above all I would like to express my deepest gratitude to my family and friends. Throughout the years they have endlessly driven me to pursue my goals in life. They have widened my perspective on what I thought was possible and have constantly encouraged me to reach for what I want to achieve. They have taught me, and often showed me, countless vital lessons proven to be invaluable to me in life. Without the support of my loved ones, I can humbly admit that my achievements in life would not be what they are today. Cheers!

Name: Seth Michael James Loggins

Date of Degree: DECEMBER, 2017

Title of Study: A MODIFIED HIGH PRESSURE APPROACH TO INVESTIGATE THE SEALING INTEGRITY OF LOST CIRCULATION MATERIALS IN COMBINATION WITH NANOPARTICLES

Major Field: Petroleum Engineering

Abstract:

This research investigates the sealing integrity of various lost circulation material (LCM) in conjunction with barite and silica fumed nanoparticles (NPs). Experimental testing in a water based mud (WBM) at different concentrations of LCM and NP's, as well as at various fracture disc sizes, enabled the analysis of sealing pressure and sealing integrity. This methodology was determined from previous literature results for LCM, as well as NP performance, in wellbore strengthening and reducing fluid loss.

A fabricated version of the "Modified Plugging Particle Apparatus" was used to conduct testing. The apparatus tested various LCM mixtures at both constant rate and constant pressure in order to determine a sealing pressure, as well as the integrity of the seal. The sealing pressure was determined by a calculated differential pressure to be seen while drilling ahead after experiencing a loss zone during drilling operations. On the other hand, the sealing integrity is how well this seal holds while drilling ahead which was analyzed through a transient pressure region after sealing was established. Three different LCM types, two concentrations and three disc sizes were used in the base test matrix. Following base case testing, NPs were used to study the effect of an increase in sealing integrity on the seal. The NPs were chosen based on low pressure fluid loss results that analyzed the effect that chemically and mechanically generated NPs had on reducing the fluid filtrate in a WBM. All experiments were conducted in a mass balance environment with consistent rheology and testing procedures.

Results showed that the apparatus can successfully analyze different LCM mixtures on a fundamental level without the influence of other effects. LCM mixtures have shown to produce higher sealing pressures in the current apparatus than what has been previously reported in the literature. Furthermore, the NPs have shown potential to strengthen the seal as the fracture realizes increasing pressure, depending on the LCM type and NP type. This research further investigates the sealing capabilities of various LCM in conjunction with NPs and introduces a new methodology of understanding the quality of these seals.

TABLE OF CONTENTS

Chapter Page

LIST OF TABLES

Table Page

LIST OF FIGURES

Figure Page

Figure Page

Figure Page

Figure Page

NOMENCLATURE

API	American Petroleum Institute
DLS	Dynamic light scattering
°F	Temperature in degrees Fahrenheit
G1	Graphite blend #1
HPHT	High-pressure High-temperature
in	Length in inches
k	Permeability (mD)
LCM	Lost circulation material
LPLT	Low-pressure Low-temperature
mL	Volume in milliliters
mm	Length in millimeters
nm	Length in nanometers
NP	Nanoparticle
NS1	Nutshell blend #1
OBM	Oil based mud
pH	Potential of hydrogen
PSD	Particle size distribution
ppb	Concentration in pound per barrel
ppg	Density in pound per gallon
psi	Pressure (lb/in^2)
PV	Plastic viscosity (cP)
(R)	Repeated test
rpm	Revolutions per minute (sec^{-1})
SCC3	Sized calcium carbonate blend #3
SG	Specific gravity
TD	Total depth (ft)
TMD	Total measured depth (ft)
TEM	Transmission Electron Microscopy
WBM	Water based mud
WBS	Wellbore Strengthening
YP	Yield point ($lb/100ft^2$)
ΔP	Differential pressure (psi)
µ	Length in micrometer
% wt.	Weight percent

CHAPTER I

INTRODUCTION

Lost circulation refers to the partial, or whole, losses of a drilling fluid system to the formation through a lithological, geo-mechanical or hydrodynamic manner. This operational hindrance has been occurring ever since the initial days of drilling and is becoming more costly as the oil and gas industry aims to drill deeper, more complex wells. As far back as the 1980's the industry has been working endlessly to solve the issue of lost circulation by developing a philosophy, or a set of guidelines, for certain treatment methods that address a particular lost circulation scenario (Canson 1985 & Vidick et al. 1988). Although numerous oil and gas operators have driven to tackle the problem of lost circulation, energy demand is increasing and technological advances steer the industry to deeper depths, inducing further concern for maintaining an adequate drilling fluid system. Whether dealing with conventional wells or modern horizontal extended reach wells, the drilling mud system must withstand the environments it will experience during the initial phases of the well construction process. Due to the detrimental impact that lost circulation has operationally, economically and environmentally, the need to design and maintain a sufficient mud system is critical.

Drilling mud systems have numerous components within the drilling process and contribute in a multitude of ways operationally. If the system is not up to standard specifications for that hole-section, efficiencies in the drilling process can drop significantly. This decrease in performance can significantly affect the economics of the well and quickly drive up the cost of operations due

to an insufficient mud system. Moreover, if the proper mud system is not utilized correctly lost circulation may be realized at the drill site which poses a great risk to the rig crew due to a removal of a safety barrier. Lost circulation, due to various reasons discussed in later sections, not only hinders operations, but further impacts the economics of the well. The fiscal impact includes the non-productive time on the rig, in addition to the cost of the replaced drilling fluid and the cost of treatment used to mitigate the losses (Lavrov 2016). Alleviating losses during the drilling process can save a significant amount of capital. As of late 2014, the average capital cost of an onshore horizontal well was projected at $7 million for drilling, completions and facilities. Considering rig time and drilling fluids make up roughly 15% of this total expenditure, any additional cost due to the fluid system can easily drive this metric above $1 million (U.S. Department of Energy 2016). In the following sections, the causes, risks and preventative measures of drilling fluid losses are discussed in detail.

1.1 DRILLING FLUID LOSS

As previously mentioned, failing to sustain a quality drilling fluid system during the well construction phase has direct implications, both operationally and economically. The fluid system serves many purposes during the drilling phase of a well. Drilling fluid transmits hydraulic power to the bit and downhole tools, cools the bit and drillstring and enables the removal of drill cuttings during drilling operations. All of these functions are critical to operational efficiency during the well construction phase. If peak performance of the mud system is not maintained the drilling operation can be hindered and significant costs could potentially be recognized. Furthermore, drilling fluid loss can have a detrimental impact on production. Fluid leak-off, or filtrate, within a hydrocarbon bearing zone can increase the amount of skin around the near wellbore. This addition of skin acts as an increased differential pressure near wellbore hindering the performance of the well (Jiao et al. 1992). It has been well documented that an engineered fluid system designed for the anticipated well conditions can significantly increase production rates (Hands et

al. 1998). Although an optimized mud system can increase production and reduce costs, more importantly, the mud system serves as a barrier for potential hazards.

1.1.1 Risks

Along with the operational functions the mud system supports during drilling, one of the most critical components it serves is controlling formation pressures and maintaining well control. During drilling operations, the mud system circulates through the drill pipe and up through the annulus. During this time, the mud must maintain a hydrostatic pressure within the fluid column that will counterbalance the forces from the formations while being drilled. If the pressure from the hydrostatic column of mud does not offset the pressures from the formation it could enable an influx of formation fluids into the wellbore. This incident is referred to as “kick” and requires immediate well control measures. On the other hand, if the pressure from the fluid column exceeds the fracture pressure it will cause fluid to emit into the formation, also known as lost circulation. In both of these cases the stability of the well is compromised and if not dealt with properly, could potentially sacrifice the well itself or harm rig personnel onsite.

1.2 RESEARCH OBJECTIVES

The main objectives of this research were to develop a new method to test and evaluate lost circulation material (LCM) in conjunction with nanoparticles. The nanoparticles were chosen based on low pressure fluid loss tests. A new apparatus was designed to achieve these objectives and enables the evaluation of these materials under constant rate and constant pressure conditions to be better understood. LCM mixtures that have been tested formerly in the literature are reexamined, and the previously tested sealing pressures of these mixtures are verified in the newly designed apparatus. The apparatus also allows the pressure “leak off” of the plugging material to be investigated after the seal has been formed under both of these conditions. A form of transient analysis is conducted on these pressure “leak off” profiles to investigate the quality of

the seal. The concept of sealing integrity is revisited and analyzed in a new light considering a higher differential pressure that can be seen operationally in horizontal well drilling. This concept was designed to account for the pressures the seal will encounter while drilling ahead after the seal has been established. The following lists the sub-objectives performed to reach the overall objective of this research:

- Design a new apparatus to effectively test the integrity of LCM with and without nanoparticles as constant differential pressure is applied to the seal.
- Evaluate previously tested LCM formulations in newly developed apparatus and establish if similar, or higher, sealing pressures can be achieved.
- Utilize nanoparticles to investigate if there are recognized benefits to increasing the sealing pressure of a formed seal.
- Assess if a new method of evaluating LCM mixtures can be established based on transient flow through the fractures.

CHAPTER II

REVIEW OF LITERATURE

This chapter defines lost circulation and discusses some of the common issues that are associated with the event. It also details previous methods that were used to evaluate lost circulation material (LCM), along with the discoveries and learnings that were made in recent years. Furthermore, it covers nanoparticle (NP) technology and the recent experimentations that have been conducted in relation to fluid filtrate and lost circulation. These works are what developed the foundation for this research and molded the overall objectives.

2.1 LOST CIRCULATION

Lost circulation is a condition during the drilling operation where fluid within the wellbore escapes into the immediate formation being drilled or a formation that has recently been penetrated. If lost circulation occurs in the production zone it is likely that other remedial techniques will be needed in order to reduce the skin damage and not sacrifice production. Furthermore, if lost circulation occurs further up the wellbore in the overburden the repercussion could be just as detrimental. Losses in this part of the zone, after drilling ahead, can cause a severe reduction in hydrostatic pressure, instigating a well control problem or even raise concern during cementing operations regarding the proper placement of cement (Lavrov 2016).

The particular circumstance that causes lost circulation to occur can vary from an induced fracture, caused by the mud system exceeding the formation fracture pressure, to a unique stratigraphic zone characteristic that causes losses, such as depletion or naturally fractured zones.

2.1.1 Lost Circulation Zones

During lost circulation, the true mechanism that is causing the losses is not always well known, but as fields develop, experience begins to mold the root problem. Figure 1 shows zones where lost circulation may occur during the drilling operation, whether initiated at the bit or up hole in the overburden.

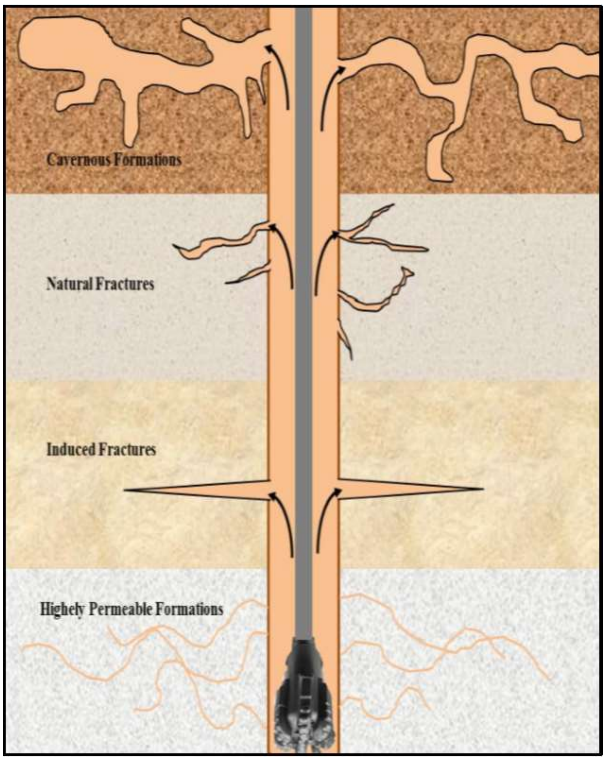

Figure 1: Potential lost circulation zones (Alsaba et al. 2015)

As shown in Figure 1, these types of zones are all susceptible areas for taking drilling fluid and can all have various rates at which it will take the fluid, as will be discussed later in the chapter. Contrary to the other three zones, induced fractures can occur at any point in the well and are primarily caused by the mud weight exceeding formation fracture pressure. At this point, a fracture is initiated by the overwhelming pressure inflicted on the formation. Fluid losses in this case are typically sudden and of drastic measure. Induced fractures are also a primary concern for

extended reach drilling in deviated wells. With pore and fracture pressure remaining the same throughout the lateral and as the well is drilled further ahead, the pressure drop required increases until it eventually meets the upper fracture pressure limitation (Lavrov 2016).

Natural fractures, unlike induced fractures, typically show gradual signs of fluid loss while drilling, but certainly have the potential for severe or total losses if drilling commences without mitigating the issue. These are typically seen within carbonate or chalk type formations, but most formations nonetheless have some form of natural fractures associated with the strata (Lavrov 2016).

Vugular and cavernous formations, although rare, have the highest impact on drilling fluid losses. These systems are a result of a geological process that enables a portion of the formation to be open at all times. They can take on any orientation and have a variable amount of void space associated with the system, but most importantly they are predominantly under-pressured below that of a fresh water gradient (Canson 1985).

Highly permeable, depleted or unconsolidated formations are the most common type of lost circulation zones, especially considering the modern day drilling philosophy of deeper, lateral shale drilling. In most cases, in order to reach these shale formations operations must endure drilling through recently produced, or depleted, formations. They are also prominent in offshore drilling where shallow sand zones can be unconsolidated. In all cases, these zones can range from minor losses to total loss of a drilling fluid system. Most times, operators will choose to drill with a more underbalanced mud system, meaning the mud weight of the fluid is closer to the pore pressure gradient of the formation. In doing this they mitigate the risk of overwhelming the formation fracture pressure, which is already dropped due to the high permeable formation. Success has been noted in cases offshore, as well as onshore unconsolidated formations, where

underbalanced drilling, in combination with an optimized fluid system has reduced fluid losses while drilling (Hannegan et al. 2002 & Cobianco et al. 2003).

2.1.2 Severity

With all the loss zones that may be encountered during drilling it is important to understand the severity level of fluid losses. Understanding the severity of fluid losses can assist in identifying the type of loss zone being drilled and help mitigate the losses being realized (Canson 1985). Losses during drilling are not always worst-case scenario. Monitoring fluid levels while drilling allows a contractor to understand the integrity of the zone being drilled and how much fluid the zone is taking in a particular time interval. Most fluid loss monitoring is conducted in bbl/hr and depending on the rate a classified severity determined. Figure 2 shows the classification of loss circulation based on their severity levels for water based, oil based and synthetic based fluids.

Fluid	Loss	Severity (bbl/h)	Scenarios
WBF	Small (infiltration)	< 25	Any type of formation (permeable Sands)
	Partial (average)	25–100	Coarse sand (gravel), natural or induzivas fractures
	Severe (massive)	100–500	Fractures, faults, vugs, caves, highly permeable formations
	Total (complete)	Impossible to maintain the wellbore full	Fractures, faults, vugs, caves,
OBF, SBF	Small (infiltration)	< 10	Any type of formation (permeable Sands)
	Partial (average)	10–30	Coarse sand (gravel), natural or induzivas fractures
	Severe (massive)	> 30	Fractures, faults, vugs, caves, highly permeable formations
	Total (complete)	Impossible to maintain the wellbore full	Fractures, faults, vugs, caves

Figure 2: Classification of lost circulation severity (Calcada et al. 2015)

It can be seen that loss severity can range from less than 25bbl/hr. to total wellbore losses. As previously discussed, each one of these cases are unique to a particular loss zone. Water losses allow for a wider range of severity as its properties are more susceptible to higher filtrate volumes than oil or synthetic based muds. Water based fluids are also less expensive and have, in some cases, been used as “sacrifice” fluids to mitigate the economic impact of fluid loss (Bruton et al. 2001). All in all, taking on losses can be expensive and operationally hazardous. Proper

techniques and preventative measures should be in place to successfully mitigate the possibilities of fluid loss during drilling.

2.1.3 Mitigation and Material Selection Criteria

Best practices have been established over the years that prevent losses from occurring initially. To mitigate the likelihood of severe losses there are preventative measures that can be implemented ahead of time. These operational methods reduce the possibility of taking on severe losses, but are no guarantee extreme cases will cease to be encountered. The best way to prevent losses from occurring is to maintaining a mud weight well below the formation fracture pressure, but this itself is not always feasible as it poses risks of wellbore stability and the possibility of an influx. Figure 3 shows a diagram representing the stages of a loss circulation management program beginning with best drilling practices as the first stage of prevention.

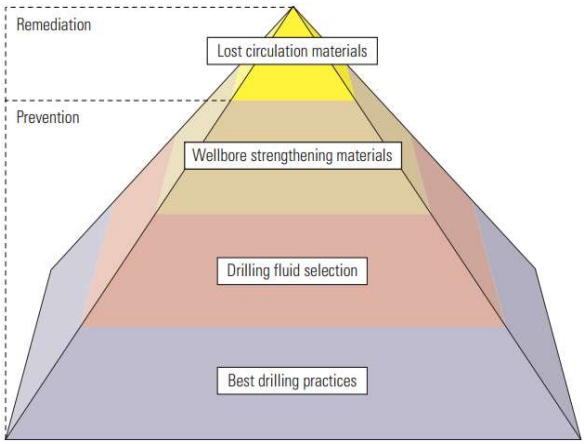

Figure 3: Lost Circulation Management Program (Cook et al. 2011)

The first line of defense when dealing with a potential lost circulation zone is establishing a set of best drilling practices. Understanding what techniques need to be used during drilling, such as certain geo-mechanical models, casing while drilling, or managed pressure drilling, as well as the details associated with your drilling plan are essential functions to first mitigating lost circulation. Secondly, knowing what fluid system will be used and the rheological properties associated with

fluid at each depth along the drill path are critical to the hydraulics program. The last line of prevention encompasses wellbore strengthening materials. These materials can be fibrous, flaked, granular, nanoparticles, acid soluble or hydratable and can be used as a standalone material or in conjunction with one another (Cook et al. 2011). These materials are introduced to the wellbore to strengthen the integrity of the formation to allow for a wider range of fluid pressure gradients to be utilized. All of these techniques are considered to be preventative measures used to mitigate lost circulation, but when cases of lost circulation occur, a different set of criteria is used to remedy to the problem.

Once losses occur immediate action is needed in order to stop further losses or prevent the acceleration of losses from happening. More concentrated volumes of granular, flakey or fibrous material can be used as well as the use of cement or high fluid loss squeezes. Although these have been known to cure losses, a set of criteria or an engineered combination of LCM is best suited to cure losses (Whitfill & Hemphill 2004 and Almagro et al. 2014). When selecting, or engineering, an LCM treatment it has been recommended that the following criteria provides the best results operationally: (1) the material should be equally effective in all anticipated loss formations (2) it should form an effective seal under high and low differential pressures (3) ensure timely placement of the material when initiated (4) handle anticipated surge and swab pressures and (5) the material can withstand the anticipated pressures expected when drilling ahead (Sweatman et al. 1997, Bruton et al. 2001 & Boukadi et al. 2004). If losses do occur and these recommendations are followed it has been noted that drilling losses will be cured properly and drilling will commence.

2.1.4 Previous Lost Circulation Experiments

The testing of lost circulation material (LCM) through some bridging apparatus has been evaluated since the 1980's (Gronewald et al. 2001). Static slot testing has been conducted in the

past to purely analyze the performance of LCM and to identify the effects that directly cause the formation to break down. Previous studies have concluded that initial fractures are stabilized by the drilling fluid until the fluid begins to enter the fracture causing it fail, which causes the need for LCM to be used, but many theories have been developed since this initial assessment was developed by the Drilling Engineering Association (Morita et al. 1990). Hinkebein et al. 1983 utilized a static slot tester to evaluate the performance of LCM that was intended to be used in geothermal wells. Five LCMs were analyzed over 266 tests in a bentonite water based mud. A sealing pressure that was determined through a calculated differential pressure of 500psi was chosen as the limit to seal, but was not limited to higher pressures. Testing commenced while pumping until max pressure was reached, which was indicated by a break in the sealing pressure. No constant pressure analysis was done during this experiment. While the analysis of sealing pressure for a bentonite water based mud was studied, a few interesting discoveries were made. First, an important take-away that was claimed in the study, was that the variance in gel strength of 9-36 $lb/100ft^2$ had no effect on the testing. Secondly, a large variance in sealing pressure was realized between the LCMs tested. It was noted that sealing pressure decreased with increased slot sizes. More specifically, it was documented that no notable sealing was formed when the slot was three times the size of the particles being used for testing.

Further tests were conducted to analyze this sealing pressure, or in some cases, a re-opening pressure that corresponds to an impairment caused by the drilling fluid after fracturing occurs. These tests were conducted with and without LCM material and never attributed this impairment to the LCM material, but more so to the drilling fluid formulation (Whitfill and Hemphill 2003). In the year 2000, the Joint Industry Projects (JIP) developed an apparatus that studied the how particles bridged across a designed fracture by analyzing fluid loss and pressures around the impermeable media (Hettema et al. 2007 and Van Oort et al. 2007). Figure 4 shows a schematic of the apparatus used in these experiments.

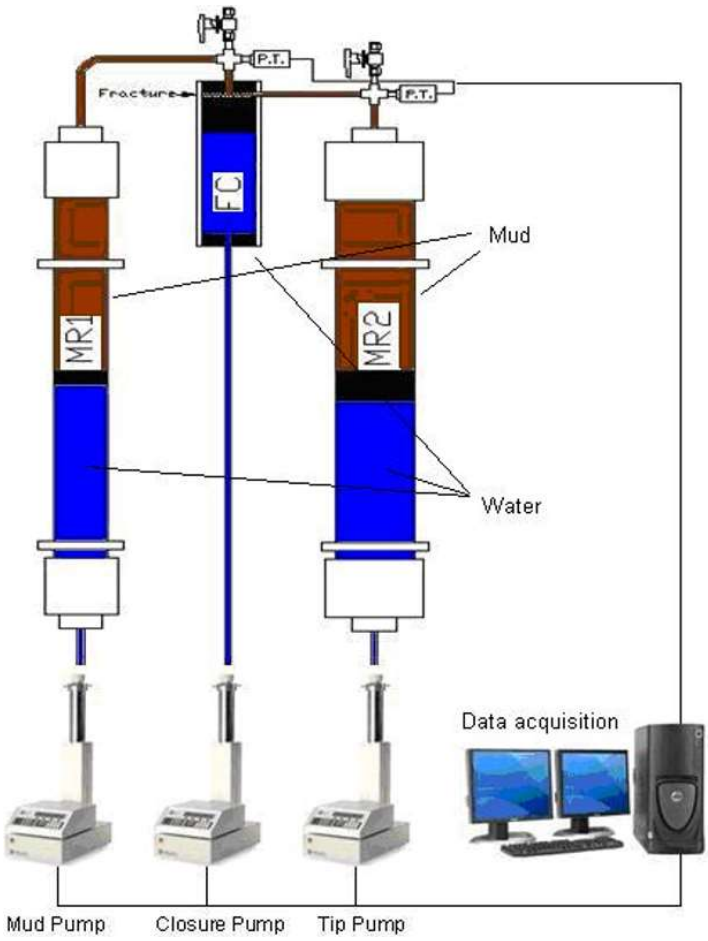

Figure 4: Impermeable Fracture Testing Apparatus (Hettema et al. 2007)

Although this device provided understanding of how particles bridged across fractures, the device had limitations regarding pressure and was limited to evaluating on fluid path location, which was at the fracture tip. Hettema et al. 2007 further studied this phenomenon by developing an innovative high-pressure testing device that evaluates drilling fluid systems and their additives. The goal of their research was to develop a device that can operate at higher pressures and manage more than one fluid system. The multi-faceted fluid system was what allowed them to not only study the physics at the fracture tip, but also through the matrix of the substrate that was being tested. This enabled a measurement to be made about the radial distance within the fracture and aid in further understanding the sealing mechanisms of a barite based drilling fluid with and

without LCM. It was able to successfully analyze the sealing effectiveness of LCM material through this radial response by measuring the fracture width. Tests were conducted by pumping fluid until a sealing pressure was witnessed. This sealing pressure was determined by the pressure at which the substrate broke, or propagated, and a pressure drop was realized. This was one of the initial experiments that looked at optimizing LCM types and concentrations for particular fracture widths. The downfall of this device was that it used ceramic plates that had 175 micron openings which seemed suitable at the time for a representative fracture. Figure 5 shows a schematic of the permeable fracturing device.

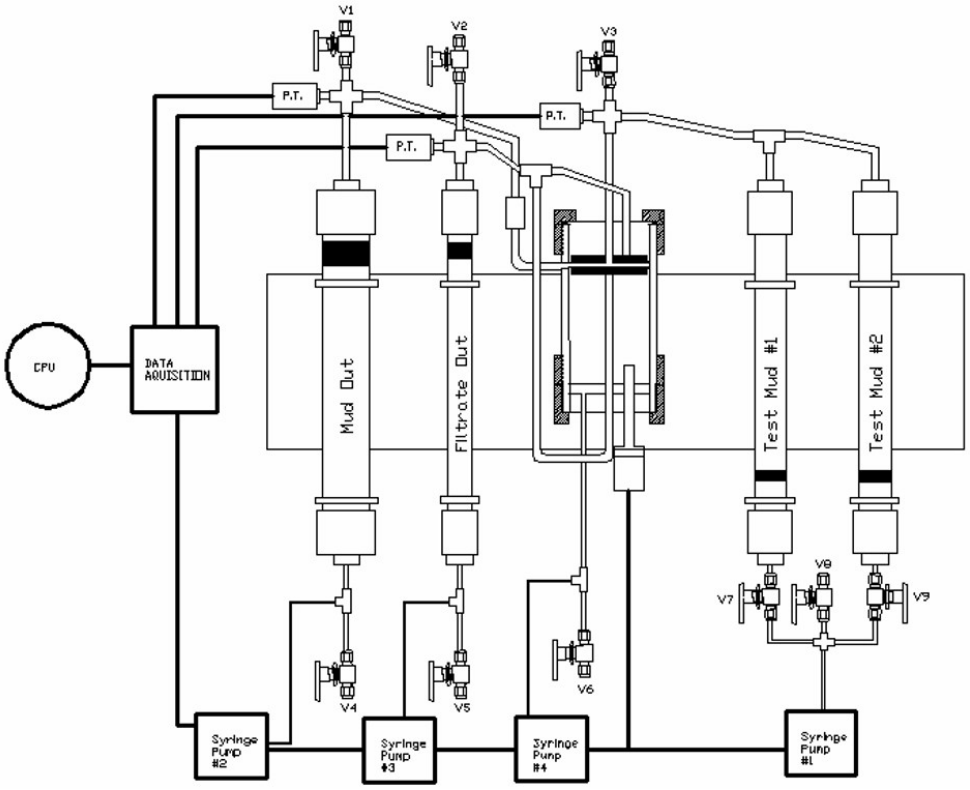

Figure 5: Permeable Fracture Testing Apparatus (Hettema et al. 2007)

Since these early tests, many studies have been done to analyze various aspects of wellbore fracturing, or more importantly, the strengthening effect that increases the resistance to fracturing. These studies have included the evaluation of wellbore models, fracture modeling, wellbore

strengthening materials, selection criteria experiments and LCM evaluations for wellbore strengthening (WBS) applications, most of which have contested the physical phenomena occurring at the wellbore (Van Oort et al. 2011, Nygaard et al. 2011 and Savari et al 2012). Many theories have been established in response to these studies, but deal more with wellbore strengthening rather than lost circulation material.

The use of lost circulation material as a remedial and preventative application has been investigated previously and is well documented in the literature. Tests have been conducted to analyze the integrity of the LCM as well as to better understand the selection criteria needed for optimized sealing. Classification of these materials have been further investigated to provide a clearer comprehension of what enables these particles to perform better under various scenarios. Parameters such as particle size distribution, shape, crushing resiliency, concentration and testing methods have been investigated for single LCM treatments as well as in combination.

Mostafavi et al. 2011 studied the resilience of LCM material through particle plugging tests and core fracturing tests. Four different types of LCM were used for testing in an apparatus that used three different slotted disc sizes, while bentonite mud was used as the drilling fluid. Testing proceeded by injecting a hydraulic fluid to push the LCM formulation through the slotted discs until a seal was formed. The path of flow was in the direction with gravity, flowing vertically downward. Pressure was monitored until the seal reached the sealing pressure, which is the pressure at which the seal breaks due to exceeding pressure. It was noted that particle mechanical properties, size distribution and concentration all played a role during testing. An analytical model that depicts the wellbore's resistance corresponding to downhole pressures was also developed. Essentially, the findings concluded that a better bridge is formed when a material has a higher resilience. Kumar et al. 2011 investigated the effect of adding combinations of ground marble into the fluid system along with graphite carbon. A similar plugging particle test was conducted using slotted discs. Sealing was also encountered while conducting these tests

providing more evidence that a combination of LCM's performs better rather than a single LCM treatment. However, during these tests a large amount of fluid loss was witnessed while measuring the sealing pressure of these materials. This led to the addition of a fiber based material to the combination, which had a reduction in fluid loss while exceeding the previous sealing pressure. One downfall to the experiments was that it was noted that the rheological change due to adding the fibers had an adverse effect on the material (Kumar et al. 2011). Kumar et al. 2011 later looked at the combination of resiliency of the LCM material along with a plugging particle apparatus. Similar to his previous study, the selection material based on the resiliency in combination of previously combined material provided higher sealing pressures coupled with lower fluid loss. Both of the previous tests were evaluated at the sealing pressure, or the limiting pressure prior to breaking.

Savari et al. 2014 considered the point at which the seal breaks to be the plug-breaking pressure (PBP). A similar plugging particle apparatus was used for the LCM tests, except the apparatus, in this case, pumped in the direction opposite to gravity. Taking this effect into account, a later study also studied the effect of particle suspension within the fluid system (Kulkarni et al. 2014). Qualitative results showed the ability of these particles to stay suspended within the drilling fluid. Both experiments combined showed an analysis of sealing breaking pressure, otherwise known as sealing pressure.

Alsaba et al. 2014 tested and discovered the various effects that LCM has on sealing pressure. Tests were conducted using a wide range of LCM that was later revisited and re-classified by Alsba et al. 2014. Various concentrations and disc sizes were used to conduct sealing pressure tests at low and high pressures. Fluid loss was monitored during all tests and temperature was applied in some cases to investigate if any degradation of the materials was recognized during testing. A total of 160 tests were carried out during the time of this investigation. Initial studies of sealing pressure were conducted to evaluate if the designed material chosen based off type, size,

shape, concentration, and particle size distribution (PSD) could seal smaller sized fractures. The sealing criteria chosen to dictate whether a material can sufficiently seal a particular fracture size was a differential pressure of 500 psi. It was found that particle size distribution had the highest effect on sealing integrity. Fibrous materials showed the highest sealing efficiency in comparison to granular calcium carbonate and graphite. Furthermore, angular particles such as nut shells had the ability to seal wider than fractures than others. Figure 6 shows the apparatuses used in these experiments.

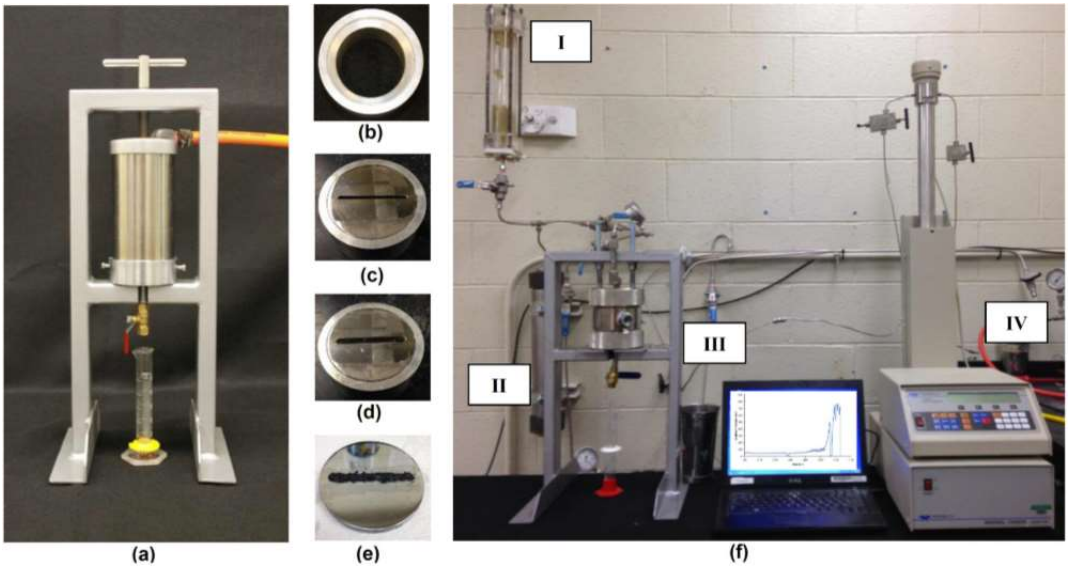

Figure 6: (a) low pressure LCM apparatus, (b) snug-fit spacer, (c) & (d) tapered discs, (e) sealed tapered disc and (f) high pressure LCM apparatus (Alsaba et al. 2014).

2.2 NANOPARTICLE TECHNOLOGY

In recent years, the use of nanoparticle technology in the oil and gas industry has become rampant. Prior to recent years, nanotechnology was primarily employed in other areas outside of the energy sector. Notable properties such as heightened durability, drug delivery, repelling effects and electronic enhancement, a number of other industries realized the benefits of this technology (Hoelscher 2012 & Bell 2004). The attractive qualities of nanotechnology began to peak interest within the oil and gas industry as the sector began to transition to unconventional,

horizontal shale plays. The locations of these hydrocarbon-bearing zones were found at deeper depths, higher pressures and elevated temperatures. These hostile conditions challenge the drilling and production equipment and push each of them to their technical limitations. Moreover, the cost of operating increased with these realized conditions calling for a technological advancement that eases the price of operating. Within that past decade, nanotechnology has proven its worth as a fluid additive in drilling, completions and workover systems to work within these operational conditions.

2.2.1 Benefits of Nanotechnology

The ability for nanoparticles to be tailored by size, shape, distribution, structure and composition enables various avenues in which nanoparticles can be implemented into oil and gas operations (Horikoshi 2013). Fundamental advantages that make the use of nanoparticles attractive in practice is the limited amount of materials needed to produce a set amount of nanoparticles, and secondly, the high surface area to volume ratio obtained from these produced particles. Figure 7 shows the number of nanoparticles and micro particles produced from one millimeter macro sphere of material.

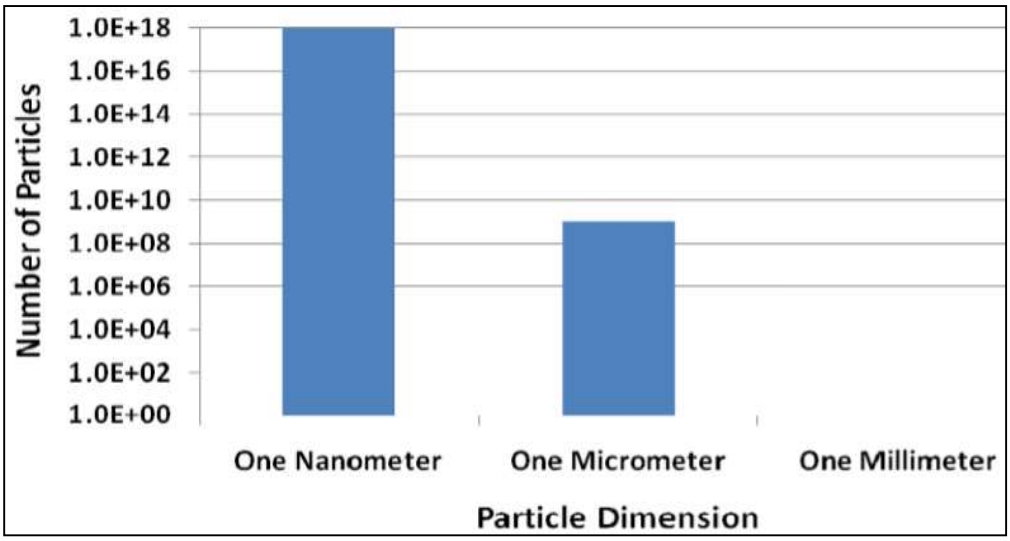

Figure 7: Number of particles produced from 1mm macro sphere (Amanullah et al. 2009)

This is significant considering the limited amount of material needed to produce such a large amount of particles. It is seen that the number of nanoparticles produced is orders of magnitude larger than the number of micrometer particles. Figure 8 shows the surface area to volume ratio of nanoparticles in comparison to micrometer and millimeter particles with the same volume.

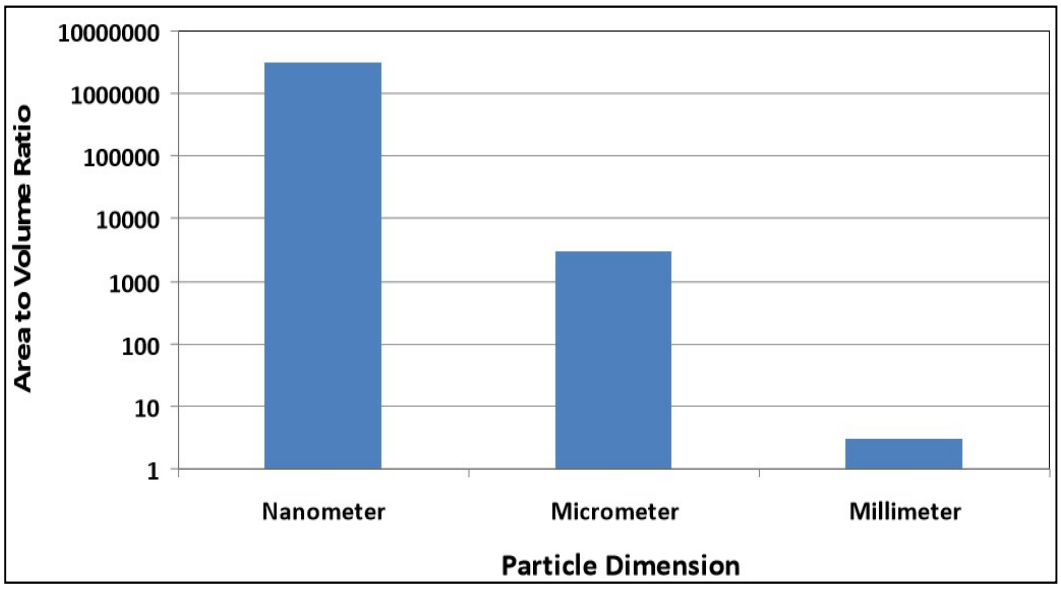

Figure 8: Surface area to volume ratio of same volume of materials (Amanullah et al. 2009)

It is clear that nanoparticles have a significantly larger surface area compared to micrometer and millimeter particles of the same volume. This relationship is critical in regards to the functionality of nanoparticles to influence a system. The large surface area enables nanoparticles to incorporate a large number of functional groups to fulfill interactions between other components within a nanoparticle system (Amanullah et al. 2009). These characteristics of nanoparticles, along with the capability to engineer them to a certain particle size, shape, size distribution, crystalline structure and composition, make the use of nanoparticles in a drilling system intriguing. Furthermore, the rheological benefits nanoparticle fluids have at higher temperatures and pressures warrant various ways for the technology to be optimized (Abdo 2013 & Kasiralvalad 2014). Numerous uses of this technology have been noted in the literature, including fluid loss

alleviation, wellbore stability, lost circulation, friction reduction, stuck pipe, clay mitigation, acid gas encounters, high-pressure high-temperature (HPHT) environments and stimulation fluids (& (Amanullah 2009 & Caldarola et al. 2016). To some extent, many of these uses have been investigated and verified within the oil and gas industry. Within the well construction phase, specifically drilling, issues like fluid loss control, well bore strengthening and formation damage have all seen significant improvements through the use of nanoparticle technology (Lecolier et al. 2005 & Zakaria et al. 2011). The following sections will cover previously tested experiments related to formation damage reduction through filtrate reduction, as well as lost circulation tests.

2.2.2 Previous Nanoparticle Experiments

Fluid loss during drilling can cause many issues, one being the issue of stuck pipe. Other than being mechanically stuck due to friction within the wellbore, stuck pipe can occur due to a strong differential pressure across a highly permeable or depleted zone. It can also become stuck due to an adhesive effect that is caused by a thick filter cake left on the wellbore. Thick filter cake is an indication that high fluid loss is being realized through the near wellbore. Introducing nanoparticles into the drilling fluid can significantly reduce the thickness of the filter cake while maintaining non-adhesive. Reducing the amount of fluid filtrate leaked off to the formation results in a significant reduction in the thickness of filter cake. Javeri et al. 2011 studied this effect utilizing silica nanoparticles. The addition of 3% by volume of silica nanoparticles was introduced to a drilling fluid and the thickness of the filter cake was measured in comparison to a drill fluid with no addition of nanoparticles. A 34% reduction in mud cake thickness was recognized when using silica nanoparticles. This effect was due to a more efficient compaction of particles within the medium causing the permeability of the filter cake to be reduced. This reduction in permeability restricted the flow of filtrate from the drill mud resulting in a thinner film of filter cake.

It has been well documented that reducing the fluid filtrate into the formation can significantly reduce the amount of formation damage that is induced during drilling (Jiao et al. 1992). Various other studies have evaluated and concluded the effect that nanoparticles are beneficial in reducing the fluid loss through a permeable media, resulting in an overall reduction of formation damage (Sensoy et al. 2009 & Contreras et al. 2014). Srivatsa et al. 2011 studied the effect of fluid loss with silica nanoparticles in a surfactant-polymer water based drilling fluid. The tests were conducted using a standard API fluid loss apparatus. They analyzed the amount of fluid lost in the drilling fluid over a 30 minutes, in 5 minute intervals, at a constant pressure of 100 psi. Xanthan gum along with a visco-elastic surfactant was used in a base case mud to test the grounds for initial fluid loss. A total of 4 base case tests were conducted to study the effects of fluid loss. Following the base case tests, silica nanoparticles were introduced to the drilling fluid and were tested accordingly. The weight percent of silica nanoparticles varied from 10% to 30%. A total of 5 drilling fluids with varying concentration of nanoparticles were tested for fluid loss. The base case fluids and drilling fluids containing nanoparticles were designed to study the effect of the addition of nanoparticles. Essentially, each base case fluid was tested with and without nanoparticles, all while maintaining the appropriate concentration of each fluid additive in each sample. Results showed a reduction in fluid loss for all samples containing nanoparticles. These results were confirmed to be due to the ability of the nanoparticles to block the small pore throats of the permeable media. Further investigation concluded that the reduction in fluid loss increases as the concentration of nanoparticles increases. Although this trend was realized, the limiting factor was discovered that increasing the concentration of nanoparticles beyond some limit caused aggregation of the particles inducing an opposite effect of the system. This effect caused the drilling fluid to form a thicker filter cake retarding the performance of the fluid.

Further experiments were conducted using nanoparticles in a water based mud and were tested for fluid loss at given permeable media size range in shale formations. Water invasion into shale

formations can cause sloughing of the formation as well as wellbore collapse and stuck pipe issues. Sensoy et al. 2009 studied the effect of using nanoparticles to reduce fluid loss into hard and soft shale formations. Two different silica nanoparticles were used in separate drilling fluids to analyze the fluid penetration into two different types of shale formations. A preserved, hard Atoka shale and a soft, Gulf of Mexico shale were obtained to conduct these experiments. Both shales contained a large portion of clay by composition. The samples were tested against separate fluids containing nanoparticles via a continuous flow apparatus. Sealing pressure, permeability and fluid loss were measured in each experiment. Results concluded that the nanoparticles reduced the fluid filtration into the Atoka shale by 16-72%. Nanoparticles also reduced the penetration of fluid into the Gulf of Mexico shale by 17-27%. Sealing pressure tended to increase with an increasing concentration of nanoparticles. 20nm silica nanoparticles showed better performance than the 5nm silica particles in regards to sealing pressure. In this case, the lower concentration limit of nanoparticles was noted at 10% wt. Dropping below this concentration reduced the ability for the particles to effectively block the pore throats of the shale.

Contreras et al. 2014 investigated the use of iron-based nanoparticles and calcium-based nanoparticles on fluid filtrate reduction through ceramic discs (k = 775 mD). Ceramic discs were used to replicate a conventional permeable media. Graphite was used as a lost circulation material for the porous media. Fluid loss was conducted using an oil-based mud (OBM) and a high-pressure high-temperature (HPHT) filter press apparatus. This apparatus was operated at 500 psi and 250°F. Additional tests on nanoparticles and graphite were conducted using a low-pressure low-temperature (LPLT) apparatus. The two nanoparticle mixtures were tested at 0.5% wt 1.0% wt and 2.5% wt concentration with 0.5% wt and 2.0% wt graphite. LPTP results showed that the iron-based nanoparticles containing 0.5% wt and 2.0% wt reduced the filtration by 100% over 30 minutes. The calcium-based nanoparticles realized about 40% reduction for both 0.5% wt and 2.0% wt graphite over 30 minutes. Both sets of results were obtained at the highest concentration

of nanoparticles for each mixture. In regards to the HPHT tests, the best results were witnesses at the lowest concentrations of nanoparticles (0.5%) for the iron-based mixture. The iron-based nanoparticles with a concentration of 0.5% wt realized a 60% and 75% reduction in fluid loss for mixtures containing 0.5% and 2.0% graphite, respectively. For the same mixture, 0.5% wt iron-based nanoparticles containing 0% graphite had a 50% reduction in fluid loss. This 50% reduction in fluid loss is an indication of the performance of only iron-based nanoparticles within the fluid. As for the HPHT test for calcium-based nanoparticles, the best results were obtained at a nanoparticle concentration of 2.5% wt. The base case fluid containing only 2.5% wt nanoparticles recognized a 30% reduction in fluid loss. A fluid loss reduction of 35% and 45% was recognized with a graphite concentration of 2.0% wt and 0.5%, respectively. Filter cake thickness had a tendency to increase with increasing graphite concentration. Overall, the utilization of nanoparticles in the OBM that was tested showed a significant reduction in fluid loss across the ceramic media.

Further research was conducted analyzing the sealing pressure through slotted discs while using barite nanoparticles and nutshells as lost circulation materials (Akhtarmanesh et al. 2016). Barite nanoparticles that were chemically and mechanically generated were used within a water based mud for the experiments. Each generated type of nanoparticles were tested at 3%wt within the water based mud. The particle plugging tests were conducted at high pressure with a 2000 micron disc. The 2000 micron disc was used to replicate a wide fracture. The experiment consisted of pumping at a constant rate of 25 ml/min and analyzing the pumping pressure over the given time interval the slotted disc was sealed. Testing proceeded by continuously pumping until a rapid drop in pressure was noticed Pumping continued to represent re-opening sealing pressure due to the loss circulation materials (LCM) ability to re-form a seal. Results showed that mechanically generated barite nanoparticles with LCM material increased the sealing pressure more than 205%, when compared to the base case. This increase in pressure was 90% greater than the chemically

generated nanoparticles. The chemically generated barite nanoparticles with LCM material increased the sealing pressure by more than 60%, when compared to the base case. These results were claimed to be due to the rampant size distribution of the particles within the drilling fluid, resulting in a better sealing pressure in comparison to traditional lost circulation material.

2.3 CRITICAL REVIEW OF LITERATURE

After studying the previous tests conducted for both lost circulation materials and nanoparticles a few key points were established after critical review. Lost circulation materials have traditionally only been studied in terms of a sealing pressure, the point at which the seal breaks as described in Section 2.1.4. This pressure was noted in the literature many times over to be the point at which the seal has formed its maximum pressure, but it has never been documented or researched if this pressure would hold its integrity as constant pressure was applied to the seal. Furthermore, most apparatuses used to study LCM utilized a traditional plugging particle apparatus where constant rate was applied until the seal was broken as seen with Hettema, Alsaba and Savari et al. The quality of the seal or how transient flow may occur through the seal has yet to be investigated. As for nanoparticles, little has been done outside wellbore strengthening to evaluate if nanoparticles are suitable candidates for lost circulation material. In terms of rheology, the literature has used consistent base muds in tests where lost circulation or nanoparticles have been tested, but have yet to thoroughly analyze these varied effects of rheology and the consequences it has on sealing integrity. These key points are what formed the basis of this research.

CHAPTER III

METHODOLOGY

The following sections detail the methodology utilized for the research herein. Descriptions of the types of fluid used, rheological studies, nanoparticle synthetization methods, apparatuses and testing methods are explained. This research was initialized based on low-pressure nanoparticle fluid loss testing to determine the proper nanoparticle selection for further experiments. Following the results from these experiments a high-pressure apparatus was designed and high pressure tests commenced. These high pressure tests were defined by the research objectives in Chapter 1.2.

3.1 LOW PRESSURE TESTING

Low pressure tests were conducted to evaluate how well a certain type of nanoparticle performs at reducing fluid filtrate in a water based mud. Two different nanoparticles were used during testing. Different concentrations of barite nanoparticles were synthesized, both mechanically and chemically, and tested at low pressure via a standard API fluid loss apparatus (Loggins et al. 2017). The performance of each nanoparticle concentration was evaluated to determine the reduction in fluid loss utilizing a water based mud. An optimal concentration was investigated in the low pressure tests, as well as unique characteristics regarding each type of nanoparticle. These tests were conducted as preliminary tests to not only investigate fluid loss reduction, but also to evaluate the feasibility of each nanoparticle to be used in high pressure testing. The following sections detail this portion of the research methodology.

3.1.1 Base Fluid Preparation

A water based mud with the absence of nanoparticles was used as a base case to compare all fluid loss results. The fluid consisted of an emulsion between 330 cc of water and 20 cc 1-hexadecene. Polysorbate-20 was used as the surfactant, as well as sodium dodecyl sulfate (SDS). Starch, a low viscosity poly-anionic cellulous (PAC-LV) and a salt friendly poly-anionic cellulous (PAC-R) were used as polymers within the WBM. Weighting agents other than barite included potassium chloride (KCl) and sodium chloride (NaCl). Bentonite and sodium hydroxide were also used as additives in the WBM to assist with the rheology. Table 1 lists the resultant rheological values for the base case WBM.

Mud Type	**Mud Weight g/cc (ppg)**	**Plastic Viscosity (cP)**	**Yield Point ($lbf/100ft^2$)**
Water Based Mud	1.21 (10.1)	17	5

Table 1: Properties for Low Pressure Base Mud

A total weight of 60 grams of barite per 350ml was used in the base case WBM. The amount of barite in the base case mud is replicated in all fluid samples. Depending on the concentration of nanoparticles, 60 grams, less the amount of the generated weight of nanoparticles produced, would be used in each fluid sample.

3.1.2 Selection of Barite Nanoparticles

Barium sulfate ($BaSO_4$), or barite, has been of wide use in drilling fluids as a weighting agent to control the density of the drilling mud. With a specific gravity of 4.5, the density of a drilling fluid containing barite can be as heavy as 19 ppg. This wide range of available density makes barite an attractive weighting agent. Moreover, barite is effective at significantly high temperatures. The material will remain stable in bottom-hole temperatures up to 500°F. This makes them a prime candidate in deep, higher temperature wells. Furthermore, barite is

essentially a non-reactive material and ensures a wide range of additives can be incorporated with this material in a drilling fluid system. This being the case, the Environmental Protection Agency (EPA) does not view barite as a hazardous waste material. Barite is commonly mined from sulfate mines making the material readily available. These benefits, along with the known advantages of nanoparticles, have driven the interest to further investigate the use of barite nanoparticles in a drilling fluid system.

3.1.3 Nanoparticle Synthetization

The use of barite nanoparticles on fluid filtrate reduction was tested and evaluated in the low pressure tests. Moreover, the reduction of fluid filtrate when using mechanically synthesized and chemically synthesized barite nanoparticles was evaluated. The two different synthetization methods use different physical processes to create nano-sized material. The top-down method, or breakdown method, uses a physical process that breaks down the material into the required size needed. The bottom-up method, or build-up method, utilizes either a solid phase or liquid phase chemical process that creates the nano-sized material. Figure 9 shows the various methods used to create nanoparticles.

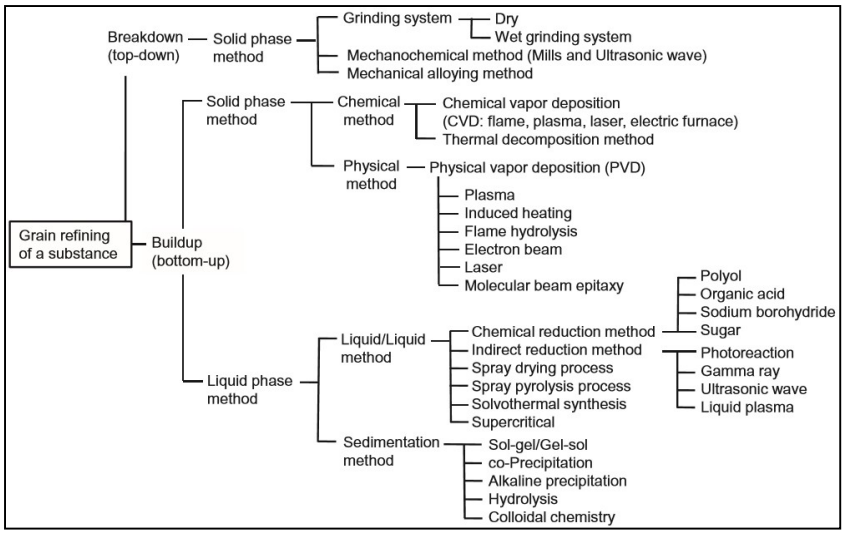

Figure 9: Various methods to create nanoparticles (Horikoshi et al. 2013)

For this research, the mechanically generated nanoparticles were created by a dry, grinding system, breakdown method. The chemically generated nanoparticles were created by a liquid phase sedimentation method via colloidal chemistry. Both types of synthesized barite nanoparticles were generated in-house. The barite nanoparticles were used in a water based mud to test the amount of fluid loss each type allowed through a given permeable media. For each synthesized type of nanoparticle, three concentrations were used within the water based mud. Different sizes of permeable media were used to analyze the efficiency of fluid loss reduction for a given concentration and synthetization type.

For the mechanically generated barite nanoparticles, an EMAX ball grinder was utilized at high speeds to mechanically break down the barite material. The grinding process was conducted in a dry environment, meaning no liquid was used during the process of grinding. Initially, 200-400 grams of normal barite was sieved through 150, 75 and 38 micron sieves for 90 minutes. Following the sieving process, only the barite that was less than 38 microns were kept and stored for future grinding. For the grinding process, 10 grams of the sieved barite was placed into the EMAX grinder along with 45 grams of 2 mm steel grinding balls. Grinding commenced at 900 rpm for 4 hours in order to achieve the desired size of nano-barite. To permit cooling of the material, grinding during the 4 hours would have 2 minutes of grinding, followed by a 2-minute rest period. The process of sieving the material and grinding the sieved material for a duration of time is what determines the particle size of the barite nanoparticles.

Chemically generated barite nanoparticles were synthesized by a sequence of a two precursor reactions. An aqueous solution of potassium sulfate ($K2SO_4$) was the first precursor mixture. The second solution of barium chloride ($BaCl_2$) was the second precursor used in the synthetization process. Each mixture contained a certain volume of 1-hexadecene, Polysorbate-20 and SDS. The two mixtures would be dissolved by mixing at 200 rpm at 75°F for 5 minutes each. After the 5-minute mixing period, the $BaCl_2$ was added to the $K2SO_4$ and was mixed for an additional 5

minutes to ensure all materials were dissolved. The reaction produces a certain volume, per desired recipe, of barium sulfate ($BaSO_4$) and potassium chloride (KCl). For the tests that were done at various concentrations, the amount of barium sulfate that was produced from the reaction would be taken into consideration when added to the fluid as a whole. Essentially, as the concentration of nano-barite increased the amount of bulk barite was reduced to ensure the fluid system had a constant overall concentration of barite. This ensured the rheology was consistent and compatible for all tests.

3.1.4 Nanoparticle Description

After synthesizing each type of generated barite nanoparticle, various tests were conducted to better describe the nanoparticles. In doing this, particle size distribution, as well as the variance in the size distribution was studied via a dynamic light scattering (DLS) apparatus. This enabled a better understanding of how each synthetization method differs from one another. Furthermore, to obtain an understanding of shape and size, transmission electron microscopy (TEM) was used to provide additional visual aid. This allowed to further describe the size of the particles, but more importantly understand how the particles were shaped and realize if any agglomeration occurred during the process. Overall, these tests were used in conjunction with the testing results to better conclude the findings from the low pressure testing and allow for the proper nano-barite selection to be made for high pressure testing.

3.1.5 Testing Apparatus and Procedure

All samples were tested using a standard API fluid loss apparatus. All experiments were low-pressure low-temperature conducted at 100 psi and 75°F. After completion of mixing each sample, weight and rheological measurements were made to ensure the proper parameters were met prior to testing for fluid loss. This was also conducted to ensure the proper values for weight

and rheology were obtained prior to changing the integrity of the sample through water extraction. Figure 10 shows a general schematic of the standard API fluid loss tester.

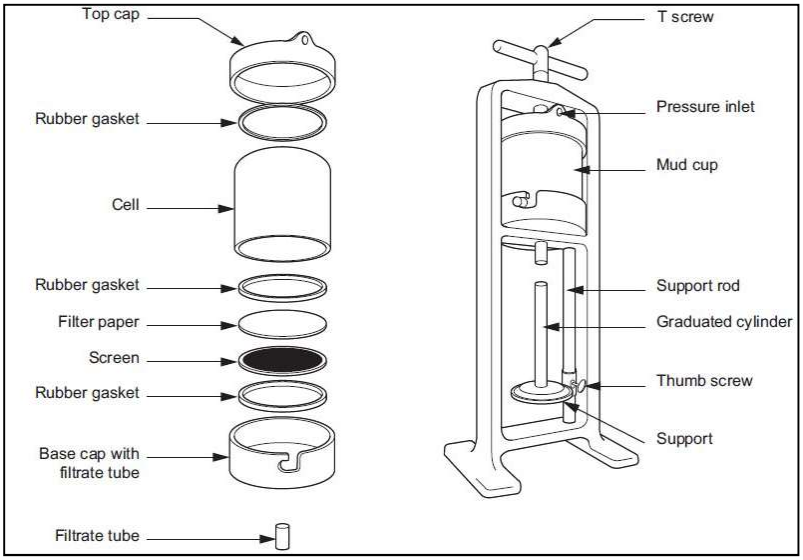

Figure 10: Schematic of a Standard API Fluid Loss Apparatus

Testing was conducted by filling the mud cap with the desired mud sample and placing it within the support structure. A pressure cap with an attached pressure regulator was then tightened via a T-screw handle. A small graduated cylinder was placed on the support plate and tightened via thumb screw. Pressure of 100 psi was then applied through the cap and fluid was measured in 5 minute intervals for 30 minutes. The final fluid loss volume was recorded and analyzed accordingly. These low pressure tests were conducted to answer the following questions:

1. Are mechanical or chemical nanoparticles more efficient at reducing fluid loss?
2. Is there an optimum concentration of nanoparticles where no reduction is recognized when increasing the concentration of nanoparticles?
3. Can the best performing nanoparticle significantly reduce fluid loss at a higher permeable filter paper size?
4. Which nanoparticle would best be suited for the high pressure testing?

Initially, tests were conducted to analyze the efficiency that each nanoparticle type had on the fluid filtrate reduction. The goal was to evaluate the effectiveness each type of nanoparticle, mechanical and chemical, had at reducing fluid loss. Filter paper sizes of 2-5 micron were tested initially to establish a fluid loss volume for a base case WBM. Fluid loss tests with 2-5 micron filter paper was then conducted with mechanical and chemical nanoparticles. Furthermore, along with nanoparticle type and filter paper size, the concentration of each nanoparticle sample was varied. Each sample was tested at 1.5% wt and 3% wt of each type of nanoparticle and was compared to the fluid loss of the base case. The performance of each nanoparticle type was recorded and analyzed accordingly to determine which type of nanoparticle reduced the filtrate the most in the WBM system. Figure 11 shows the API fluid loss apparatus used for the experiments.

Figure 11: API Fluid Loss Apparatus

Following the tests for mechanical and chemical nanoparticles, a secondary test was conducted using the same chemical nanoparticles. This test was conducted on the same 2-5 micron filter paper using a WBM system under different rheological properties (MW = 9.1, PV = 35 cP, YP = 42 lb/100ft^2). This test was conducted to look at a comparison view of fluid loss using a different

mud and also to analyze the reduction in fluid filtrate as the concentration of nanoparticles continuously increases. The goal was to evaluate if there was an optimum concentration of nanoparticles where no further reduction in fluid loss was witnessed with an increase in concentration.

Lastly, the best performing nanoparticle was then tested at 5-10 micron filter paper to evaluate the reduction in fluid loss at a higher permeable size. This test was conducted to see if the chemical nanoparticles had the ability to reduce the fluid filtrate in a larger permeable media. Furthermore, these tests determined if there was an optimum concentration where no more fluid loss was recorded when the concentration of chemical nanoparticles was further increased. The results for these experiments are further described in the following section.

3.2 HIGH PRESSURE TESTING

A newly developed approach of analyzing lost circulation material with and without nanoparticles was established through the design of a fabricated Modified Plugging Particle Apparatus (MPPA). Testing conditions were established through a calculated differential pressure calculation that can be encountered in a modern horizontal well drilling operation. These tests were all evaluated in the same base mud, in which rheology was extensively analyzed and settling tests were conducted. Initially, previously reported LCM formulations with their respective disc sizes were tested in the newly developed apparatus to realize similar or higher sealing pressures as well as to establish repeatability. Following these initial tests, the testing matrix was evaluated for the LCMs of interest to investigate higher sealing pressures at the designed differential pressure limitation and a constant pressure evaluation after reaching the initial sealing pressure. Nanoparticles were also introduced into the testing matrix to evaluate the potential sealing benefits of two different nanoparticles. The following sections detail the methodology for the high pressure testing portion of this research.

3.2.1 Apparatus

A fabricated version of the "Modified Plugging Particle Apparatus" was developed for the high pressure LCM and nanoparticle testing. The main objective in designing this apparatus was to aim at developing a mass balance system that analyzes pressure, rate and volume automatically. The goal in designing this apparatus was to develop a system that could test sealing pressures, the pressure at which the seal breaks, and also test particles under constant pressure to evaluate the integrity of the material. It was also a goal to be able to analyze the pressure transient once these two pressure limits were reached and pumping stopped, which would not remove pressure from the system, but only allow the measurement of pressure depletion through the testing media. To achieve this a 5,000 psi permeability plugging tester made by OFITE Testing Equipment, Inc. was used as a baseline foundation for the testing cell. Figure 12 shows a visual representation of the tester.

Figure 12: OFITE Permeability Plugging Tester

This equipment was originally made to be operated with a manual hand pump, as shown, but was unable to operate at constant rate. It was designed to test fluid samples through slotted discs by a hydraulically actuated piston which was controlled by the manual hand pump, which is shown in Figure 12. The fluid leak-off would then exit through the bottom portion of the back pressure

regulator to allow measurements of fluid loss. The first modification to this piece of equipment was to remove the back pressure regulator and manual pump. This would allow the attachment of a cylindrical pump to the flow manifold and enable a large flow-out port for exiting testing fluids containing LCM. In doing this, the thread port on the top cap that held the back pressure regulator was increased to a 1/2” thread to allow a Swagelok fitting to attach to 1/4” stainless steel tubing. This was deemed a sufficient size of tubing to allow the flow of fluid containing LCM.

To attach a cylindrical pump to the permeability tester the flow manifold was fabricated in order to attach the required tubing. The manual pump was removed and 1/4" tubing was attached via Swagelok fittings. A 3,500 psi Vindum Engineering, dual cylindrical pump was selected for the apparatus. Figure 13 shows a representative pump that was used for the apparatus.

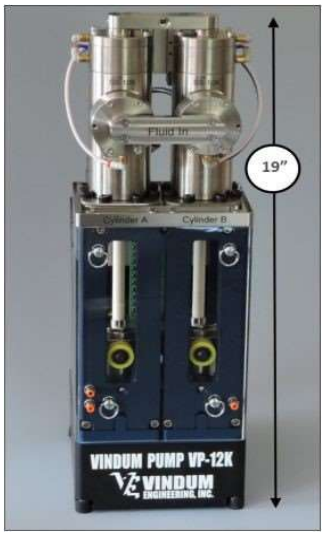

Figure 13: Vindum Engineering Pump

The continuous-flow, high-pressure, dual cylinder pump has the ability to operate with non-stop pulse free flow. It allows higher accuracy with multiple operating modes. It can be operated in constant pressure and rate delivery modes. The pump can also be operated in constant rate and delivery modes. It can dispense and receive fluids either operating under constant rate or pressure. Although the cylinders can operate in tandem, they can also be set to operate independently of

each other. Pressure transducers and computer controlled software allows for the immediate monitoring of pressures, volumes and rates. In designing the apparatus, the pump was set up to pump water as the hydraulic fluid and utilized clean nitrogen gas to operate the solenoids that control the valves on the pump.

The last fabrication to the apparatus was to design a way to monitor the mass of the fluid as it exited the flow-out tubing. Being aware of the density of the fluid being tested, obtaining the mass of the material would allow the volume of the material to be calculated as it exiting the apparatus. To accomplish this a portable OHAUS scale was used at the flow out port. This scale allowed for constant and immediate measurements to be made and transferred to the computer. Following these main attachments and fabrications to the original apparatus the testing procedure was ready to be established. Figure 14 shows a visual schematic of the testing apparatus with all of its components.

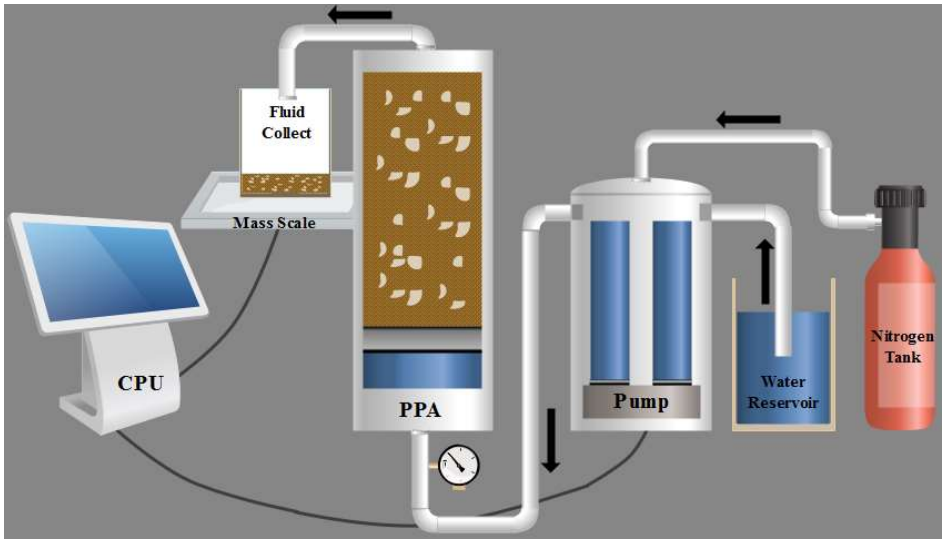

Figure 14: High Pressure Testing Schematic

The modified apparatus was operated by using DI water as the hydraulic fluid within the pump. Nitrogen was used as the operating gas to control the valves during pumping. Fluid would be received through a water reservoir into the pump and displaced through the tubing into the

apparatus. The mud sample and hydraulic fluid would be separated by a piston inside the testing apparatus to ensure quality of the mud. At the top of the testing cell a spacer was placed to ensure a proper gap was established between the fracture disc and the exit port. This ensured the pressure acting on the cylinder was also being transferred across the entire fracture slot and not just the flow port. The testing fluid containing the particulates would pumped across the fracture disc until a seal was formed. Fluid that escaped past the fracture disc would flow up through the flow-out tubing and exit into a container that was placed on the mass scale to enable mass measurements. Figure 15 shows a visual representation of the apparatus utilized for the high pressure experiments.

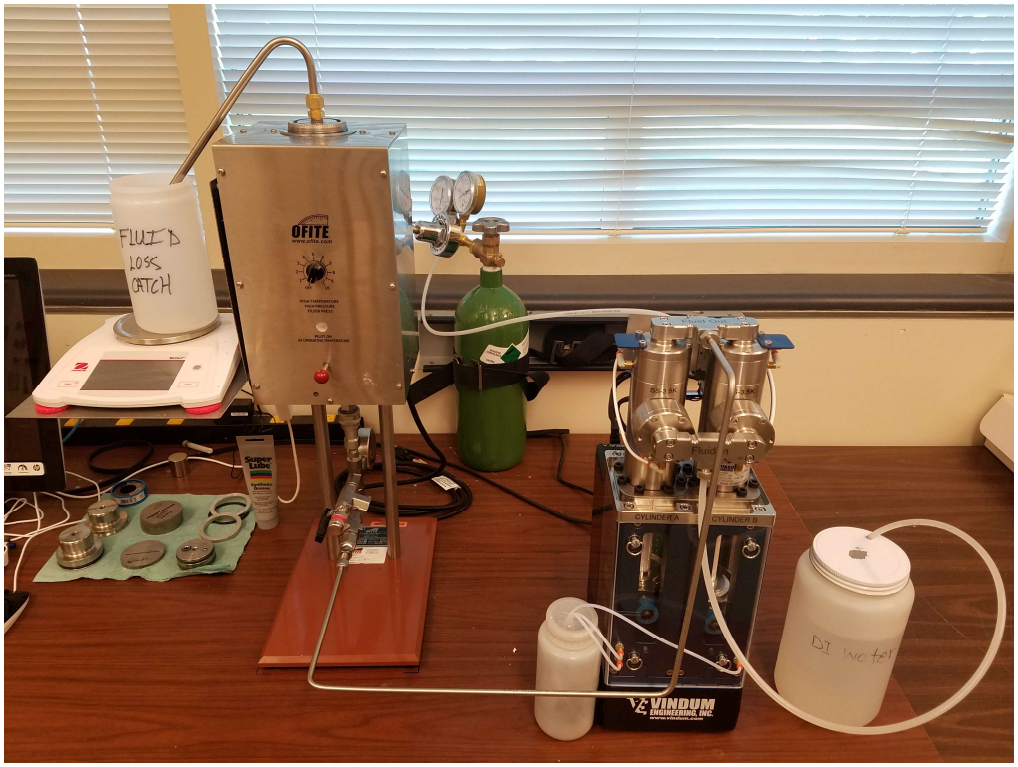

Figure 15: High Pressure Testing Apparatus

The exit tubing was open to the atmosphere so the pump pressure was theoretically the differential pressure, not considering minimal frictional losses in the system. The angled flow-out tubing had a capacity of 12 ml which was taken into account during the evaluation process in

regards to fluid loss. All testing was done under a mass balance environment and analysis was conducted accordingly.

3.2.2 Differential Pressure Selection

Various differential pressures have been used in the past to evaluate LCM and their ability to withstand pressures incurred during drilling operations. Previous studies have taken a differential pressure of 500 psi to be an acceptable pressure to consider LCM performance as sufficient. For this research, a differential pressure of 1200 psi was calculated as an acceptable pressure to be encountered during operations. This differential pressure is what was selected to test the LCM and nanoparticles to while proceeding with the experiments. This pressure was determined based on a common drilling scenario that can occur in modern horizontal drilling operations. The rock mechanics of the formations were not considered, due to the aspect that fracturing stress regimes were not part of the direct scope if this research. Therefore, a simplified scenario based on previous drilling experience in South Texas was created to justify and reason the selected differential pressure. This scenario includes a mono-bore well design drilled to a true vertical depth of 12,500 ft. It is assumed that lost circulation will occur in a depleted, weak zone at a depth of 7,000 ft while drilling with a 10 ppg mud. Considering hydrostatic pressure of that mud at the point of lost circulation, the depleted zone would have had to take on fluid at a pressure of 3,640 psi. At this point, drilling operations spot an LCM pill that is expected to cure losses and also handle anticipated pressures to be incurred while drilling ahead. In order to reach total measured depth, the drilling operations must utilize a 13.5 ppg mud for the entirety of the lateral. During this time, the zone that took on losses earlier with a 10 ppg mud is now realizing a 13.5 ppg mud for the remaining of the operation. This mud weight at the 7,000 ft loss zone corresponds to a hydrostatic pressure of 4,914 psi. Figure 16 provides a crude visual aid for the lost circulation scenario.

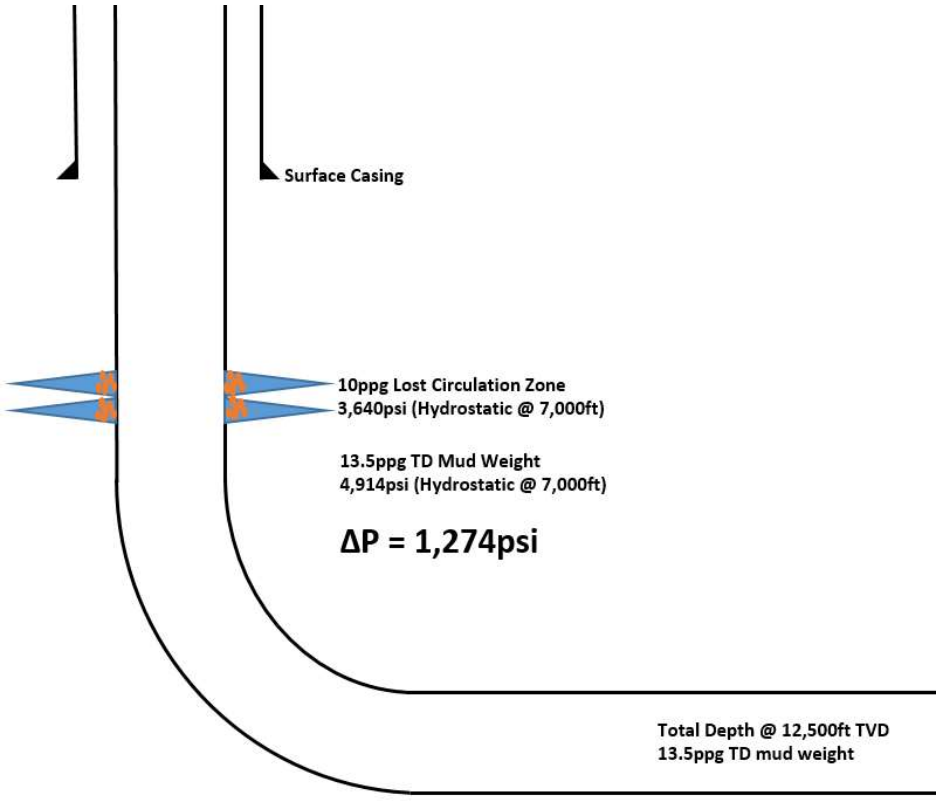

Figure 16: Lost circulation scenario for differential pressure selection

The difference between this pressure and the pressure that corresponded to the lost circulation event is 1,274 psi. This is the pressure that the LCM seal will not only encounter, but will have to withstand until cementing operations are finished securing the well. It should be noted that even though this scenario was more so assumed, the conditions of this drilling environment are rather conservative in terms of total depth (TD) mud weight and depths. It is this scenario and more importantly this pressure that is determined as the testing differential pressure for this research.

3.2.3 Testing Procedure

The testing procedure for the high-pressure experiments was developed specifically for the research objectives. A methodical approach to priming the pump and prepping the fluid was established to ensure accuracy and consistency of the results. These methods were better recognized and further developed over the course of fabricating the apparatus. Outside of the

specifications of each piece of equipment, a set testing procedure was developed after the design was completed and familiarity was established through preliminary tests.

Initially, 350 ml of base mud was measured out and prepped to be re-mixed for hydration purposes. The testing volume of 350 ml of base fluid was used to simplify the LCM measurements, seeing as one gram of lost circulation material is equivalent to one pound per barrel. During this time the required amount of LCM material and nanoparticles, if applicable, were weighed out and set to the side in order to be added to the base mud. While the mud was rehydrating, the piston was placed in the apparatus and fluid was pumped through the bleed port to ensure air was removed from the system. The bleed port was then close and 45 ml of fluid was pumped to move the piston upward and ensure the piston seals were still sufficient. The 45 ml of fluid was established to ensure that when the LCM mixture was placed in the testing cylinder the fluid level would be right at the tapered disc. This eliminates the air gap at the top of the cylinder and enables immediate testing of the fluid against the tapered disc. The LCM is then added to the base mud and is mixed for one minute to ensure proper distribution of the particles. During this time the top O-ring and spacer is added to the upper portion of the cylinder. The mud is then added to the testing apparatus and the tapered disc is placed on top of the spacer ring. The top seal cap and flow-out tubing is then secured on top of the cylinder. At this time testing is ready to commence.

A specific pumping schedule was established to ensure the desired results of evaluating the sealing integrity of each seal as it encounters the established differential pressure. Initially testing commenced by pumping at a constant rate of 25 cc/min until the differential pressure of 1,200 psi was reached. The moment this pressure is reached the pumped shuts down and pressure is monitored for five minutes. After the five-minute interval, pumping resumes at a constant pressure in increments of 100 psi to ensure the pressure does not drastically exceed the differential pressure. Once the differential pressure is re-established, constant pressure of 1,200

psi is applied for five minutes. After the five-minute interval the pump stops once again and pressure is monitored. Figure 17 shows a graphical representation of the pressure profile for each test for visual purposes only.

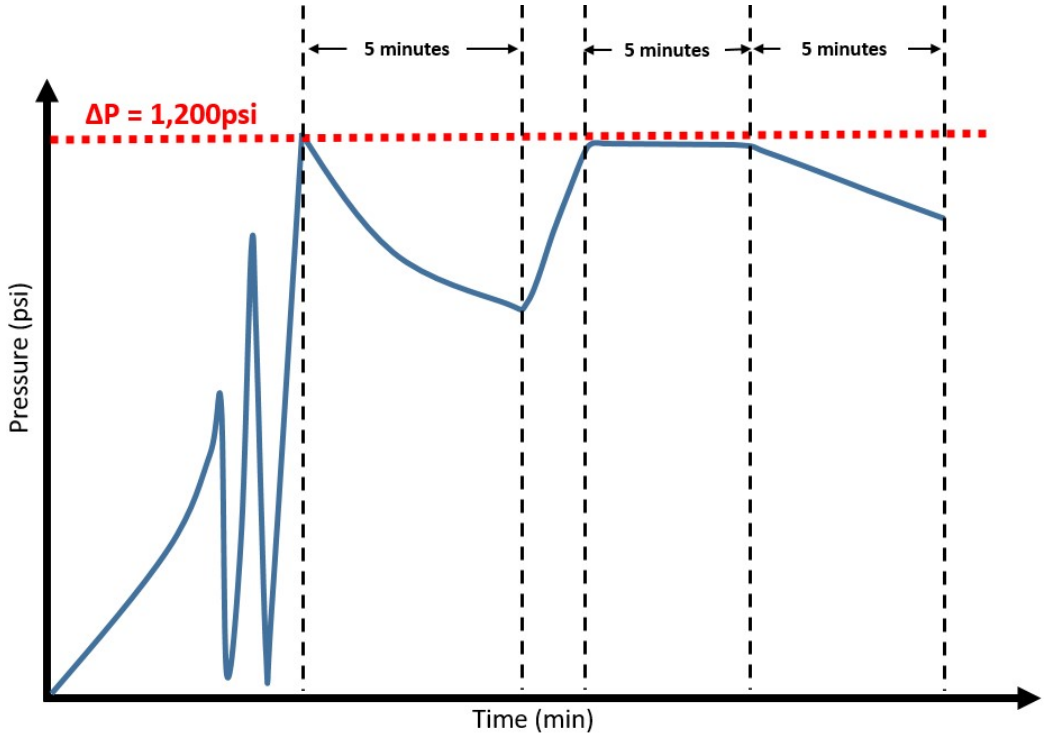

Figure 17: Typical pressure profile for high pressure testing

Cumulative volume, rate and mass are all be monitored during the entirety of the pumping process. The initial pumping schedule of 25 cc/min had a maximum limitation of how much volume can be pumped without seeing a sealing pressure of 1,200 psi. This limit was set at 300 cc and was established as a testing criteria in regards to timely placement of the LCM, as well as a safety precaution. (Note: The Standard Operating Procedure can be found in the Appendices)

3.2.4 Base Fluid Preparation

The base fluid used in the tests was chosen based on previous experiments. The mud formulation was a 7% wt bentonite water based mud (WBM). This mud was chosen to ensure all other effects

of weighting materials and lubricity materials were not affecting the results. Table 2 lists the values obtained for the mud measurements once the mud was sheared and rehydrated.

Mud Type	Mud Weight g/cc (ppg)	Plastic Viscosity (cP)	Yield Point ($lbf/100ft^2$)
Water Based Mud	1.05 (8.8)	14	35

Table 2: Rheological properties of the bentonite mud for high pressure testing

The mud was mass mixed every three days to ensure the rheological properties stayed consistent. This time period is further explained within the rheology section of this chapter. During mixing, the batches were prepared by individually mixing 35 grams of bentonite in 465 ml of water using a Hamilton Beach mixer. Each sample was mixed for five minutes to ensure proper mixing and to initiate the hydration process. After batch mixing was concluded, the mass batches were allowed to sit for 24 hours to ensure full hydration of the bentonite was established within the mud. This was done due to pH of the mixing water, which was measured at 6.8. Considering bentonite mud requires a pH of nearly 8.0, extra time was added to ensure proper hydration had occurred. To safeguard proper monitoring of the mud mixing process within the lab, a logbook was scribed to ensure all members associated with other laboratory equipment were aware of the age of the mud. Mud weight and rheology was frequently checked to maintain quality control.

3.2.5 Rheology Evaluation and Settling Tests

An extensive rheology study was conducted on the base mud for a number of reasons. First, considering the base mud was represented from previous tests dating as far back as the 1980's from the study Sandia Labs concluded, consistency in rheology was needed to ensure proper results were obtained from these tests. Moreover, this particular study conducted by Sandia Labs concluded that a large variance in gel strengths was observed for the bentonite mud. Considering the newly developed apparatus is pumping in a static environment against the direction of gravity

it was critical that the proper gels and yield strengths were established prior to testing. In doing this, a number of tests were piloted to investigate these effects.

As previously stated, the bentonite mud was mass mixed and allowed to age no longer than three days. To ensure that the mud quality was consistent over these three days an extensive rheology study was piloted. This evaluation studied the effect that hydration had on the quality of the bentonite mud, as well as how un-sheared, freshly mixed, and sheared, re-mixed in the blender, mud increases the rheology of the mud. All tests were conducted using a standard FANN 35 viscometer. The evaluation began by mass mixing two gallons of bentonite mud and testing for rheology immediately after mixing without allowing the bentonite to hydrate. Plastic viscosity, yield point and gel strengths were all measured immediately after mixing. The gel strengths were measured at 10 s, 30 s, 1 m, 5 m, 10 m, 30 m, 1 hr, 2 hr and 24 hr. Following the 24 hr period, rheology and a 5-minute gel strength was conducted without re-shearing the mud. The mud was then allowed to age for three days and tests for rheology were conducted on day two and day three. Each set of tests included testing the rheology and gel strengths, specifically at 10s, 30s, 5m and 30m. Tests were conducted on un-sheared and sheared mud and the effect of shearing the mud and allowing the mud to rehydrate was investigated. Tests were repeated to ensure quality of results.

After the rheology analysis was finished, a settling test was conducted to ensure the particles would not settle to the bottom of the testing apparatus during testing. A qualitative settling test was conducted using a clear 600 ml beaker. A 350 ml mixture of 50 ppb, 1000 micron sized graphite was used for the evaluation. The mixture was placed and video recorded for a duration of 30 minutes. Still-shot pictures were taken in 5-minute intervals for documentation purposes. The 30 minute interval was established by preliminary tests conducted in the newly developed apparatus. It was determined 30 minutes was a sufficient amount of time considering the maximum amount of volume restricted from being pumped was 300 ml.

3.2.6 Lost Circulation Material

The lost circulation material and tapered discs used in these experiments were selected based on previous tests conducted Alsaba et al. 2014. Considering the newly developed apparatus, a comparison of previous LCM performance was needed for proper evaluation of the materials. This allowed the previously concluded sealing pressures under their respective disc sizes to be evenly matched. All LCM mixtures were single LCM treatments and did not contain a combination of different type of LCMs. Graphite (G1), nut shells (NS1) and sized calcium carbonate (SCC3) were the LCMs used for the experiments. The treatments contained various sizes of the same material to satisfy the particle size distribution that was previously tested. In all experiments, various concentrations and disc sizes were used for evaluation purposes. Table 3 shows the particle size distribution for each of the mixtures and their respective concentrations.

Particle Size Distribution (microns)						
LCM Blend	Total Conc. (ppb)	D10	D25	D50	D75	D90
G 1	15	60	85	320	800	1300
G 1	50	60	95	340	800	1300
NS 1	15	180	400	1000	1600	2000
NS 1	50	180	400	1000	1600	2400
SCC 3	50	250	360	680	950	1200

Table 3: Particle size distributions for LCM mixtures

A total of 11 tests were conducted in regards to LCM type, concentration and disc size combinations with eight out of the 11 combinations tested for repeatability. An additional test using G1 at a higher disc size was conducted to evaluate sealing in a larger fracture size. Table 4

lists the testing matrix with the LCM combinations and their respective concentrations, fracture disc size, and previously reported sealing pressures and fluid loss values.

Test #	LCM Blend	Repeated	Concentration (ppb)	Disc Size (microns)	Slotted Disc	Previous Sealing Pressure (psi)	Previous Avg. FL (ml/cycle)
1	G 1	No	15	1000	TS1	414	8.3
2	G 1	Yes	50	1000	TS1	449	7.6
3	G 1	No	50	1500	TS2	N/A	N/A
4	NS 1	Yes	15	1500	TS2	1754	11.8
5	NS 1	Yes	15	1000	TS1	984	3.5
6	NS 1	Yes	15	2000	TS4	441	24.5
7	NS 1	Yes	50	1000	TS1	2202	2
8	NS 1	Yes	50	1500	TS2	2027	19.2
9	NS 1	Yes	50	2000	TS4	755	18.3
10	SCC 3	Yes	50	1000	TS1	589	13.3
11	SCC 3	No	50	1500	TS2	162	31.3

Table 4: High Pressure Testing Matrix for LCM Mixtures

These tests were evaluated to study the newly developed apparatus and to also compare sealing pressures and fluid loss with previously documented results. Following the high pressure LCM mixture evaluations two out of the eight LCM combinations were chosen to be tested utilizing nanoparticles.

3.2.7 Nanoparticle Selection

Two types of nanoparticles were chosen for high pressure testing. The low-pressure fluid loss testing using the in-house generated nanoparticles were analyzed and chosen accordingly. The mechanically grinded barite nanoparticles with a nominal size of 62 nm were chosen to be utilized in the high pressure testing. It was determined that the addition of mechanical nanoparticles into the LCM mixture would allow for an easier mixing process considering the nanoparticles are generated in a dry grinding system. Furthermore, the chemical nanoparticles are generated by creating an emulsion as a precursor prior to the colloidal generation of the nanoparticles. This was not seen as an ideal process due to the time needed to mix one batch of chemically nano-based WBM and also due to the addition of further additives in the system that could hinder the fundamental analysis of the LCM and nanoparticles.

Fumed silica nanoparticles were the second type of nanoparticles chosen for high pressure testing. These nanoparticles were provided by SIGMA Life Science Co. and had a nominal size of 200-300 nm. These nanoparticles were selected due to the differing average particle size, in comparison to the mechanically generated barite nanoparticles. Furthermore, these nanoparticles have been well documented in the literature for reducing fluid loss and increasing wellbore stability. For this reason silica nanoparticles were deemed as a prime candidate for high pressure testing.

Both type of nanoparticles were used in combination with the previously tested LCM mixtures. These LCM mixtures were tested in the high pressure apparatus and then tested with the addition of nanoparticles. Concentrations of 1% wt and 3% wt of both types of nanoparticles were used in the experiments. NS1 and SCC3 were selected as candidates for high pressure testing containing nanoparticles. A concentration of 50 ppb of each LCM was used and tested individually utilizing

a 1500 micron tapered disc. Table 5 details the testing matrix for the nanoparticle and LCM high pressure testing.

Test #	LCM Blend	NP Type	NP Conc. (wt. %)	Repeated	LCM Conc. (ppb)	Disc Size (microns)
1	NS 1	Barite	1%	No	50	1500
2	NS 1	Barite	3%	Yes	50	1500
3	SCC 3	Barite	1%	No	50	1500
4	SCC 3	Barite	3%	No	50	1500
5	NS 1	Silica	1%	No	50	1500
6	NS 1	Silica	3%	No	50	1500
7	SCC 3	Silica	1%	Yes	50	1500
8	SCC 3	Silica	3%	No	50	1500

Table 5: Nanoparticle high pressure testing matrix

A total number of eight assessments were conducted for the nanoparticle high pressure testing with two of the combinations tested for repeatability. The LCM combinations were chosen based on the previously tested high pressure results. Due to the responses encountered in the high pressure testing, these LCM combinations were selected to be used in conjunction with nanoparticles to realize if additional benefits were seen with using either type of nanoparticle.

CHAPTER IV

FINDINGS

After low pressure testing concluded the mechanically generated nanoparticles were selected for high pressure testing. Furthermore, along with the barite nanoparticles, fumed silica nanoparticles were chosen to be included with the high pressure testing matrix. A previously tested set of LCM combinations were chosen for high pressure testing. Two combinations were chosen to be tested with both types of nanoparticles. The newly developed apparatus allowed for a different form of analysis than what has previously been done in recent years. The sections herein detail the findings and results associated with both sets of tests.

4.1 LOW PRESSURE RESULTS

Both types of nanoparticles were tested in a WBM at concentrations of 1.5% wt and 3% wt on 2-5 micron filter paper. Chemical nanoparticles proved to be the best at reducing fluid loss, therefore, another set of tests were conducted using a different WBM with varying rheological properties on 2-5 micron filter paper. Chemical nanoparticles were also tested on 5-10 micron paper to see if further fluid loss reduction was witnessed at a higher pore throat size. These nanoparticles were tested at concentrations of 1% wt, 2% wt, 3% wt and 4% wt. Overall, the chemical nanoparticles proved to reduce the fluid filtrate of the WBM more effectively than the mechanical nanoparticles. Although the chemical nanoparticles performed better than the mechanical, the process in which these nanoparticles were synthesized caused the selection

of mechanical nanoparticles to be more attractive for high pressure testing. The process of generating chemical nanoparticles is not only time consuming, but also requires an emulsion of oil and water, which was deemed unattractive in regards to the rheology. The goal was to select a nanoparticle that does not hinder the mud system in order to purely analyze LCM and nanoparticles. For this reason, silica nanoparticles were also introduced into the high pressure testing matrix. The following describes the description of each type of barite nanoparticle, as well as the accompanying fluid loss results.

4.1.1 Barite Nanoparticle Classification

Classifications of each type of nanoparticle were developed in order to better understand and conclude the fluid loss results. In doing so, one form of classifying the particles was to look at the size distribution of the nanoparticles. To help aid in this process a dynamic light scattering (DLS) apparatus was used to determine the particle size distribution and size variance of the particles. Figure 18 shows the size distribution for the chemically generated nanoparticles.

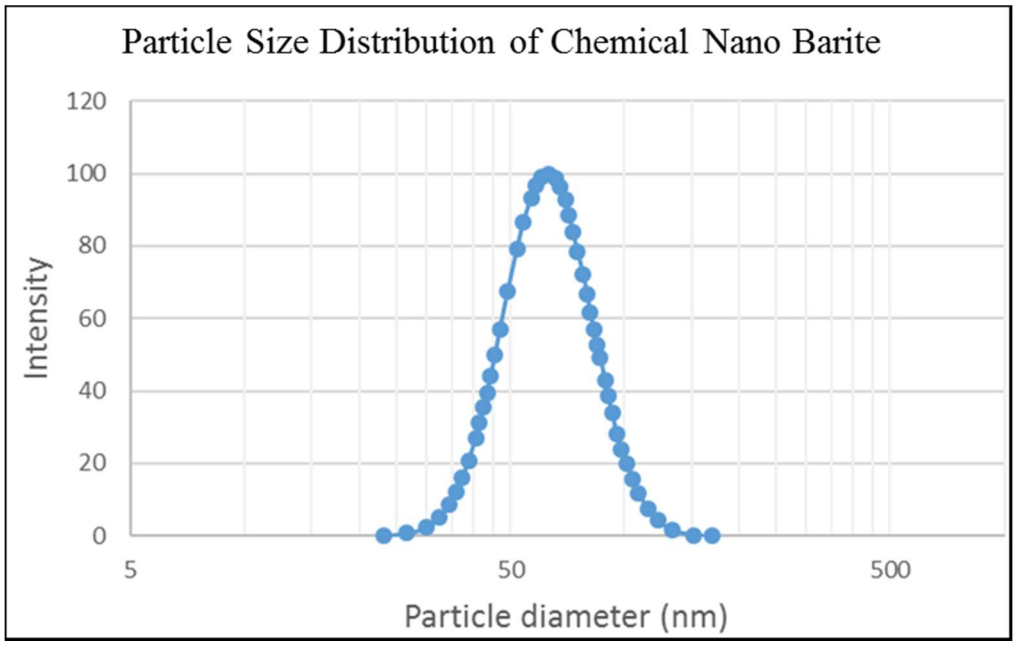

Figure 18: Particle Size Distribution of Chemically Generated Nanoparticles

It can be seen from the DLS analysis that the chemically generated nanoparticles have a nominal particle size of roughly 62 nm. The variance in this distribution is represented by the thinness of the normal distribution curve. This represents the other sizes of particles associated within the sample. It can be seen that the chemically generated nanoparticles have a small variance of size distribution as it ranges from 30 nm to 125 nm on a normal distribution. For comparison, this same evaluation was conducted for mechanically generated nanoparticles. Figure 19 show the size distribution for the mechanically generated nanoparticles.

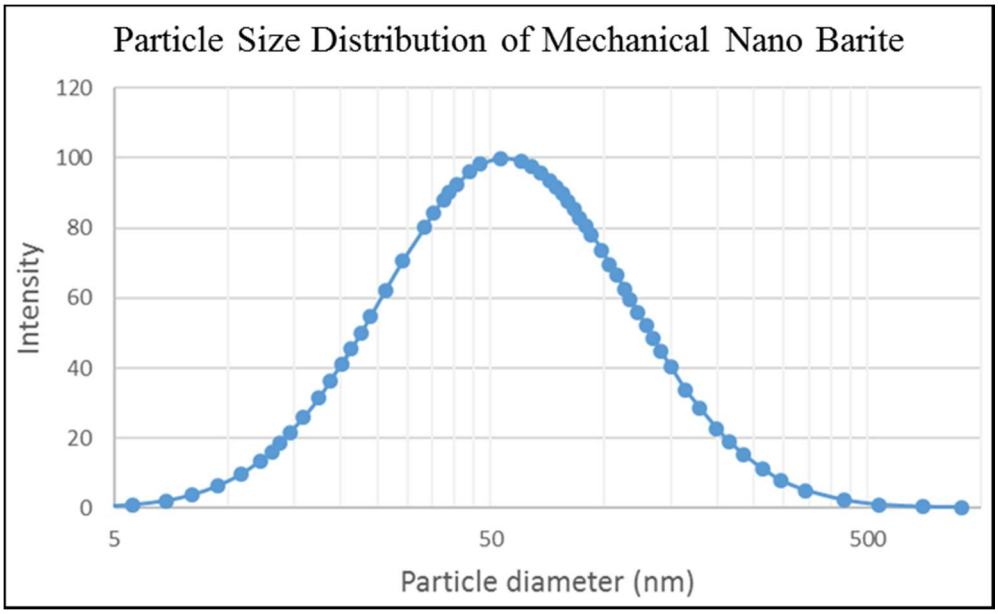

Figure 19: Particle Size Distribution of Mechanically Generated Nanoparticles

In comparison to the chemically generated nanoparticles, it can be seen from the DLS analyzer that the mechanically generated nanoparticles have relatively the same nominal particle size diameter. Although the diameters are relatively the same, the size variance in the mechanical nanoparticles is much larger. This can be seen from the wider form of the normal distribution curve consisting of particle sizes ranging from 10 nm to 300 nm.

TEM imaging was also coupled with DLS analysis to infer the particle size, as well as the shape and sorting of the particles. This enabled the evaluation to study how the nanoparticles interacted

with each other in solution. The question of agglomeration was raised while synthesizing the nanoparticles, especially with the mechanical nanoparticles. Figure 20 shows an image showing the mechanical nanoparticles in solution.

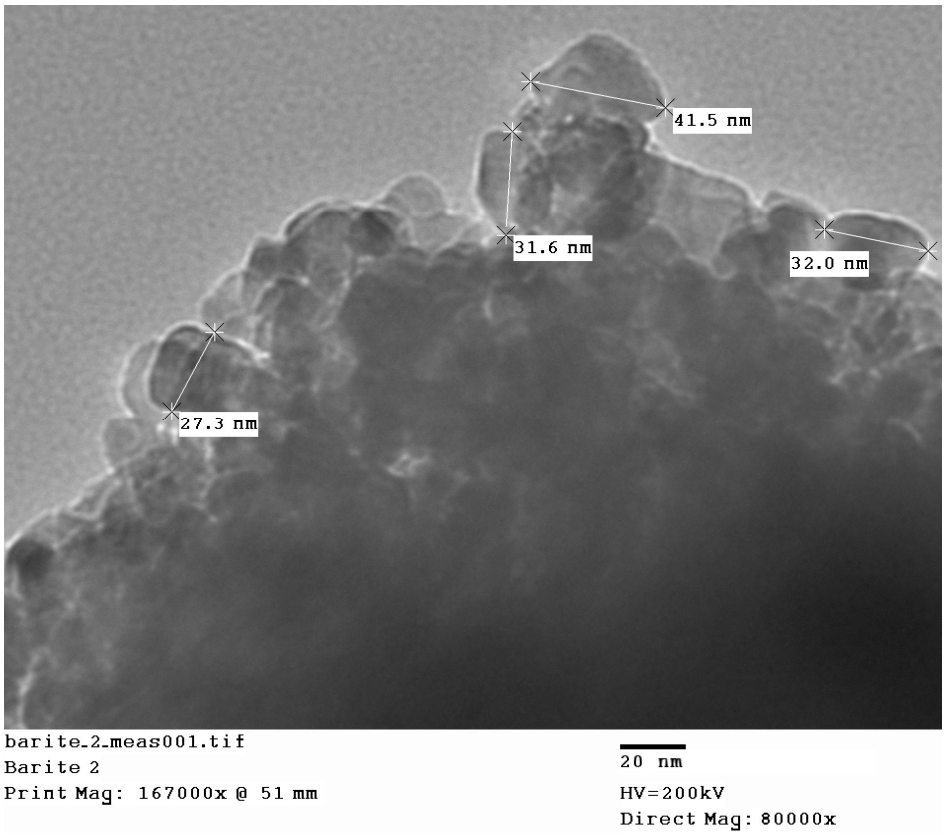

Figure 20: TEM Image of Mechanical Nanoparticles

It can be seen from the image that small particles less than 100 nm are present. These particles have shown to have an affinity towards other particles and agglomeration has occurred. This agglomeration increases the distribution of the particle sizes in relation to the DLS analysis. This is partly due to the preparation method of the particles and as well as the particle affinity after being placed in solution. After mixing, it was noted that the particles had a high tendency to agglomerate to each other. This issue was not mitigated during the low-pressure testing for the sake of consistency, although other methods of post mixing storing was established for high pressure testing. These methods included aggravated the particles through a sieve to ensure the

particles were re-separated. The shape of these particles can also be noted to be more angular, but considering the size and number of particles this was not deemed as critical. The same analysis was conducted on the chemically generated nanoparticles. Figure 21 shows an image showing the chemical nanoparticles in solution.

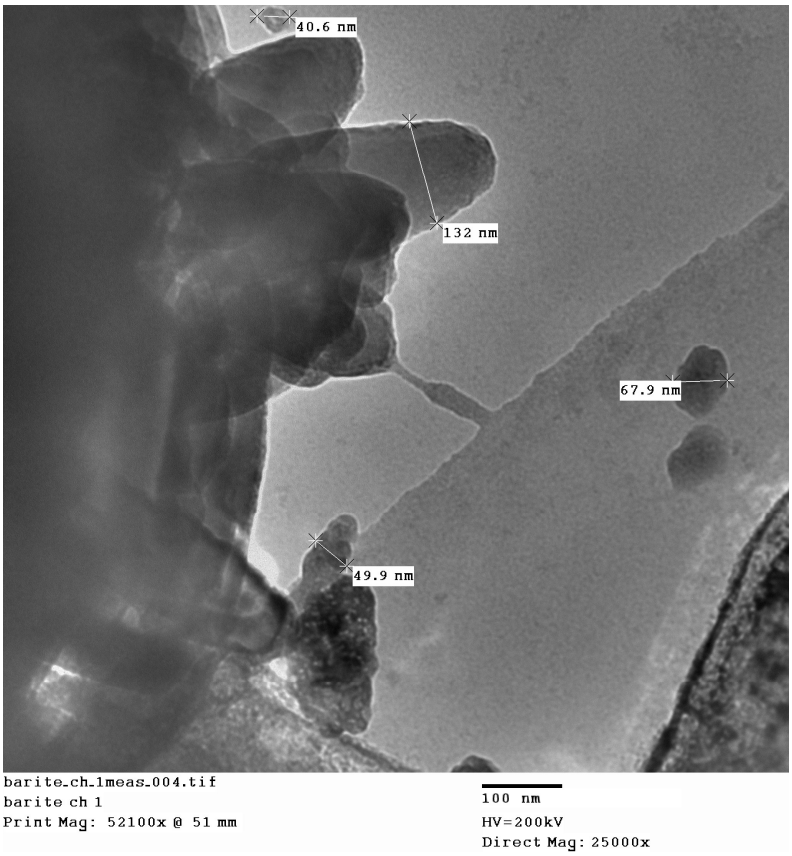

Figure 21: TEM Image of Chemical Nanoparticles

As for the chemical nanoparticles, roughly the same size distribution can be seen from the imaging. These particles did not agglomerate as severely, in comparison to the mechanical nanoparticles. This contributed to the tighter variance in particle size distribution in regards to the DLS analysis. It can also be noted that these particles were well rounded in comparison to the mechanical nanoparticles. These methods of describing the nanoparticles provided great insight in terms of the low pressure evaluations.

4.1.2 Nanoparticle Fluid Loss Results

Fluid loss results were achieved for all concentrations and nanoparticle type. An identified trend was realized between the two types of barite nanoparticles at each concentration. Each fluid loss test was compared to the base case fluid loss test. Figure 22 below shows the fluid loss results for a filter paper size range of 2-5 micron for mechanically generated nanoparticles at 1.5% wt and 3% wt concentration.

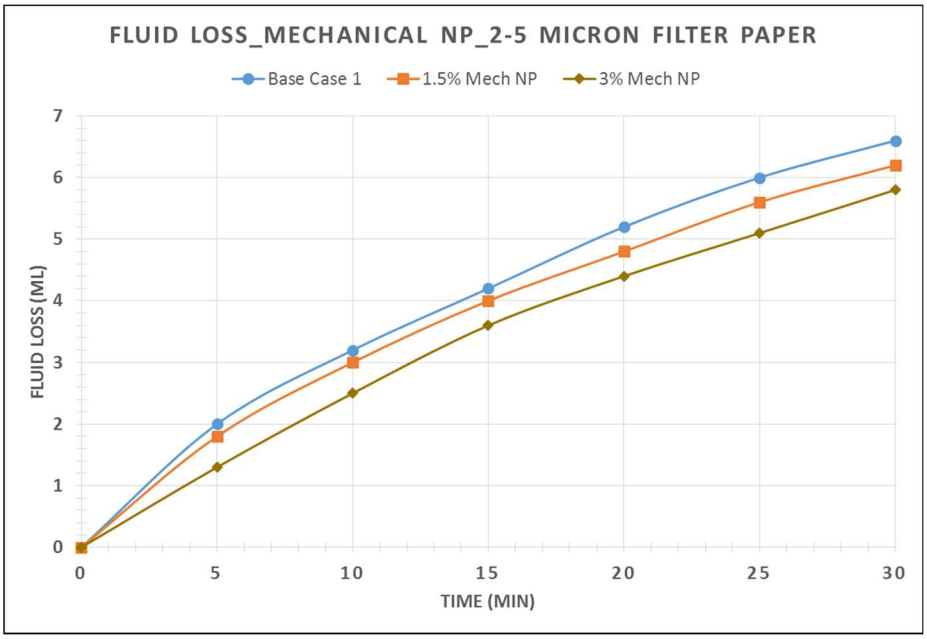

Figure 22: Mechanical Nanoparticles Fluid Loss for 2-5 micron filter paper

The base case fluid loss was measured to be 6.6 mL over the 30-minute interval. It can be seen from Figure 22 that mechanical nanoparticles have the ability to reduce the fluid filtrate in the water based mud. By using 1.5% wt mechanical nanoparticles the fluid filtrate in the WBM system was reduced from 6.6mL to 6.2 mL. Furthermore, a fluid filtrate reduction from 6.6 mL to 5.8 mL was realized when using 3% wt mechanical nanoparticles. The same base case value was used to analyze the efficiency of chemical nanoparticles on the reduction of fluid filtrate. Figure 23 below shows the fluid loss results for the chemically synthesized barite nanoparticles.

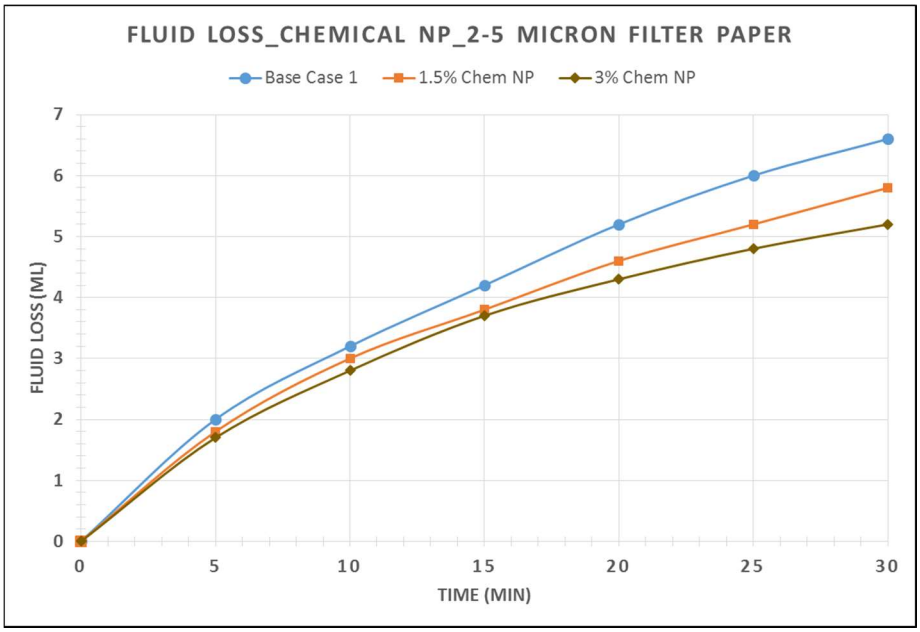

Figure 23: Chemical Nanoparticles Fluid Loss for 2-5 micron filter paper

Figure 23 illustrates that chemical nanoparticles also have the ability to reduce the fluid filtrate in a WBM. Comparing the reduction in fluid loss to the base case of 6.2 mL, chemically generated nanoparticles at 1.5% wt and 3% wt concentration reduce the fluid loss to 5.8 mL and 5.2 mL, respectively. Table 6 condenses the results obtained within the fluid loss tests for the 2-5 micron filter paper sizes.

Test Fluid	Fluid Loss (mL)	% Reduction
Base Case	6.6	0%
1.5% Mechanical	6.2	6%
3.0% Mechanical	5.8	12%
1.5% Chemical	5.8	12%
3.0% Chemical	5.2	21%

Table 6: Fluid Loss Results for 2-5 micron filter paper

A comparison of the two types of nanoparticles shows that the chemical nanoparticles are more efficient at reducing the fluid loss than the mechanical nanoparticles. This could be a result of a packing difference between the two types of synthesized nanoparticles due the size variance and shape of particles. While the cake is being formed, these differences in size and shape can cause packing to happen differently for the two types of nanoparticles. Table 7 summarizes the performance of each type of nanoparticle through a direct comparison of fluid loss reduction.

Nanoparticle Concentration	Fluid Loss Reduction Ratio ($\%_{Chemical}/\%_{Mechanical}$)
1.5%	2
3.0%	1.75

Table 7: Fluid Loss Reduction Comparison for 2-5 micron filter paper (%chem/%mech)

For the 2-5 micron filter paper size, it is clear that the chemical nanoparticles are more effective at reducing the fluid loss than the mechanical nanoparticles. At a concentration of 1.5% barite nanoparticles, the chemically generated nanoparticles are two times more effective than the mechanically generated nanoparticles. Furthermore, for 3.0% concentration, chemically synthesized nanoparticles are 1.75 times more effect than mechanical.

Knowing that chemical nanoparticles perform better at reducing fluid loss than mechanical nanoparticles, further testing was conducted to better understand the performance of the chemically generated nanoparticles. Tests were conducted from 0-4% wt concentration of nanoparticles in 1% wt increments to evaluate the effect of concentration. Furthermore, the magnitude of fluid loss reduction was also studied. Figure 24 shows the fluid loss results for chemical nanoparticles at the various concentrations.

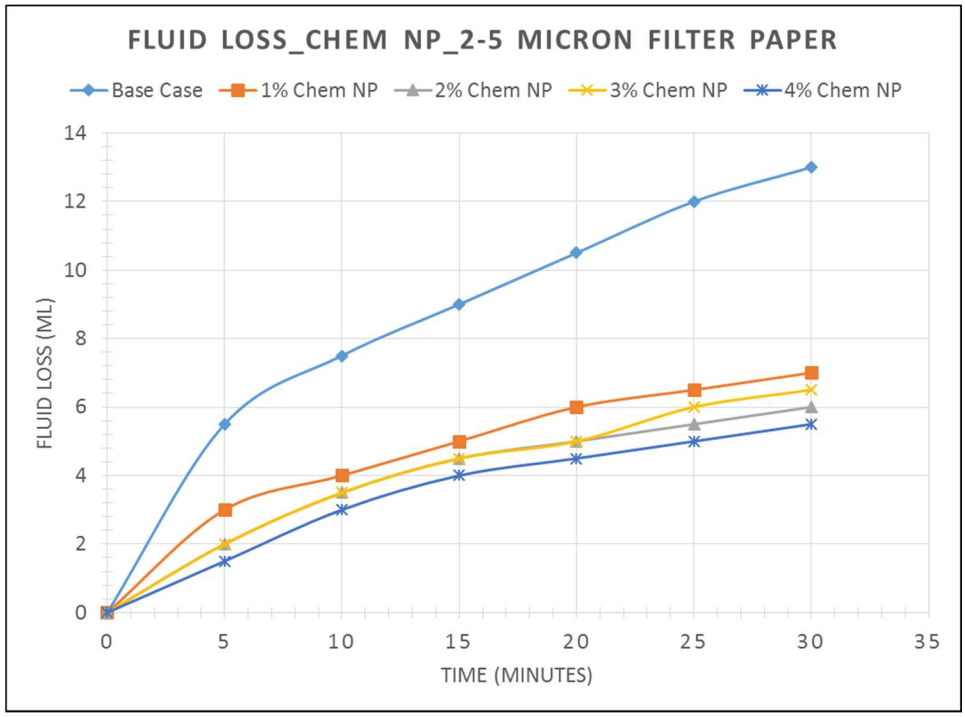

Figure 24: Chemical fluid loss for 2-5 micron filter paper with varying concentration

A significant decrease in fluid loss was recognized using chemical nanoparticles for this WBM system. Initial fluid loss for the base case was 13 mL. The addition of 1% wt chemical barite nanoparticles decreased the fluid loss by 46% to 7 mL. This reduction in fluid loss was larger than what was realized in comparing mechanical and chemical nanoparticles. Table 8 summarizes the results for the fluid loss tests at 2-5 micron filter paper over the various concentrations.

Test Fluid	Fluid Loss (mL)	Reduction %
Base Case	13	0%
1% Chemical	7	46%
2% Chemical	6	54%
3% Chemical	6.5	50%
4% Chemical	5.5	58%

Table 8: Fluid Loss results for chemical nanoparticles at varying concentration for 2-5 micron

It can be seen that fluid loss is drastically reduced with the introduction of 1% wt chemical nanoparticles. A continued reduction in fluid loss is witnessed with further addition of chemical barite nanoparticles. It should be noted that at 2% wt chemical nanoparticles, the fluid loss reduction is 54%, followed by a 50% reduction in fluid filtrate using 3% wt nanoparticles. This additional 1% wt concentration from 2% wt to 3% wt nanoparticles does not further reduce the fluid loss. It can be concluded that the optimum concentration of chemical nanoparticles is roughly 2% wt for this WBM system.

Further testing of fluid loss was conducted on a larger filter paper size. This test was conducted using the same chemical nanoparticles as the previous tests. The goal was to see how fluid filtrate was reduced when using chemical barite nanoparticles on a larger permeable media. Furthermore, the same evaluation of optimum concentration was conducted, as done previously. The tests were conducted on a filter paper size range 5-10 micron. Figure 25 shows the fluid loss performance of the chemical nanoparticles on the 5-10 micron filter paper.

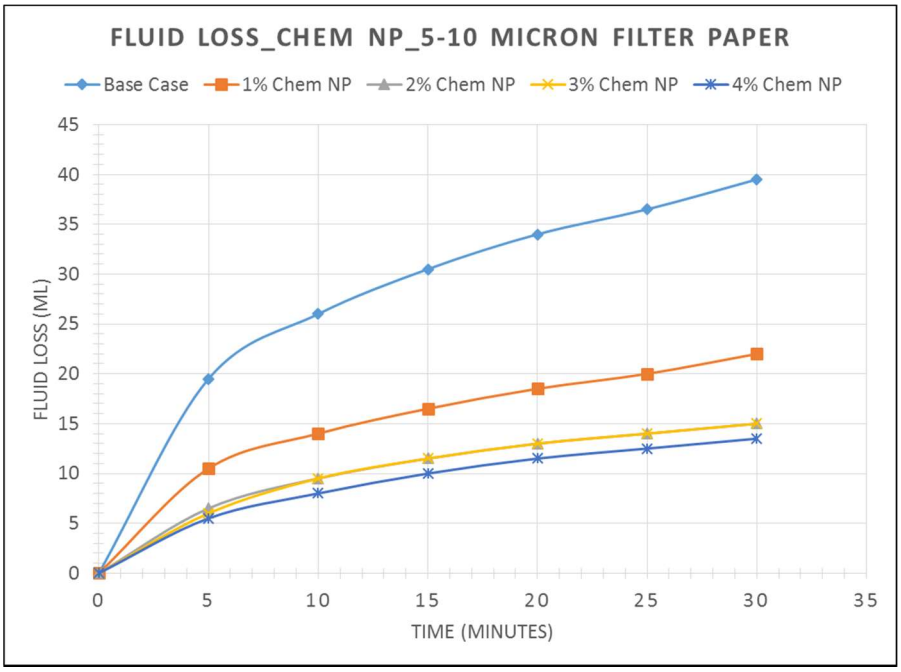

Figure 25: Chemical fluid loss for 5-10 micron filter paper with varying concentration

It should be noted that a larger volume of fluid loss was encountered in the base case. This was expected considering the large median pore throat size in the filter paper that allows for more initial flow before cake build-up. Nonetheless, a similar reduction in fluid filtrate is witnessed when 1% wt chemical nanoparticles is introduced to the WBM. This reduction in fluid filtrate from 39 mL to 22 mL is a 44% reduction, overall. As seen in previous tests, the fluid loss results show a continued decrease in fluid loss with a continued addition of chemical nanoparticles. Table 9 summarizes the results for the fluid loss tests at 5-10 micron filter paper over the various concentrations.

Test Fluid	Fluid Loss (mL)	Reduction %
Base Case	39.5	0%
1% Chemical	22	44%
2% Chemical	15	62%
3% Chemical	15	62%
4% Chemical	13.5	66%

Table 9: Fluid Loss results for chemical nanoparticles at varying concentration for 5-10 micron

Fluid loss is considerably reduced with the introduction of 1% wt chemical nanoparticles. A further reduction in fluid loss is realized with additional chemical barite nanoparticles. It should be noted that at 2% wt chemical nanoparticles, the fluid loss reduction is 62%, followed by the same 62% reduction in fluid filtrate using 3% wt nanoparticles. This additional 1% wt concentration from 2% wt to 3% wt nanoparticles does not further reduce the fluid loss. As in the previous test for 2-5 micron filter paper, it can be determined that the optimum concentration of chemical nanoparticles is 2% wt for this WBM system.

These tests were conducted to prove that in-house prepared nanoparticles have the ability to reduce fluid loss in a WBM. This evaluation not only concludes that nanoparticles have the ability to reduce fluid loss, but that there is also an optimal concentration of nanoparticles in

regards to fluid loss reduction. Furthermore, it can be concluded that both types of nanoparticles have the ability to reduce fluid loss in a low pressure environment. Although the chemical nanoparticles seemed more attractive from a performance outlook, the mechanical nanoparticles were chosen based on the ease of introducing these particles to a WBM system containing LCM. Moreover, fluid loss reduction is not as large with mechanical nanoparticles, but the addition of mechanical nanoparticles did not alter the base mud for high pressure testing. For these reasons, the mechanical nanoparticles were chosen as the testing candidate for high pressure testing. The introduction of silica nanoparticles was also chosen based on similar reasons, as well as the diversity in particle size distribution.

4.2 HIGH PRESSURE RESULTS

High pressure testing consisted of a thorough evaluation of rheology and particle settling tests to ensure the LCM and nanoparticles could withstand the static environment while being pumped. High pressure results concluded a successful evaluation of LCM with nanoparticles was established. Results showed the designed apparatus can successfully analyze sealing processes under constant pressure and constant rate environments. The following sections herein detail the observations during this portion of testing.

4.2.1 Rheology and Settling Evaluation

Rheology of the bentonite WBM was thoroughly evaluated to ensure the quality of the mud was consistent and that the particles that would be placed in the mud would be able to be suspended for the proper amount of time. Consistency in the mud was critical to understand as it is the essential foundation for all testing. It was decided to thoroughly test rheology on the mud as preliminary high pressure tests showed a large variance in pressure transient after sealing (Note: results from these tests can be found in the Appendices). In order to evaluate this variance,

rheology was taken at the time right after mixing and 24 hrs after mixing. Figure 26 shows the results for the rheology measurements taken right after mixing and 24 hours after mixing.

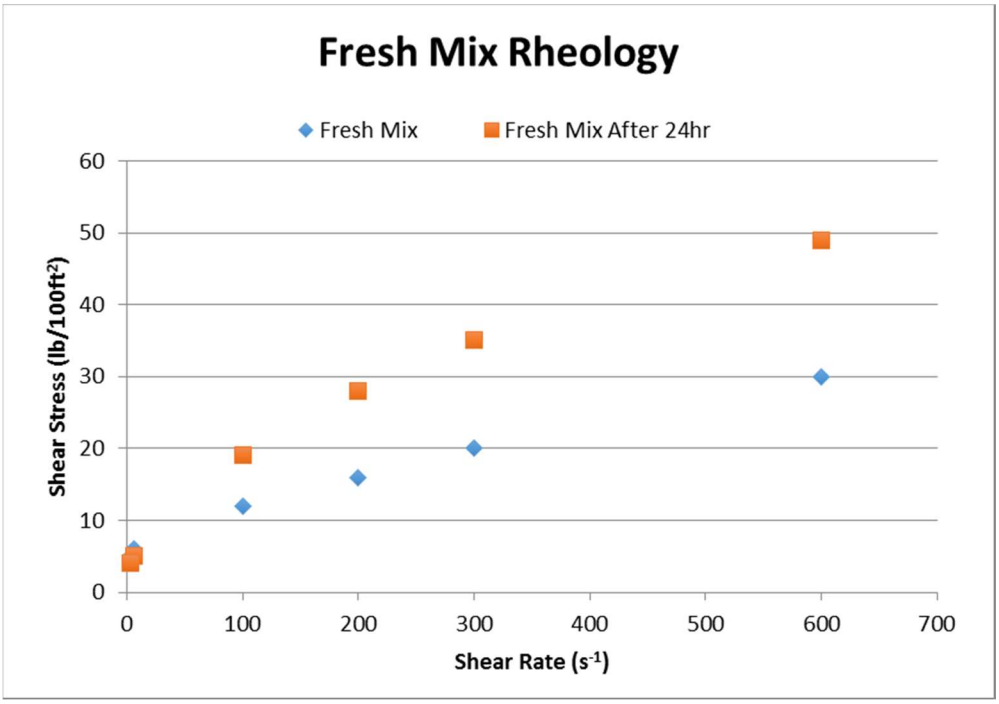

Figure 26: Fresh Mix Bentonite Rheology at 24 hours after mixing

The freshly mixed mud had a PV of 10 cP and an YP of 10 lb/100ft^2 right after mixing. The mud was undisturbed and allowed to rest for 24 hours and measurements were taken once again. After 24 hours of mixing the PV increase to 14 cP and the YP increased to 21 lb/100ft^2. To further understand this effect, gel strengths were taken at the API standard of 10 seconds and 10 minutes, but were also evaluated up to 24 hours. It should be noted that the tests that were repeated, denoted with an "R", were tested separately from the original mud. These repeated tests were of the same mixed batch and also in the same time period of the original mud. These tests were conducted on a separate viscometer to ensure the other tests were not interfered with in regards to the time evaluation. Figure 27 shows the results from the gel strength tests.

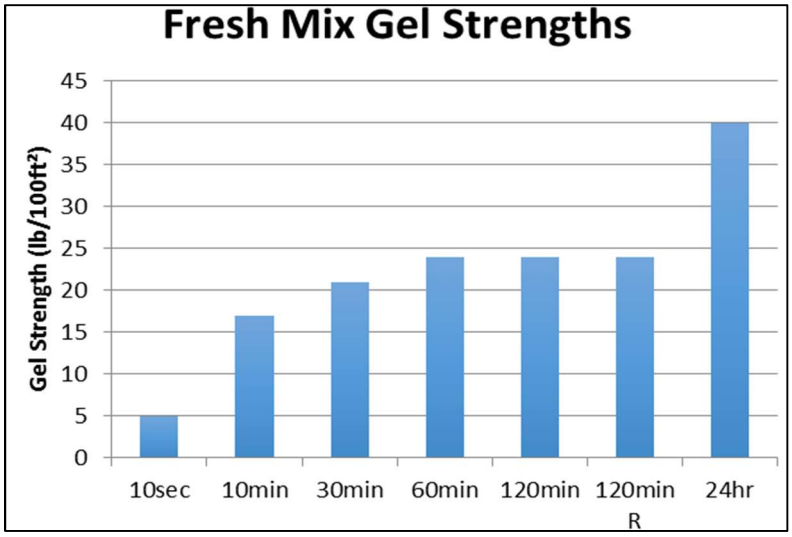

Figure 27: Gel strength results from freshly mixed mud up to 24 hours

It should be noted that pH tests of the mix water concluded that the water was slightly acidic at a pH of 6.4, which adds to the hydration time of the mud. As previously noted, preliminary high pressure tests showed a large variance in transient pressures after sealing. To further investigate this phenomenon, rheology and gel strength tests were conducted at 2 and 3 days after mixing on un-sheared and sheared mud. Figure 28 shows the results of the 10 second gel strength tests.

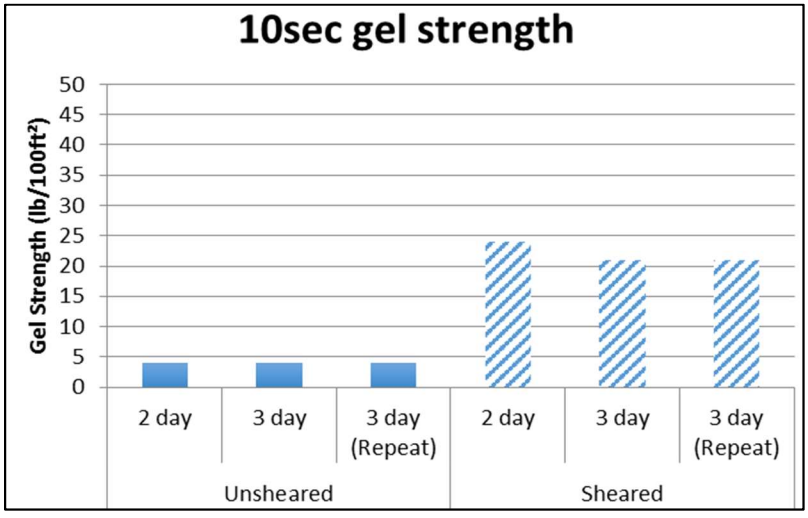

Figure 28: 10 second gel strengths for un-sheared and sheared mud

It can be seen that the mud gains a significant amount of gel strength once the mud is re-mixed, or sheared. This can be seen for 2 and 3 days after mixing. Similar tests were conducted for 30 minute gel strengths. Figure 29 shows the results from the 30 minute gel strength tests.

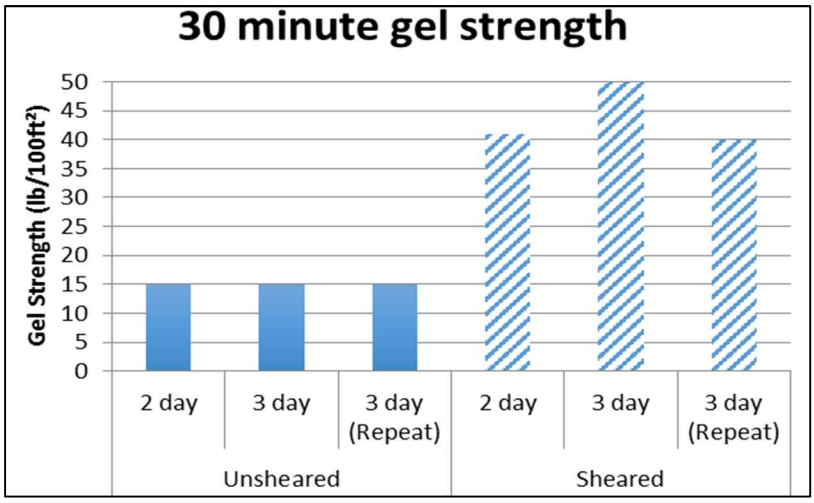

Figure 29: 30-minute gel strengths for un-sheared and sheared mud

Similar results of increased gel strengths can be noted from the 30 minute gel strength tests. Furthermore, rheology was studied at each phase of these gel strength evaluations and were noted as the averages realized during these tests. Figure 30 shows the results from the rheology tests.

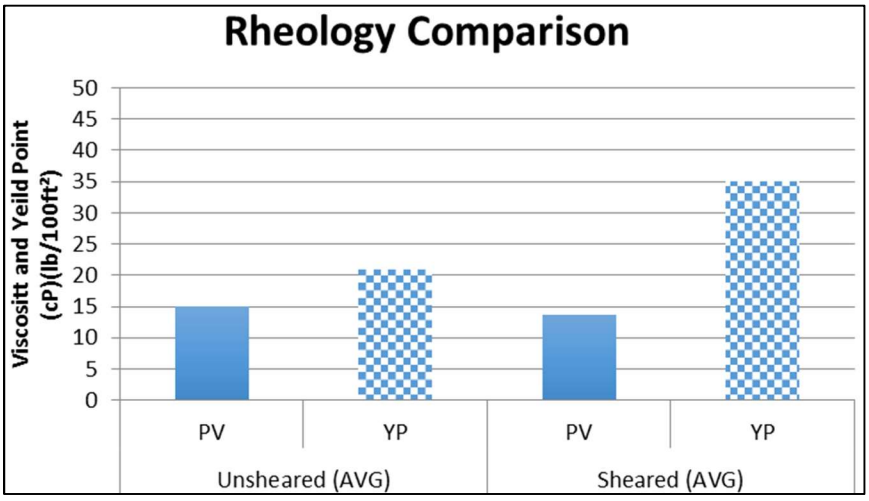

Figure 30: Average rheology during gel strength evaluations

Looking at the rheology findings as a whole it can be concluded that the bentonite mud needs 24 hours to hydrate in order to establish a baseline rheology. Furthermore the mud needs to be re-sheared, or mixed, prior to testing to re-gain its yielding and gel strength characteristics.

Knowing that the mud needs an initial time period for hydration additional tests were conducted to qualitatively analyze the settling of particles within the mud. The test had roughly 350 ml of WBM and particles were placed in a beaker and monitored via video recorder for 30 minutes in 5-minute intervals. This was done using a 50 ppb mixture of 1000 micron graphite (SG=2.3). The 1000 micron was chosen based on the fact that the D50 of all LCM mixtures were no larger than 1000 micron. Figure 31 shows the results of the tests at 0 min, 15 min and 30 min.

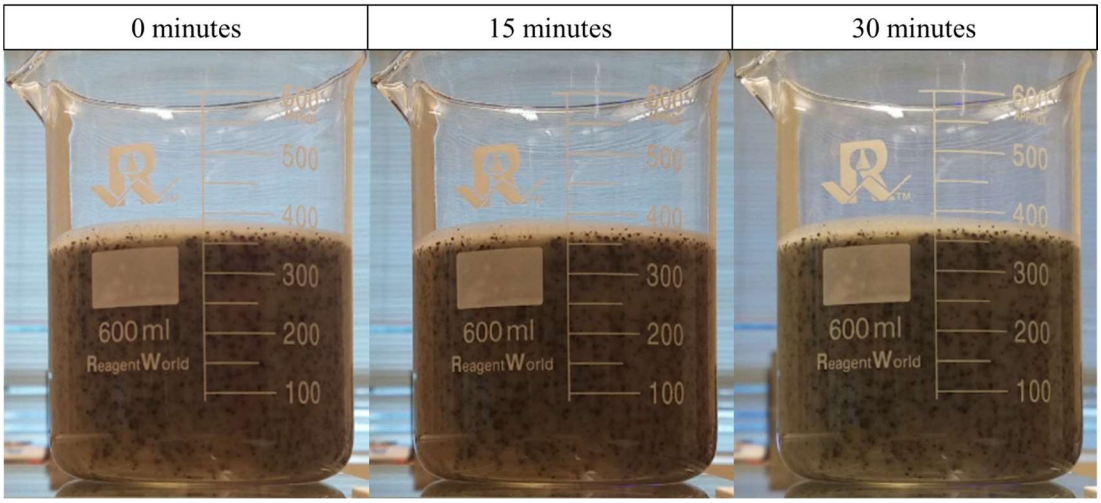

Figure 31: Settling test results for 1000micron 50ppb graphite

It is clear that the settling tests showed no particle drop within the 30 minute period. Pictures regarding the 5 in, 10 min, 20 min and 25 min were not included for this reason. This, coupled with the results from the rheology assessment, validates that the static environment for high pressure testing would suffice for future assessments of LCM and nanoparticles. Furthermore, the 30-minute time period required for testing was concluded to be sufficient based on the particles used within the fluid system for the settling tests.

4.2.2 Lost Circulation Material Testing

A total of 24 high pressure LCM tests were conducted using the newly developed apparatus. Eight out of the 24 tests were repeated to test the reliability of the apparatus. These tests were compared to the previously reported sealing pressures in the literature for the same LCM combinations, as well as the reported fluid loss per cycle. It should be noted that a cycle is referred to herein as the point at which the seal breaks and a significant drop in pressure is witnessed. At this point, the pressure will continue to climb as the pump is operated under a constant rate of 25 cc/min. These tests were evaluated based on whether the previously reported sealing pressure was reached, how long it took to reach the differential pressure of 1,200 psi, how much fluid loss was realized compared to previously reported losses, how the seal holds under constant pressure and the increased pressure integrity recognized after constant pressure was applied. The first tests ran were conducted on a 1000 micron disc using 50 ppb sized calcium carbonate (SCC3) in order to establish repeatability. Figure 32 shows the pressure tests for these three evaluations.

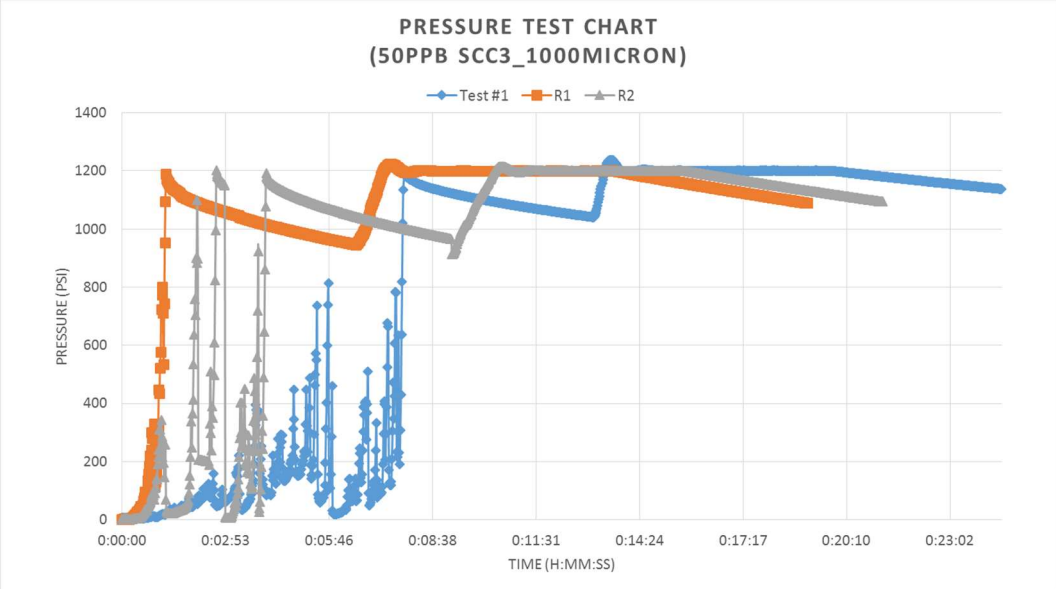

Figure 32: 1000 micron_50 ppb sized calcium carbonate tests

Looking at the pressure test for the SCC3 it can be concluded that an acceptable level of repeatability can be achieved using this apparatus. All three tests were able to reach the differential pressure of 1,200psi. It can be seen that the time it takes to establish the seal varies from the rampant amount of cycles in each test. Once the differential pressure was reached the transient region for each test showed similar trend and magnitude of pressure loss. Each test was able to maintain the seal under constant pressure for the 5-minute interval. Following the constant pressure, it was noted that the second pressure transient region encountered less pressure drop than the first region. Moreover, the pressure transient through the seal in the second region underwent a change in trend. This was expected due to a constant force applied to the seal rather than an instantaneous seal establishment. Figure 33 shows the first and second pressure transient regions for this test.

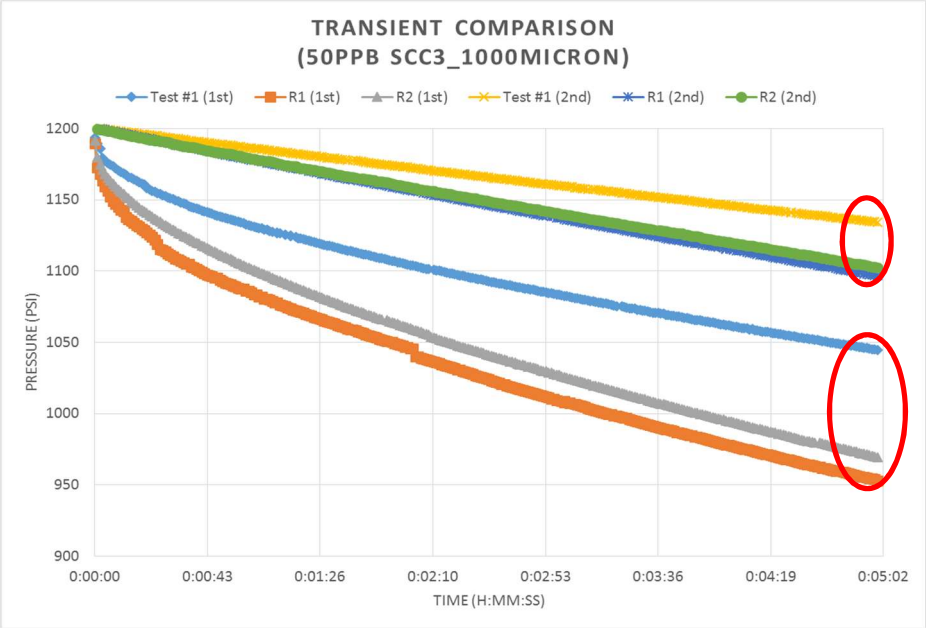

Figure 33: Transient pressure zones for 1000 micron_50 ppb sized calcium carbonate

Evaluating the trends and magnitude of pressures of these two graphs, it can be concluded that these tests are repeatable. The level of variance in pressure is less than 100 psi for the first transient and less than 50 psi for the second transient zone. A qualitative analysis was utilized for

these evaluations due to the lack of fluid loss resolution built into the apparatus. The lack of fluid loss, or flowrate, during constant pressure and pressure transient regions eliminated the possibility of using conventional Darcy flow equations. Furthermore, after calculating the Reynolds number using the three disc sizes and particle size distributions of the LCM mixtures, it was concluded that the flow regime is outside the Darcy flow number (Reynolds number < 1). Although these qualitative measurements were used for the first and second transient regions, a good deal of metrics were able to be gathered from these pressure tests for comparisons purposes. (Note: All LCM pressure tests including repeated tests can be found in the Appendices)

One of the goals in designing the apparatus was to see if previously documented sealing pressures could be recognized under the same testing conditions. Moreover, it was a goal to evaluate if these LCM mixtures could obtain higher sealing pressures based on the calculated differential pressure of 1,200 psi. The findings showed that every single LCM mixture was able to obtain higher sealing pressures than what was documented previously. Furthermore, every single mixture was able to reach the differential pressure of 1,200 psi. Figure 34 shows the tests with their previously tested sealing pressure compared to the differential pressure of 1,200 psi.

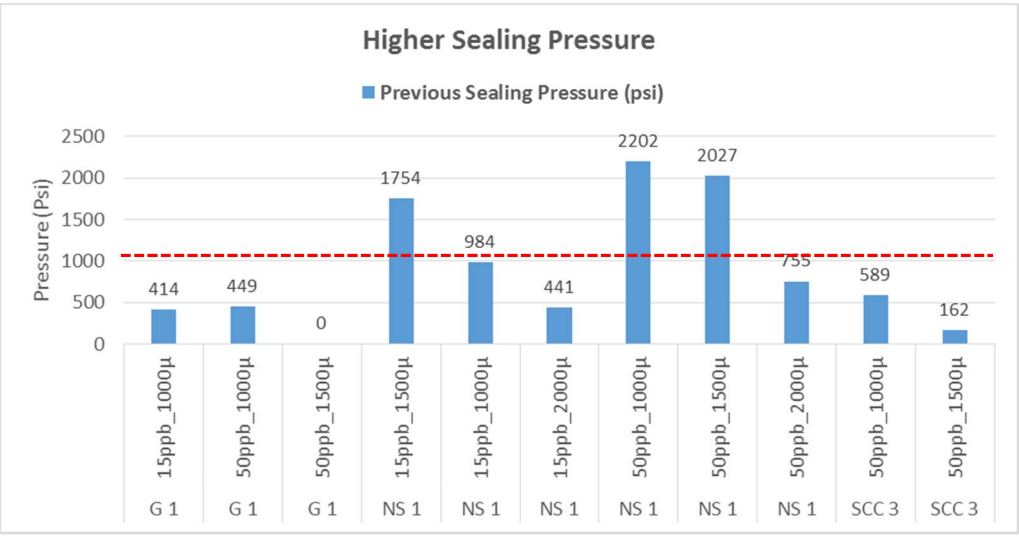

Figure 34: Previously noted sealing pressures compared to the obtained differential pressure

It can be seen that seven out of the ten LCM mixtures were able to obtain higher sealing pressures than previously documented. The 50 ppb graphite (G1) tested at 1500 micron was not evaluated previously which is why the previous sealing pressure is listed at zero. It should be noted that the three nutshell (NS1) tests were previously documented to have higher sealing pressures. Testing to these pressures was not conducted, as it was only the objective to reach the 1,200 psi differential pressure.

It was found that the apparatus allowed for analyzing the time it took each LCM mixture to reach the differential pressure, as well as the number of cycles that occurred prior to reaching this sealing pressure. This was deemed as a critical evaluation method due to the importance of LCM placement in application. Figures 35-37 shows the sealing time and number of cycles for the NS1, SCC3 and G1 tests. Note that tests with an "R" indicates a repeated test.

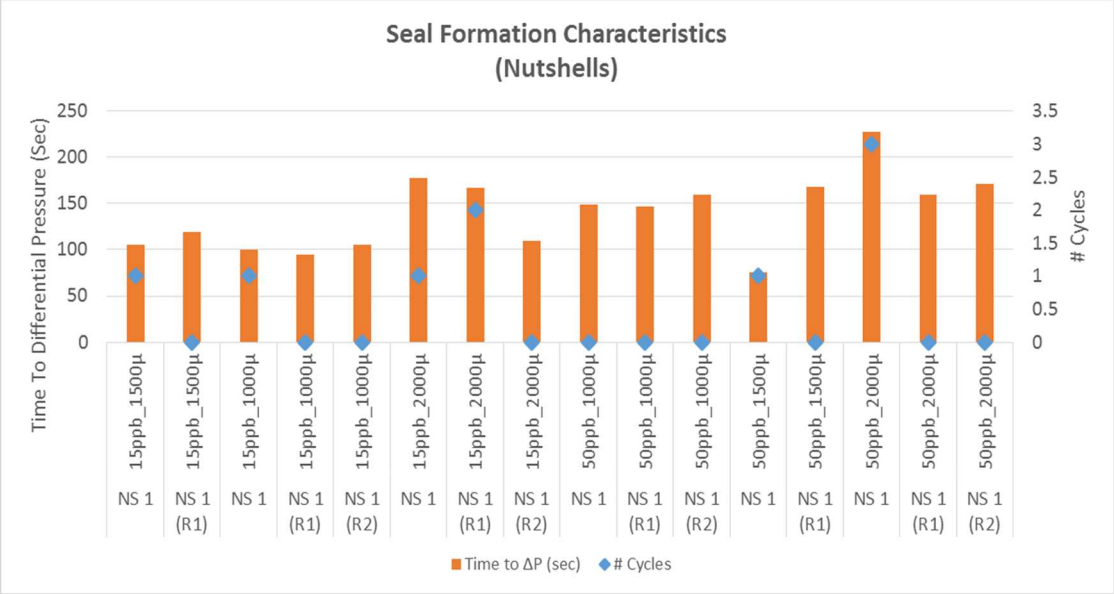

Figure 35: Seal formation characteristics of nutshells (NS1)

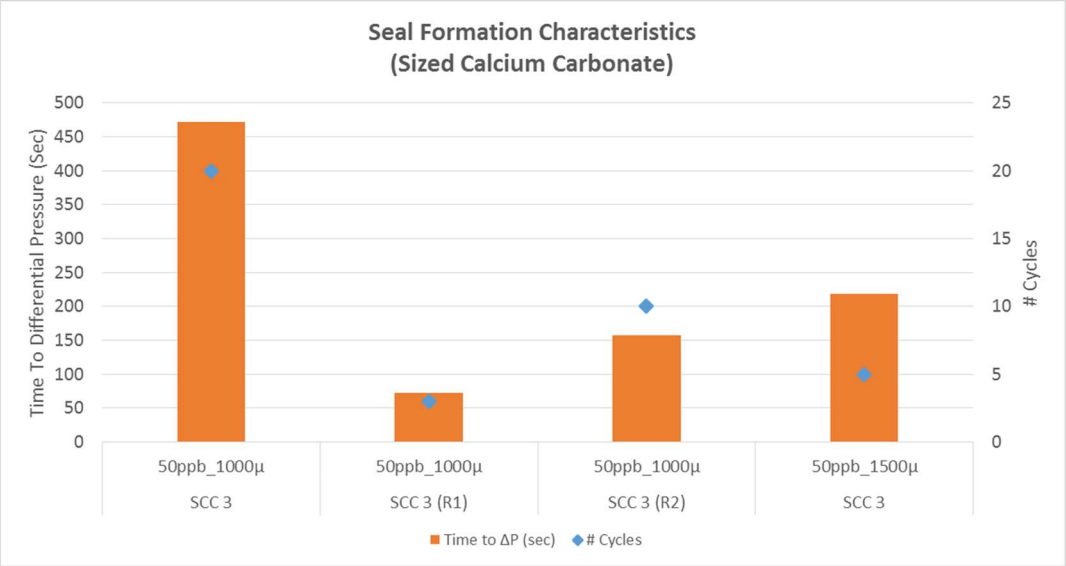

Figure 36: Seal formation characteristics of sized calcium carbonate (SCC3)

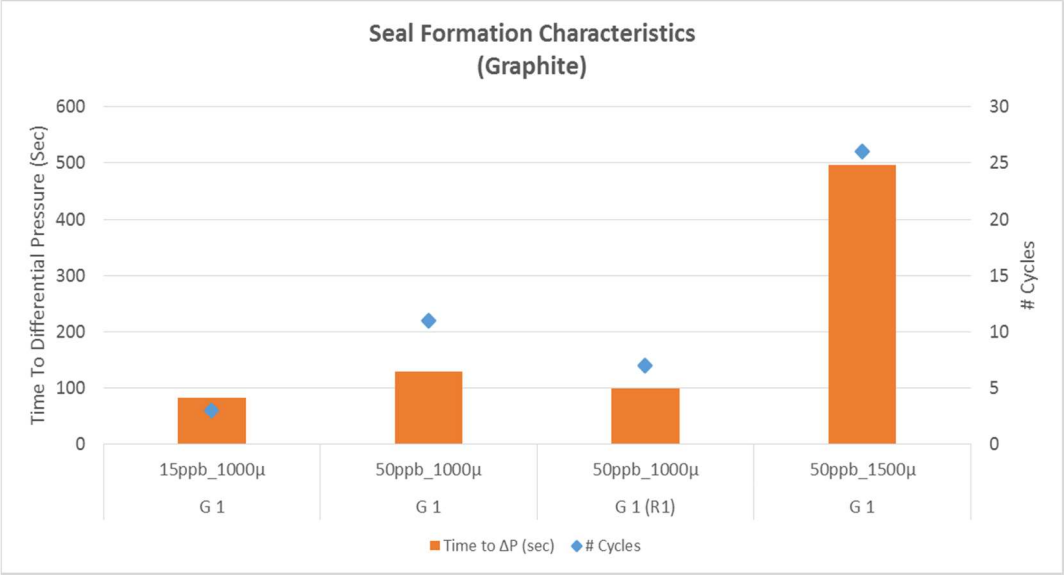

Figure 37: Seal formation characteristics of sized calcium carbonate (SCC3)

It can be seen that the average time for a NS1 mixture to reach the 1,200 psi differential pressure and seal is roughly two minutes. It should be noted that in most cases the NS1 blends had zero cycles. The trend recognized during the pressure tests was that all NS1 tests typically have a smooth increase in pressure until the differential pressure is reached. It can also be noted that an

increase in concentration does not always result in a decrease in sealing time. This trend was also witnessed in the transient regions. In the other LCM mixtures, higher sealing times and cycles were recognized. More cycles occurred in both the SCC3 and G1 tests. Although the graphite did undergo more cycles, it replicated a very similar trend that was seen with the nutshells. The SCC3 tests were the most sporadic in terms in cycles and time to seal, as these tests showed large variability in these metrics.

Fluid loss was also measured and used as a metric for the new apparatus. Knowing previous fluid loss data for each mixture allowed for a clear comparison. It should be noted that all fluid loss was encountered and measured during constant rate prior to reaching the differential pressure of 1,200 psi. Fluid loss was analyzed by taking the total amount of fluid loss and dividing by the number of cycles prior to reaching the sealing pressure of 1,200 psi. These values were compared to previously reported values for each mixture. Figures 38-40 show the fluid loss per cycle values for the NS1, SCC3 and G1 tests.

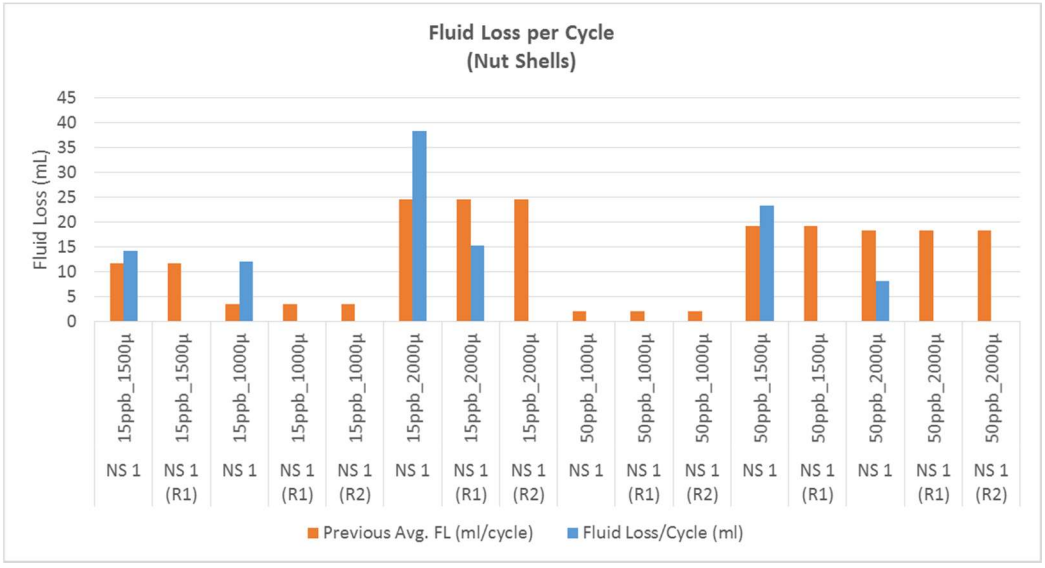

Figure 38: Fluid loss per cycle for all NS1 tests

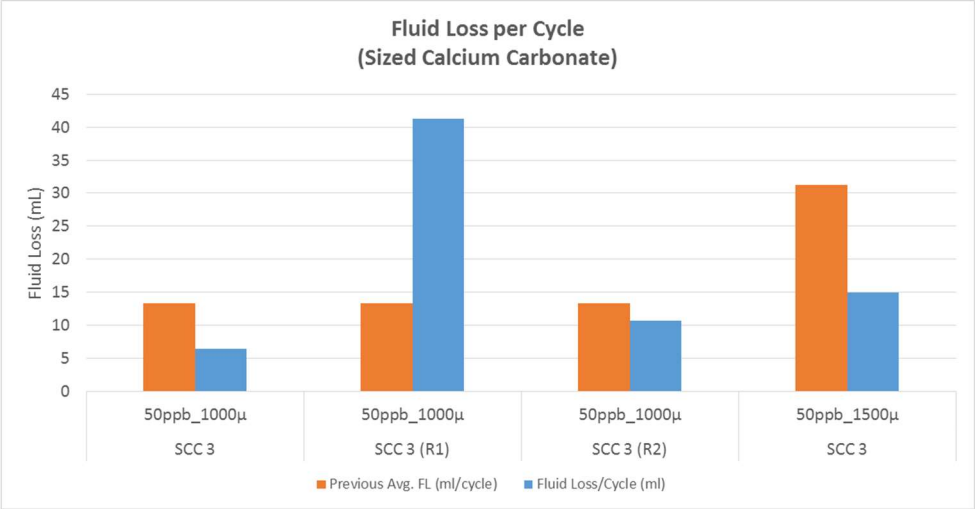

Figure 39: Fluid loss per cycle for all SCC3 tests

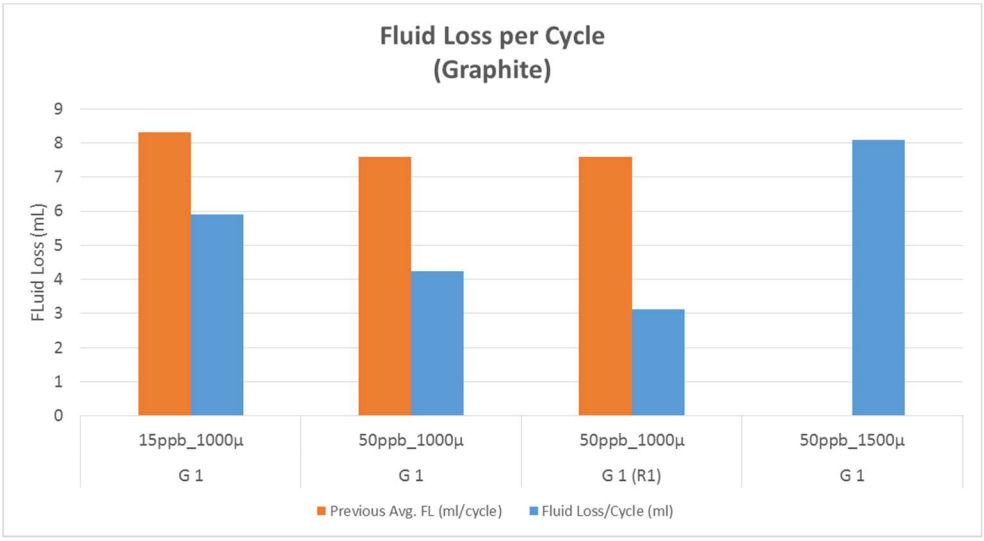

Figure 40: Fluid loss per cycle for all G1 tests

The fluid loss evaluation confirmed similar fluid loss values that have previously been reported. Based on a cycle basis, the graphite tests witnessed the least amount of fluid loss. These tests were also better performing in regards to sealing, which will be addressed here after. Higher fluid loss volumes were also noted in the NS1 and SCC3 tests, but were also in agreement with what was previously shown in the literature. It should be noted that some tests did not have any fluid loss volumes. These low volumes were only recognized with the NS1 tests. Although there was

no fluid loss recorded, a potential volume of fluid loss equivalent to 12 ml could have been realized due to the design of the apparatus. The flow out tube was directed against gravity and had a volume of 12 ml, which in some cases residual fluid was witnessed after testing. For these cases an accurate measurement could not be made and was assumed that the total fluid loss was zero. This lack in fluid loss resolution is what was discussed earlier as the determining factor that called for qualitative analysis. This flaw is what prevented the measurement of flow and eliminated the possibility of Darcy equations or other flow equations to be used for the transient regions of the test.

Besides the hindrance of flow monitoring, the apparatus was able to successfully evaluate the LCM mixtures under constant pressure conditions. This is critical in application as LCM has to be able to handle higher pressures as a well drills deeper depths past the point of lost circulation. Table 10 details which LCM mixtures that failed under constant pressure.

LCM Blend	Test	Higher Sealing Pressure?	Seal Break During Constant Pressure?
G 1	15ppb_1000µ	Yes	No
G 1	50ppb_1000µ	Yes	No
G 1	50ppb_1500µ	N/A	No
NS 1	15ppb_1500µ	No	No
NS 1	15ppb_1000µ	Yes	No
NS 1	15ppb_2000µ	Yes	Yes
NS 1	50ppb_1000µ	No	No
NS 1	50ppb_1500µ	No	Yes
NS 1	50ppb_2000µ	Yes	Yes
SCC 3	50ppb_1000µ	Yes	No
SCC 3	50ppb_1500µ	Yes	No

Table 10: List of LCM mixtures that failed under constant pressure

The table details whether each LCM blend was tested higher than the previously reported sealing pressure, as well as which LCM mixtures failed under constant pressure for all tests. The table shows that the SCC3 and G1 mixtures were able to hold a seal under constant pressure conditions for all tests. It was noted that three LCM mixtures containing NS1 failed under constant pressure conditions. One of these mixtures was not tested above its previously reported sealing pressure, while the other two tests were tested above at the differential pressure of 1,200 psi. These pressures are listed with the following figures as reference. Figures 41-43 show the pressure graphs where each seal failed during constant pressure for each of the mixtures.

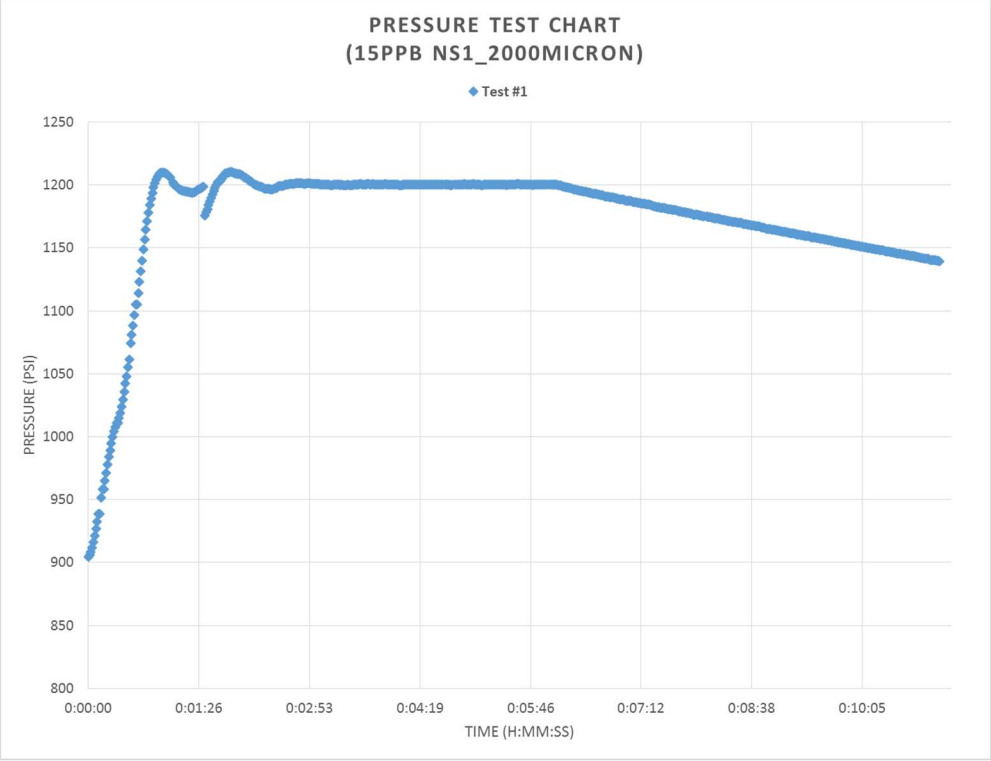

Figure 41: Seal failure for 15 ppb NS1_2000 micron (Previous Sealing Pressure = 441 psi)

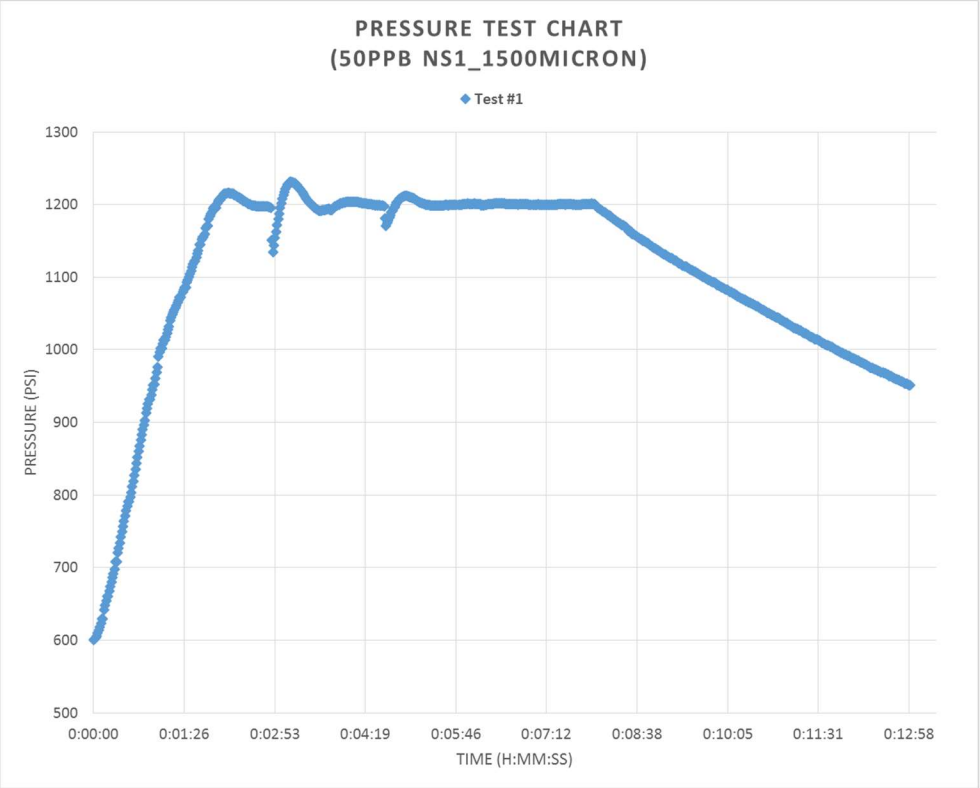

Figure 42: Seal failure for 50ppb NS1_1500micron (Previous Sealing Pressure = 2,027psi)

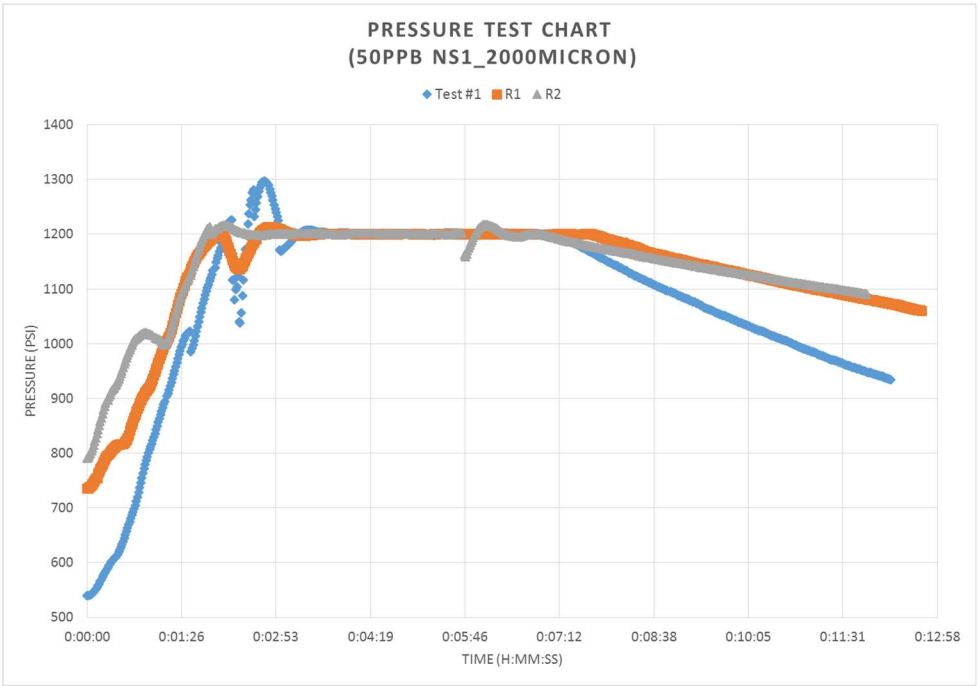

Figure 43: Seal failure for 50ppb NS1_2000micron (Previous Sealing Pressure = 755psi)

It should be noted that all five tests that failed under constant pressure consisted of NS1 mixtures. Both mixtures at 15 ppb and 50 ppb failed under constant pressure for a 2000 micron tapered disc. Each of these tests had previously been reported to have lower sealing pressures. It can be seen that the 50 ppb mixture had a significant drop in pressure once the seal broke under constant pressure. For this test, the repeatable evaluations also showed a failure under constant pressure. As for the 15 ppb mixture, it was only noted that this test failed once under constant pressure, as the other repeatable tests did not fail. In regards to the 50 ppb 1500 micron test, a break in the seal was also encountered under this differential pressure of 1,200 psi.

Aside from analyzing constant pressure and how well the seal holds under 1,200 psi, a comparison of the transient pressure was evaluated. This was conducted to see how the integrity of the seal strengthens after the constant differential pressure was applied to the seal. The final pressure encountered after the first transient period was compared to the final pressure seen in the second transient zone. Figure 44-47 shows the final pressure for the first and second pressure transient zones for SCC3, G1 and NS1 for 15 ppb and 50 ppb.

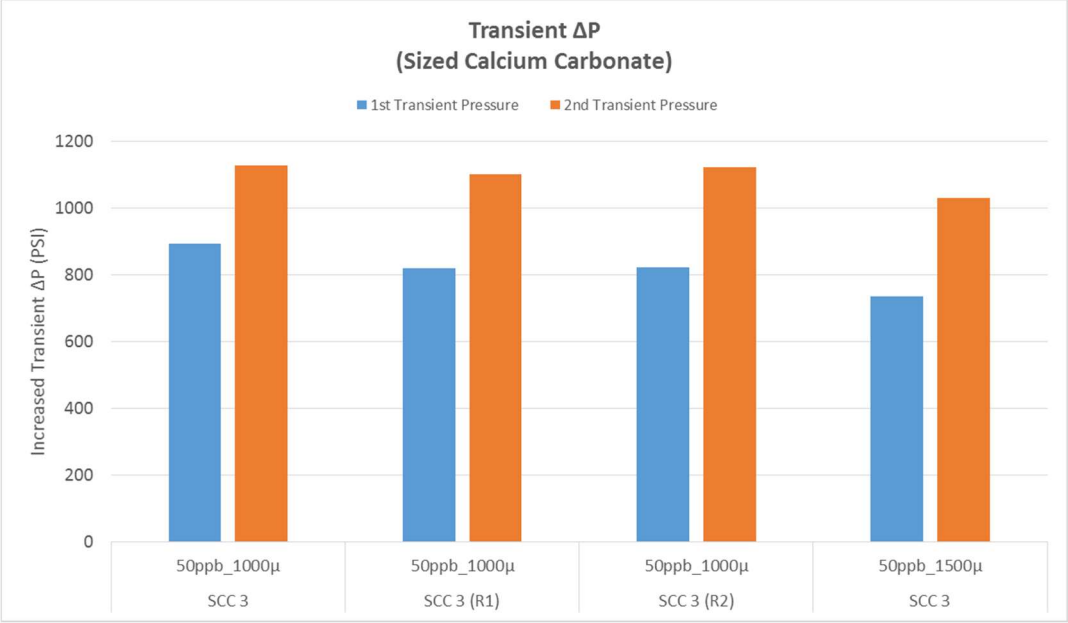

Figure 44: First and second transient pressures for SCC3

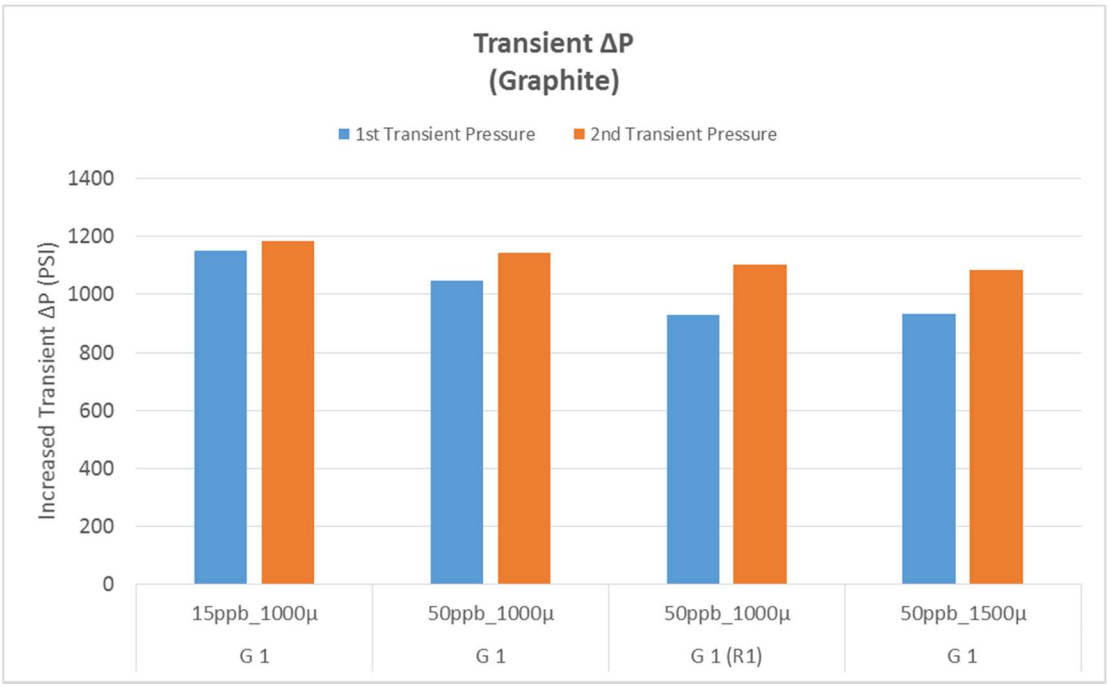

Figure 45: First and second transient pressures for G1

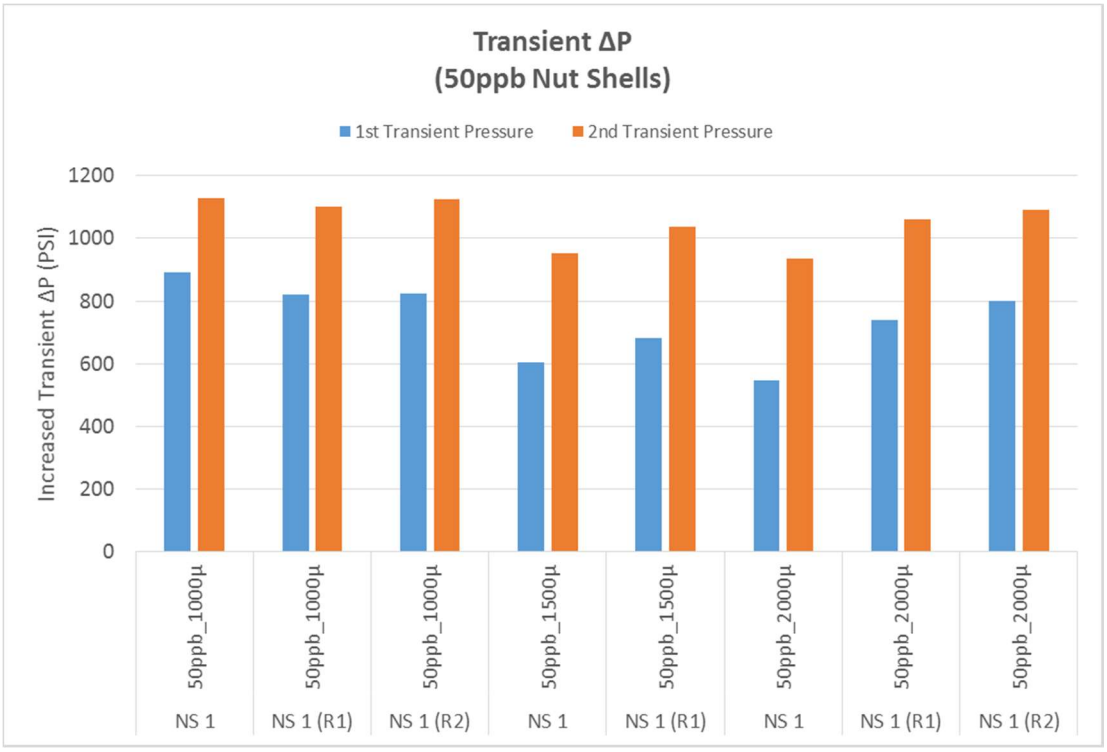

Figure 46: First and second transient pressures for 50 ppb NS1

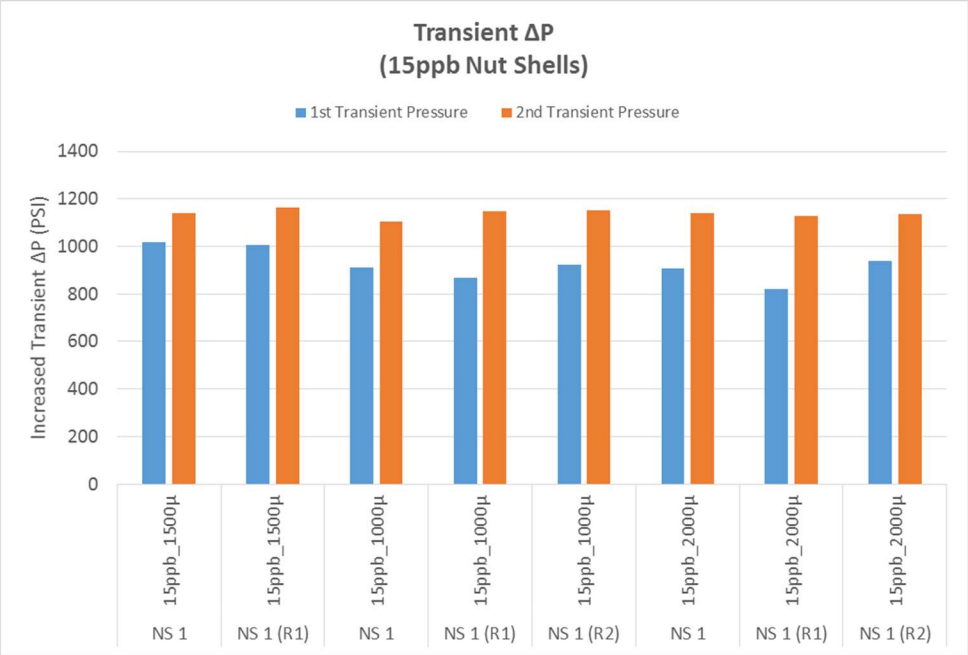

Figure 47: First and second transient pressures for 15 ppb NS1

(Note: All transient test comparisons can be found in the Appendices) It is clear after analyzing the difference in transient pressures that strengthening of the seal occurs due to the constant differential pressure. It should be noted that this constant pressure period was set at 5 minutes. It is recommended that future tests apply pressure for a longer period of time to see further integrity formation of the seal. It can be seen from the data that the G1 mixtures performed the best in terms of seal integrity. The initial transient pressures for these tests did not see a lot of pressure depletion. This is an initial indication of the quality of the seal. The second transient pressure is more so related to how the seal is strengthened through a permeability reduction caused by compaction. This can clearly been seen in the other tests regarding the SCC3 and NS1. The 50 ppb NS1 tests realized the highest drop in pressure after initiating the seal. In some cases these pressures dropped more than 50% of the designated differential pressure of 1,200 psi. In regards to the 15 ppb NS1 tests, first transient pressure drop was not as severe as seen in the 50 ppb tests. This was opposite to the expected result of an increased pressure with an increasing concentration. The SCC3 also showed decent performance with initial quality of the seal as the

majority of these tests did not drop below 800 psi during first transient. The only exception was the 50 ppb 1500 micron SCC3 test, which is the mixture that was chosen for NP testing. As for seal strengthening, all tests were able to strengthen the seal above 1,000 psi in most cases. The only exception was the 50 ppb NS1 1500micron and 50 ppb NS1 2000 micron tests. It was chosen that the NS1 and SCC3 for 50 ppb 1500 micron would be tested with silica and barite nanoparticles.

4.2.3 Nanoparticle Testing

Following the high pressure LCM testing, a similar workflow was conducted to see the effects that barite and fumed silica NPs have on the sealing characteristics in conjunction with LCM. The main objectives in analyzing the nanoparticles were to study if a decrease in fluid loss or sealing time was realized, whether the nanoparticles prevented failure of the seal during constant pressure and how the nanoparticles strengthened the seal through a qualitative analysis. Figures 48-51 show the total fluid loss results containing NPs for SCC3 and NS1 compared to the LCM tests.

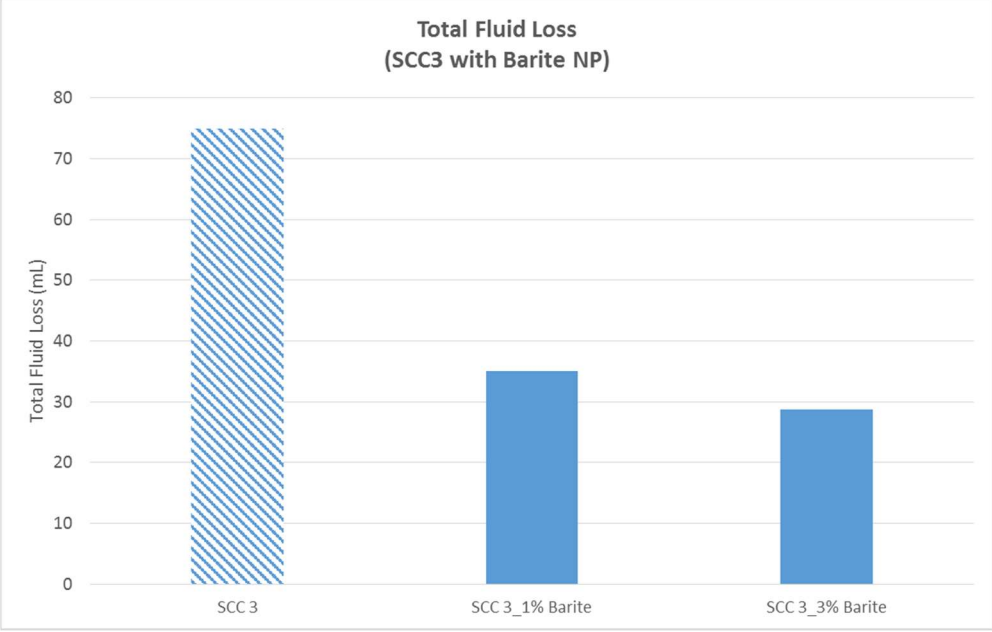

Figure 48: Total fluid loss for SCC3 LCM mixture containing 1% and 3% barite NP

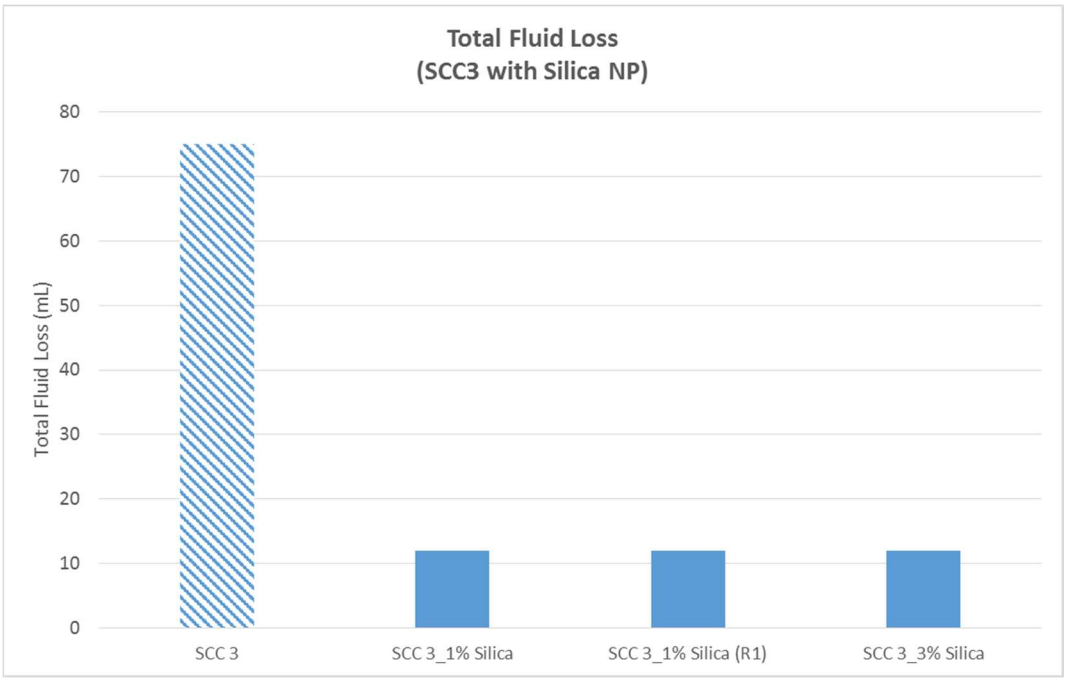

Figure 49: Total fluid loss for SCC3 LCM mixture containing 1% and 3% silica NP

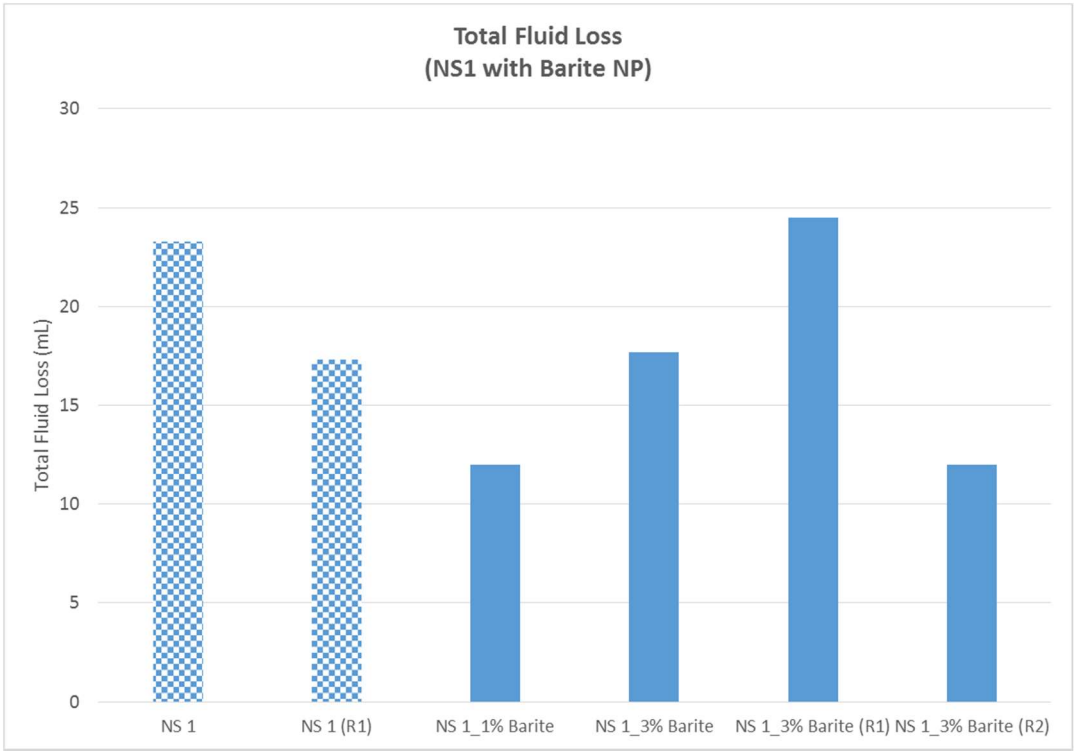

Figure 50: Total fluid loss for NS1 LCM mixture containing 1% and 3% barite NP

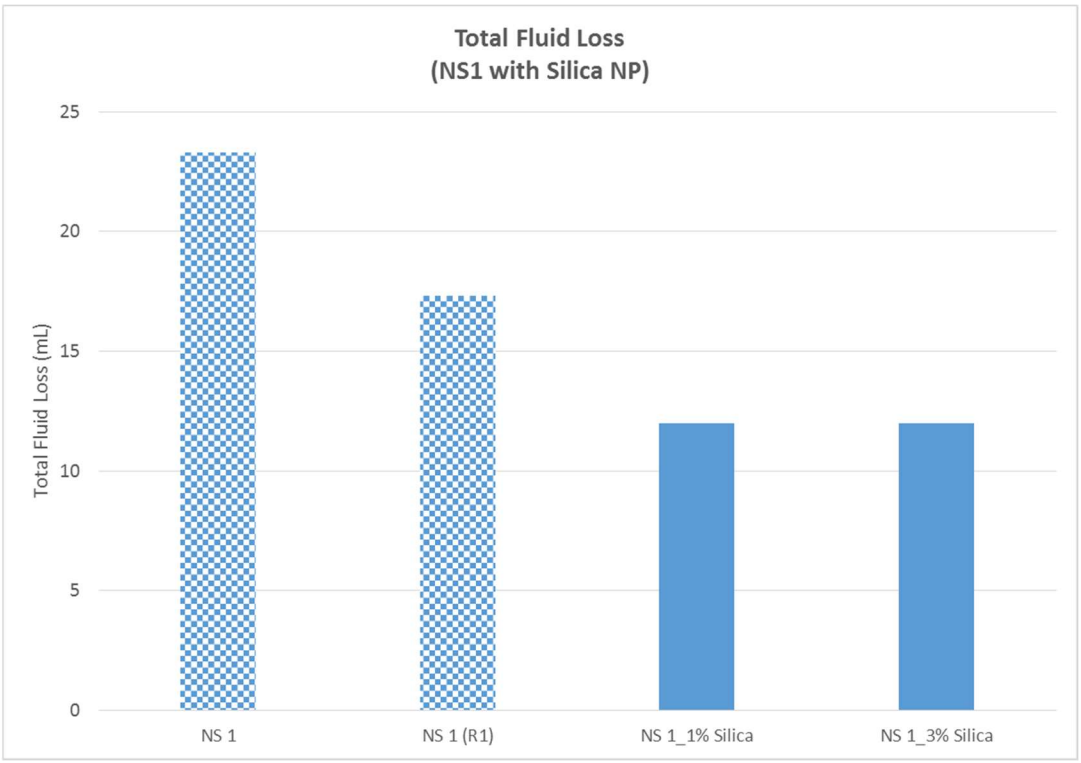

Figure 51: Total fluid loss for NS1 LCM mixture containing 1% and 3% silica NP

A significant reduction in fluid loss was witnessed in regards to the SCC3 mixture. This reduction was recognized with both barite and silica based nanoparticles. In all cases regarding the SCC3, a reduction in 50% fluid loss was measured. The greatest reductions were seen with the silica NPs. As for the NS1 mixtures, only the silica NPs witnessed a reduction in fluid loss. This reduction was seen to be roughly 30% of the original fluid loss. The barite NPs failed to significantly reduce the fluid loss in the NS1 mixture. At 1% barite NP a slight reduction was recognized, but inconsistency in fluid loss results were seen with 3% barite NPs. This is to be expected from low pressure testing, as well as silica NP performance covered in the literature.

The time for the sealing pressure to reach the differential pressure of 1,200psi was also evaluated. This provided further insight into the performance of the NPs. Figures 52-55 show the time it took the SCC3 and NS1 mixtures containing NPs to reach the differential pressure of 1,200psi.

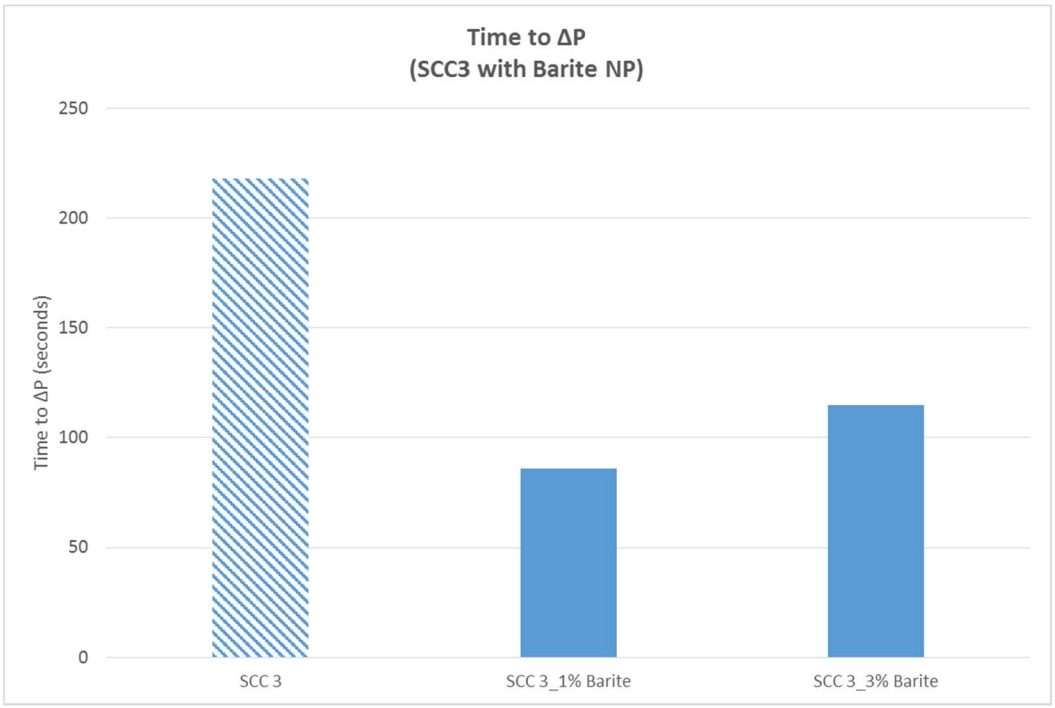

Figure 52: Time to reach differential pressure for SCC3 mixture with 1% and 3% barite NPs

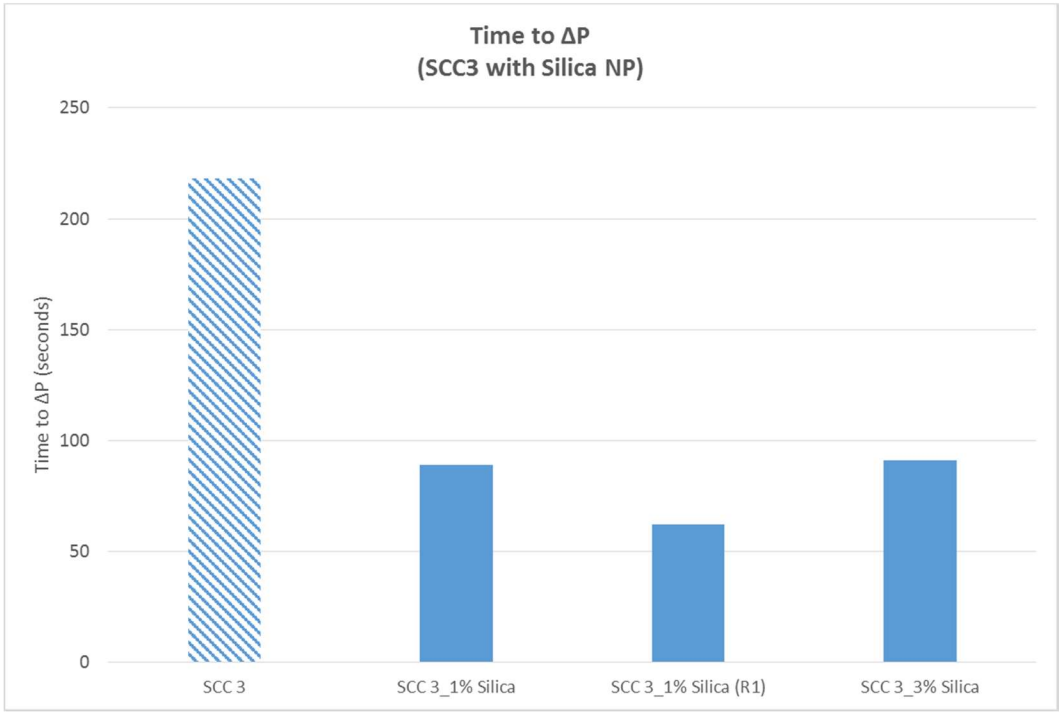

Figure 53: Time to reach differential pressure for SCC3 mixture with 1% and 3% silica NPs

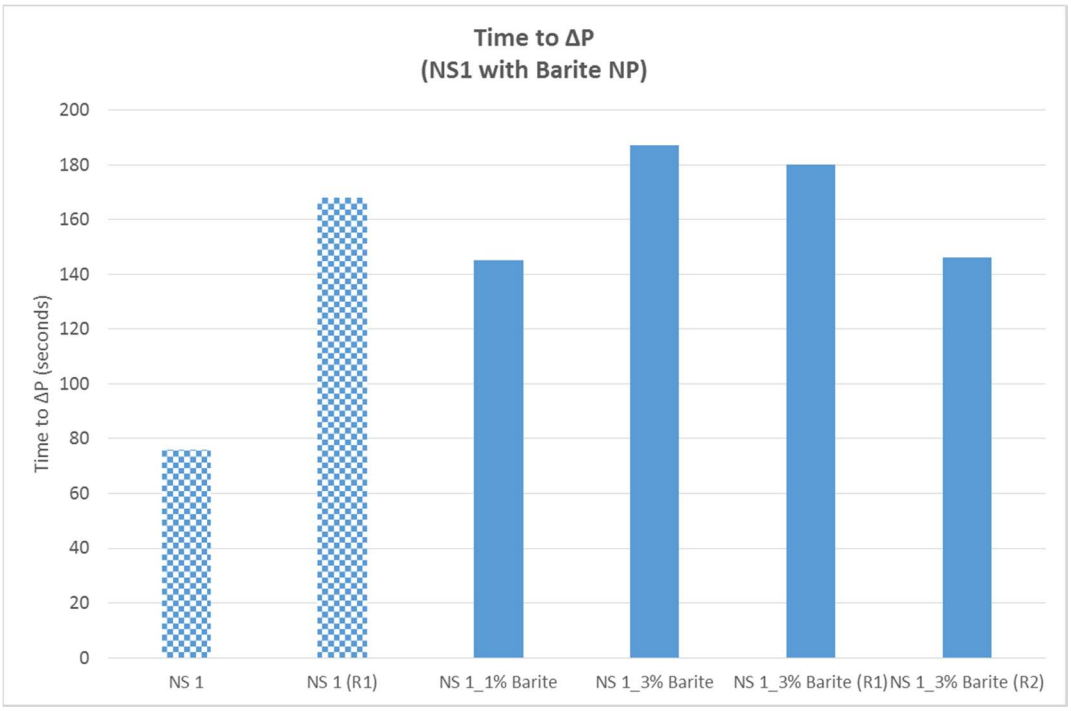

Figure 54: Time to reach differential pressure for NS1 mixture with 1% and 3% barite NPs

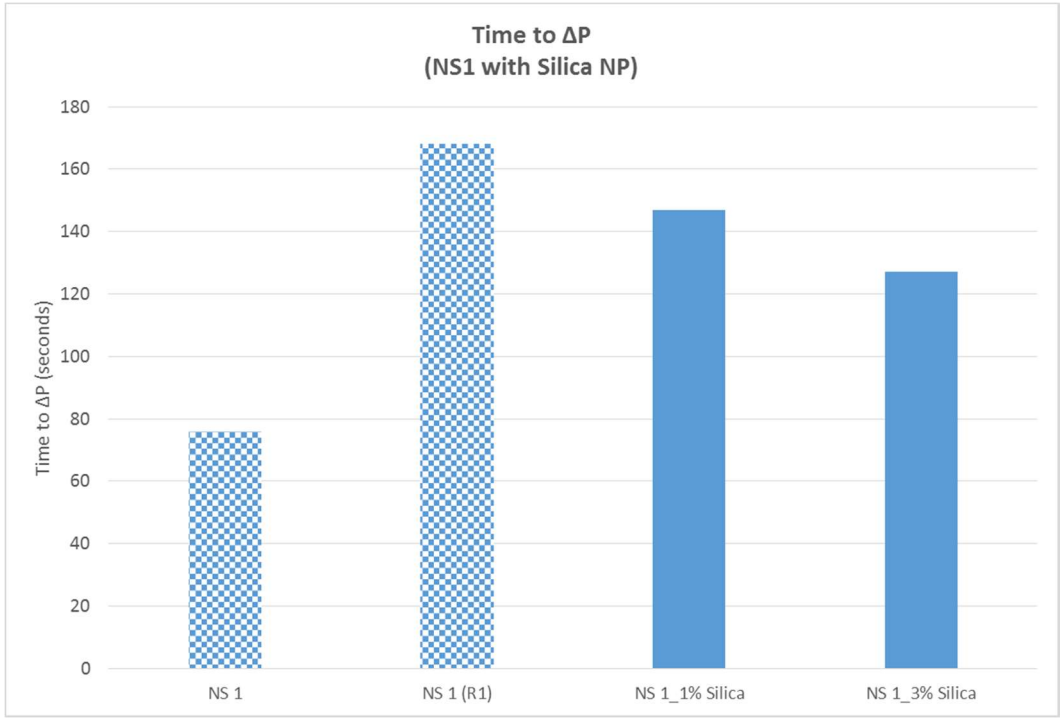

Figure 55: Time to reach differential pressure for NS1 mixture with 1% and 3% silica NPs

The time it takes to reach differential pressure is reflective of the same trends realized with the fluid loss data. It can be seen with the SCC3 mixtures containing both types of nanoparticles that a significant reduction in sealing time was witnessed. Once again, it should be noted that the silica NPs performed better than the barite NPs in this case. In regards to the NS1 mixtures, neither type of NPs had a notable influence on reducing the time to reach sealing pressure.

Knowing the NS1 blend broke in the high pressure testing, the addition of NPs were also studied to see if either type had the ability to prevent the failure of the seal breaking. Considering the SCC3 mixture did not break during high pressure testing, this will not be listed herein, but should be noted the SCC3 blend did not fail with the addition of NPs. Table 11 lists the original NS1 LCM blends and details which NP tests failed under constant pressure.

LCM Blend	**Seal Break During Constant Pressure?**
NS 1	Yes
NS 1 (R1)	No
NS 1_1% Barite	Yes
NS 1_3% Barite	Yes
NS 1_3% Barite (R1)	Yes
NS 1_3% Barite (R2)	No
NS 1_1% Silica	No
NS 1_3% Silica	No

Table 11: List of NP tests in NS1 mixtures that failed under constant pressure

As noted prior, the original NS1 blend failed under constant differential pressure of 1,200 psi. This was also recognized when the addition of 1% and 3% barite NPs were used for testing. This was not seen with the silica NPs as the seal maintained integrity for the duration of constant

pressure. Figure 56 shows the original NS1 test, as well as the NP tests that failed under constant pressure.

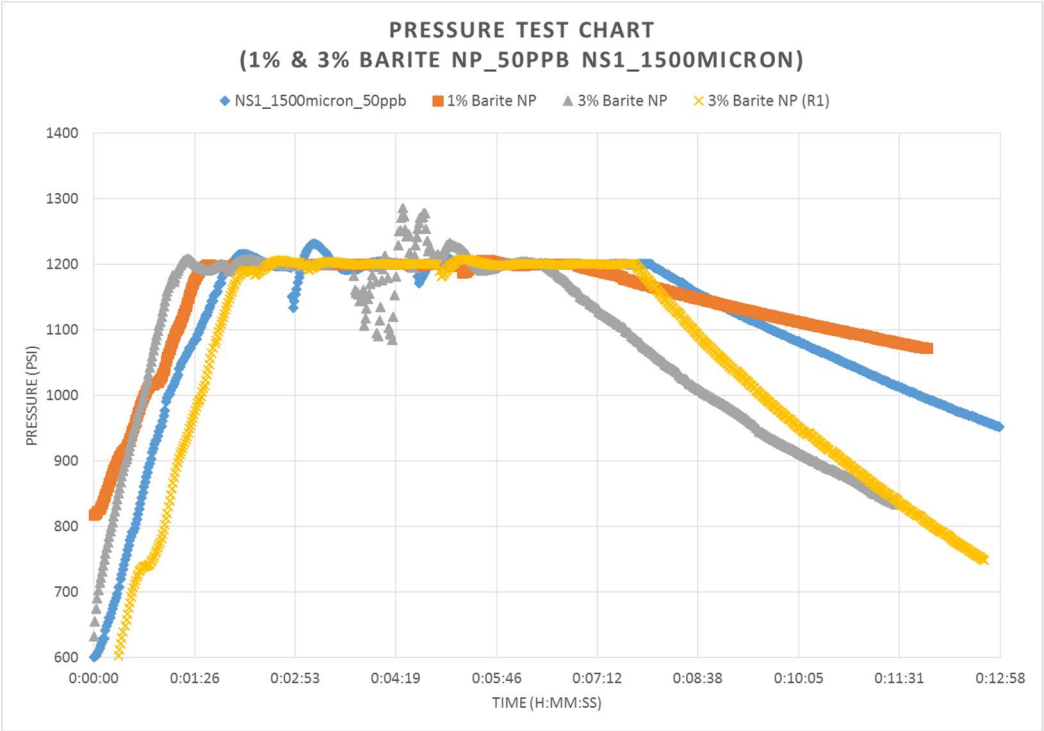

Figure 56: Seal failure under constant pressure with 1% and 3% barite NP for a NS1 mixture

It can be seen that the magnitude of seal failure was not reduced in any manner regarding the barite NP tests. It should be noted that no realized trend of failure was noticed in regards to timing of the seal failure.

Lastly, an investigation was conducted to see how NPs increase the sealing integrity of the mixtures and if an increase in seal strength was recognized. Similar to the LCM tests, the addition of NPs were analyzed based on the increase in pressure realized after the second transient region. This pressure is compared to the last pressure encountered in the first transient region. All NP tests and LCM mixtures were compared to the original LCM high pressure results. Figure 57-60 shows the results for the SCC3 and NS1 mixtures containing barite and silica NPs.

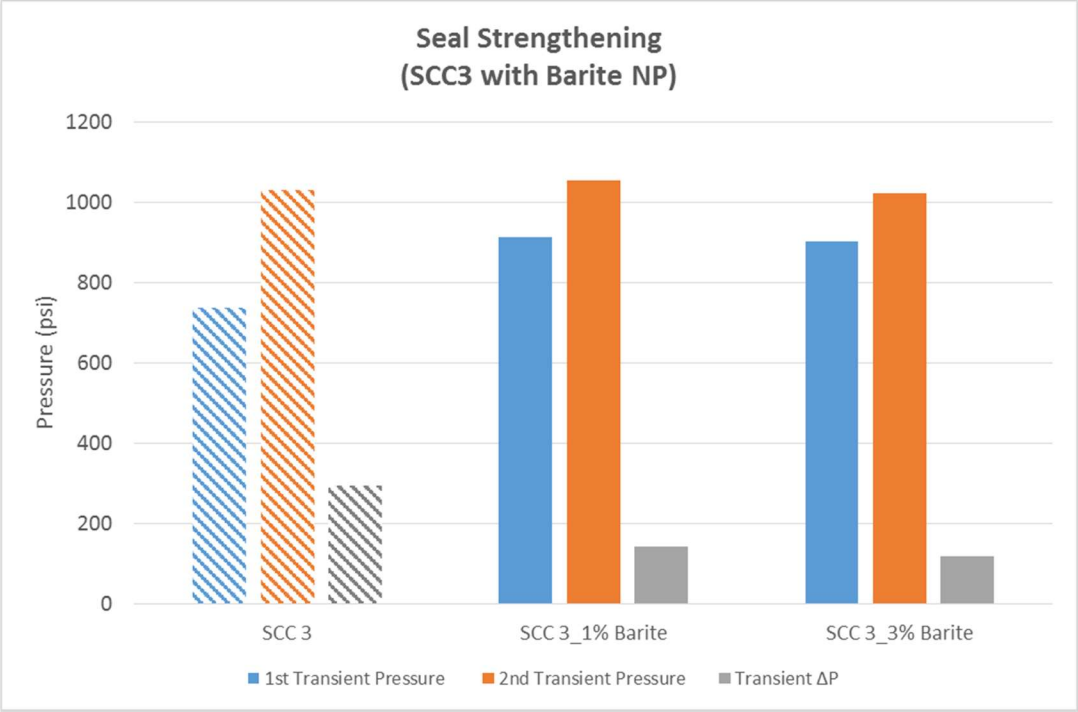

Figure 57: Seal strengthening of SCC3 mixture containing 1% and 3% barite NPs

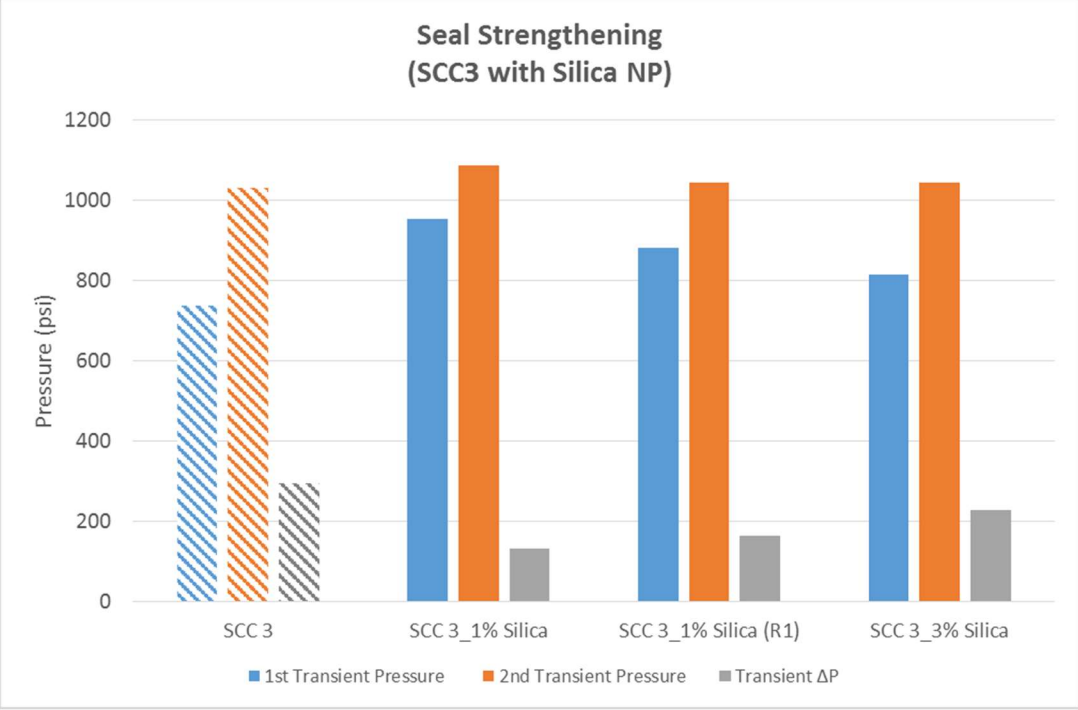

Figure 58: Seal strengthening of SCC3 mixture containing 1% and 3% silica NPs

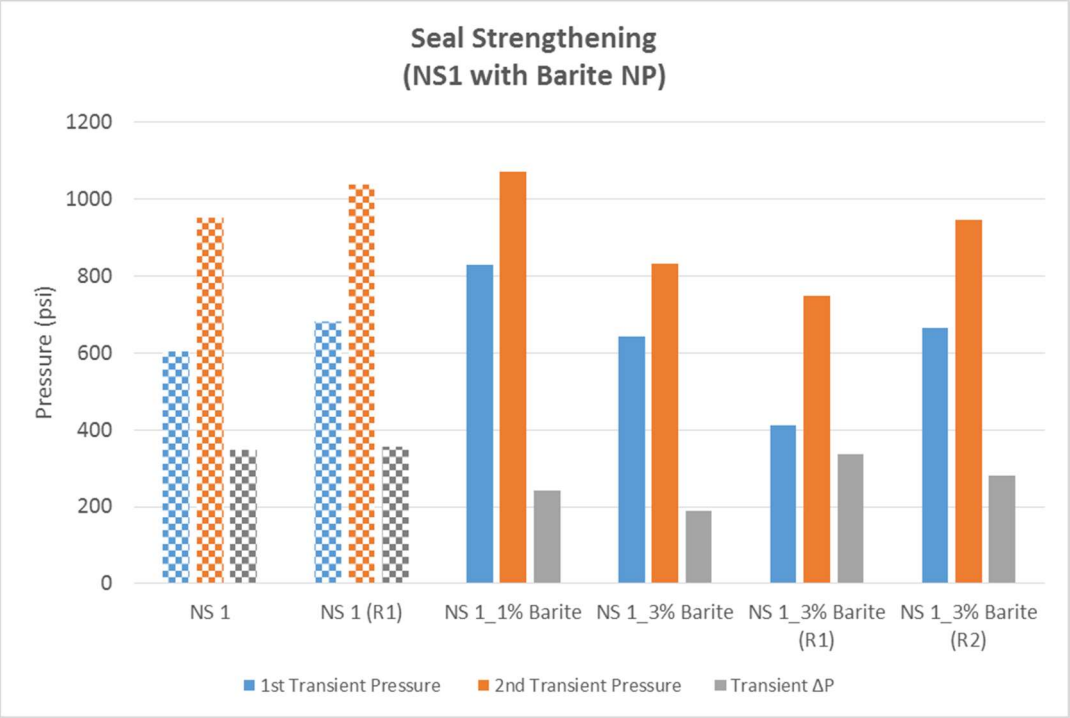

Figure 59: Seal strengthening of NS1 mixture containing 1% and 3% barite NPs

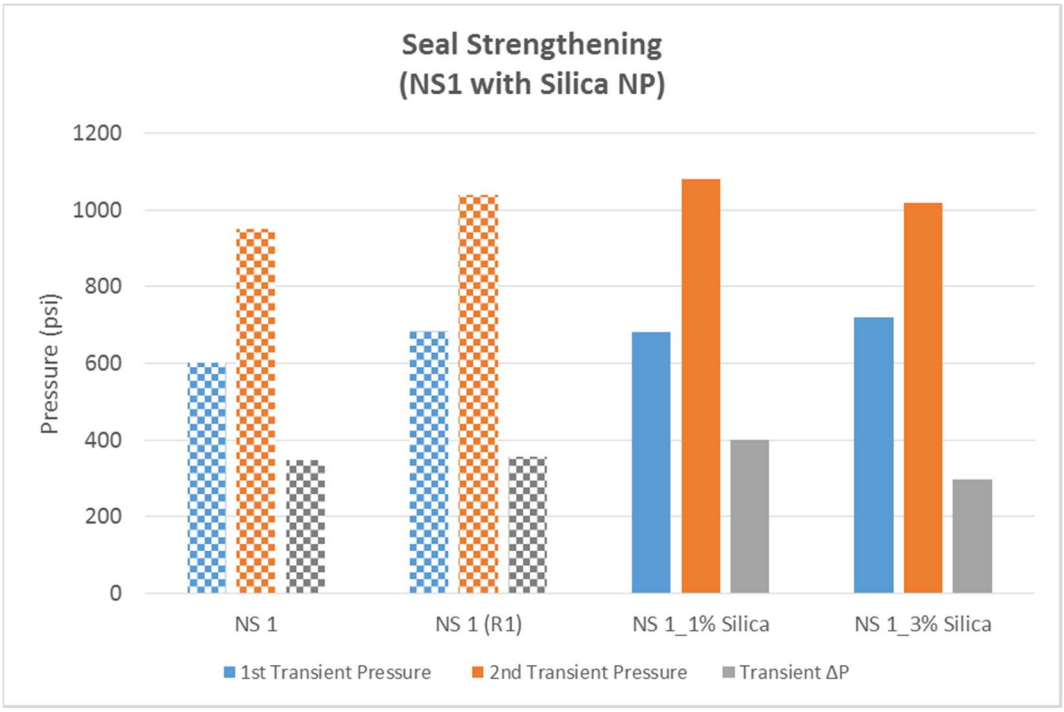

Figure 60: Seal strengthening of NS1 mixture containing 1% and 3% silica NPs

It was found that the NPs have the ability to affect the quality of the initial seal, but fail to significantly affect the strength of the seal in the second transient region. This can be seen with the SCC3 mixtures for both types of NPs. The initial transient pressure for the base case SCC3 mixture was 730 psi. The addition of NPs increased this pressure above 900 psi with the exception of 3% silica NPs. The final pressure recognized with NPs was within 50 psi for all SCC3 tests. This provides clarity that NPs can increase the quality of the initial seal but do not enhance, nor hinder, the second pressure transient, which is more so related to the strength of the seal. As for the NS1 tests, neither type of NP drastically increase the quality of the seal, nor the strength of the seal after constant pressure was applied. It should be noted that the silica NPs showed better results in comparison to the barite NPs for the NS1 mixtures. It was seen that barite NPs actually hindered the seal for the NS1 mixtures. This is believed to be due to the rheological effect the barite NPs have on the fluid mixture once increased above 1%. All in all, these results for the NS1 mixtures were to be expected considering the fluid loss results, timing results and constant pressure analysis all hinted towards the lack of performance within the NS1 mixture. (Note: All nanoparticle tests including transient comparisons can be found in the Appendices)

CHAPTER V

CONCLUSION

The aim of this research was to develop a new method to evaluate the sealing qualities of LCM and NPs. The goal in designing this apparatus was to improve the quality of analyzing LCM and NPs and to extend the analysis of these materials beyond only looking at sealing pressures, or the point at which the seal breaks. Furthermore, it was designed to look at previously tested materials and evaluate if higher sealing pressures could be established and maintained by applying constant differential pressure. The apparatus was used to accomplish these goals by testing LCM as well as LCM in conjunction with NPs. The conclusions, limitations of the work and future recommendations are detailed herein.

5.1 APPARATUS PERFORMANCE

The newly developed apparatus for high pressure testing was successfully able to evaluate LCM and NP materials under new conditions that have previously not been conducted. Traditional analysis of sealing pressures, or the point at which the seal breaks, were able to be analyzed along with new testing techniques enabled by the design. The introduction of constant pressure analysis was established and successfully implemented into testing. Furthermore, the analysis of pressure transient once the seal first establishes at the designated pressure, as well as after constant pressure has been applied was also enabled through the design. The monitoring of fluid loss was beneficial for fundamental analysis, but can certainly be improved to monitor fluid loss at higher resolutions. The set-up of the apparatus was successful considering the range of operational

parameters that can be controlled during testing. The following points list the primary conclusions, recommendations and limitations regarding the newly developed apparatus.

- The apparatus can evaluate LCM and NPs by traditional methods of testing materials until the seal pressure breaks, known as sealing pressure.
- The apparatus allows a new method of testing that enables testing under constant pressure to better understand how various materials handle continuous pressure when drilling ahead after lost circulation has occurred.
- The apparatus enables the analysis of pressure transient regions before and after constant pressure has been applied to study the initial quality of the seal and how the seal strengthens through compaction.
- Filtrate monitoring allowed for a rudimentary evaluation of fluid loss, but hindered the transient and constant pressure analysis due to a lack of measurement resolution.
- Darcy flow equations were not able to be utilized due to a high Reynolds number caused by the flowrate and possibly the disc sizes.
- Alterations to the mass scale instrumentation can be made in order to enable traditional flow equations to be used for transient and constant pressure analysis.

5.2 LCM TESTING

Previously tested LCM mixtures were evaluated on the newly developed apparatus. These tests were chosen in order for repeatability to be established. Moreover, these previously tested LCM mixtures had a reported sealing pressure for each mixture which was desirable for comparison purposes. The following points list the main conclusions, recommendations and limitations for the LCM testing.

- Previously evaluated LCM treatments were able to be replicated under new testing conditions with the newly designed apparatus with repeatability.

- A calculated differential pressure of 1,200psi based on field experience was established as a new baseline for a sufficient sealing pressure.
- All LCM mixtures were successfully tested to this newly established differential pressure.
- Eight out of the 11 LCM mixtures were determined to have higher sealing pressures than previously reported in the literature based on the new differential pressure.
- Settling evaluations confirmed that performance is not hindered by pumping against the direction of gravity for the rheology of choice.
- All LCM mixtures showed an intriguing pressure transient zone after initial sealing, or when the differential pressure was reached which is indicative of the quality of the seal.
- Previous fluid loss results were replicated and confirmed with measurements that were dynamically evaluated.
- Each LCM mixture was successfully evaluated based on how fast each mixture formed a seal which corresponded to the fluid loss that was encountered.
- LCM mixtures were tested under constant pressure and were successfully evaluated to study how the seal holds in this pressure environment.
- Failure of the seal for three NS1 mixtures was observed which provided clarity of not only the apparatus but also the performance of the seal.
- LCM mixtures that have higher sealing pressures did not always perform the best under constant pressure which indicates packing of the seal is necessary to establish seal integrity.
- Constant pressure tests concluded that LCM selection may need to be based on how well seals perform under constant pressure rather than a breaking point in pressure.
- Secondary transient zones all showed that the seal strengthens, but clear trends could not be established based on a lack of fluid loss resolution to monitor flow that would enable flow equations.

5.3 NANOPARTICLE TESTING

Nanoparticles were screened initially in a low pressure environment to establish a baseline for high pressure tests. It was decided that the mechanically generated barite nanoparticles, although not the better performing particles, were to be used in high pressure testing. This was decided based on the ease of operating with the nanoparticles in comparison to the chemically generated nanoparticles. Silica nanoparticles were also introduced to high pressure testing to provide an additional testing metric. The following points list the primary conclusions, recommendations and limitations regarding the nanoparticles.

- Low pressure testing concluded fluid loss reductions are realized with both chemical and mechanical barite nanoparticles.
- Mechanically generated nanoparticles have more of an angular shape with poor size distribution as compared to the chemical nanoparticle which are more rounded and finely sized.
- Repeatability was successfully established in regards to the high pressure testing for both types of nanoparticles.
- In regards to high pressure testing, both types of nanoparticles were able to replicate similar fluid loss reductions with the SCC3 mixture, but the NS1 mixture failed to see similar benefits.
- The time to form a seal was reduced by utilizing nanoparticles and in the worst case did not seem to hinder the sealing process with either nanoparticle.
- Silica nanoparticles were able to prevent the NS1 mixture from failing under constant pressure conditions, but the barite nanoparticles did not show a benefit in preventing this occurrence as the seal with barite nanoparticles also failed under these conditions.
- Both types of nanoparticles were able to increase the quality of the seal initially for the SCC3 mixture but failed to replicate the same results for the NS1 mixture.

- Seal strengthening was not recognized with either type of nanoparticle due to a lack of apparatus resolution that prevented robust flow analysis.
- Overall, the silica nanoparticles performed better in all aspects of the analysis in comparison to the barite nanoparticles.

5.4 FUTURE WORK

During the course of this research a number of recommendations or procedural alterations were noticed and documented. These adjustments were noticed during the course of testing as well as after testing was concluded and analysis had commenced. The following points list the primary recommendations for future work regarding this research.

- A more efficient method of monitoring flowrate during constant rate and constant pressure operations should be established to enable the use of conventional flow equations to describe the newly developed testing methods.
- Knowing chemical barite nanoparticles perform better than mechanical barite nanoparticles, it would be ideal to establish a method that would enable the use of chemical nanoparticles in the high pressure testing apparatus.
- Continue to use silica nanoparticles as a baseline due to the realized benefits the material has in not altering the rheology of the fluid.
- Further evaluate the phenomena of seal failure under constant pressure conditions to better understand LCM selection criteria.
- Establish a new set of testing conditions, or better evaluate future conditions to enable Darcy flow to be used based on a sufficient Reynolds number.

REFERENCES

Abdo, J. & Haneef, M. D. (2013). Clay nanoparticles modified drilling fluids for drilling of deep hydrocarbon wells. Applied Clay Science, 86, 76-82.

Akhtarmanesh, S., Al-saba, M., Cedola, A. E., Qader, R., Caldarola, V. T., Hareland, G., & Nygaard, R. (2016, June). Barite Nano-Micro Particles with LCM Seals Fractured Form Better in Weighted Water Based Drilling Fluids. In 50th US Rock Mechanics/Geomechanics Symposium. American Rock Mechanics Association.

Almagro, S. P. B., Frates, C., Garand, J., & Meyer, A. (2014). Sealing Fractures: Advances in Lost Circulation Control Treatments. Oilfield Review, 26(3), 4-13.

Alsaba, M., Nygaard, R., & Hareland, G. (2014, April). Review of lost circulation materials and treatments with an updated classification. In AADE National Technical Conference and Exhibition, Houston, TX, Apr (pp. 15-16).

Alsaba, M. T., Nygaard, R., Saasen, A., & Nes, O. M. (2014, September). Lost circulation materials capability of sealing wide fractures. In SPE Deepwater Drilling and Completions Conference. Society of Petroleum Engineers.

Amanullah, M., & Al-Tahini, A. M. (2009, January). Nano-technology-its significance in smart fluid development for oil and gas field application. In SPE Saudi Arabia Section Technical Symposium. Society of Petroleum Engineers.

Bell, M. R. (2004, November). A case for nanomaterials in the oil and gas exploration and production business. In International Congress of Nanotechnology (ICNT) (pp. 7-10).

Boukadi, F., Yaghi, B., Al-Hadrami, H., Bemani, A., Babadagli, T., & De Mestre, P. (2004). A comparative study of lost circulation materials. Energy sources, 26(11), 1043-1051.

Bruton, J. R., Ivan, C. D., & Heinz, T. J. (2001, January). Lost circulation control: evolving techniques and strategies to reduce downhole mud losses. In SPE/IADC drilling conference. Society of Petroleum Engineers.

Calçada, L. A., Neto, O. D., Magalhães, S. C., Scheid, C. M., Borges Filho, M. N., & Waldmann, A. T. A. (2015). Evaluation of suspension flow and particulate materials for control of fluid losses in drilling operation. Journal of Petroleum Science and Engineering, 131, 1-10.

Caldarola, V. T., Akhtarmanesh, S., Cedola, A. E., Qader, R., & Hareland, G. (2016, June). Potential Directional Drilling Benefits of Barite Nanoparticles in Weighted Water Based Drilling Fluids. In 50th US Rock Mechanics/Geomechanics Symposium. American Rock Mechanics Association.

Canson, B. E. (1985, January). Lost Circulation Treatments for Naturally Fractured, Vugular, or Cavernous Formations. In SPE/IADC Drilling Conference. Society of Petroleum Engineers.

Cobianco, S., Pitoni, E., Ricci, P. N., & Galli, M. (2003, January). Optimized drill-in fluid leads to successful open hole gravel pack completion installation in unconsolidated reservoirs-case history. In SPE European Formation Damage Conference. Society of Petroleum Engineers.

Contreras, O., Hareland, G., Husein, M., Nygaard, R., & Al-Saba, M. (2014, February). Application of in-house prepared nanoparticles as filtration control additive to reduce formation damage. In SPE International Symposium and Exhibition on Formation Damage Control. Society of Petroleum Engineers.

Contreras, O., Hareland, G., Husein, M., Nygaard, R., & Al-saba, M. T. (2014, October). Experimental investigation on wellbore strengthening in shales by means of nanoparticle-based drilling fluids. In SPE Annual Technical Conference and Exhibition. Society of Petroleum Engineers.

Cook, J., Growcock, F., Guo, Q., Hodder, M., & van Oort, E. (2011). Stabilizing the wellbore to prevent lost circulation. Oilfield Review, 2012(23), 4.

Gronewald, P. J., Mansure, A. J. & Staller, G. E. (2001). Indonesian LCM Evaluation Tests Using a Modified API Bridging-Materials Tester [Lost Circulation Materials] (No. SAND2001-2400). Sandia National Labs, Albuquerque, NM (US); Sandia National Labs, Livermore, CA (US).

Hands, N., Kowbel, K., Maikranz, S., & Nouris, R. (1998). Drill-in fluid reduces formation damage, increases production rates. Oil and Gas Journal, 96 (28).

Hannegan, D., & Divine, R. (2002, January). Underbalanced drilling-perceptions and realities of today's technology in offshore applications. In IADC/SPE Drilling Conference. Society of Petroleum Engineers.

Hettama, M., Horsrud, P., Taugbol, K., Friedheim, J., Huynh, H., Sanders, M. W., & Young, S. (2007, January). Development of an innovative high-pressure testing device for the evaluation of drilling fluid systems and drilling fluid additives within fractured permeable

zones. In Offshore Mediterranean Conference and Exhibition. Offshore Mediterranean Conference.

Hinkebein, T. E., Behr, V. L., & Wilde, S. L. (1983). Static slot testing of conventional lost circulation materials (No. SAND-82-1080). Sandia National Labs., Albuquerque, NM (USA).

Hoelscher, K. P., De Stefano, G., Riley, M., & Young, S. (2012, January). Application of nanotechnology in drilling fluids. In SPE international oilfield nanotechnology conference and exhibition. Society of Petroleum Engineers.

Horikoshi, S. A. T. O. S. H. I., & Serpone, N. I. C. K. (2013). Introduction to nanoparticles. Microwaves in Nanoparticle Synthesis: Fundamentals and Applications, 1-24.

Javeri, S. M., Haindade, Z. M. W., & Jere, C. B. (2011, January). Mitigating loss circulation and differential sticking problems using silicon nanoparticles. In SPE/IADC Middle East Drilling Technology Conference and Exhibition. Society of Petroleum Engineers.

Jiao, D., & Sharma, M. M. (1992, January). Formation damage due to static and dynamic filtration of water-based muds. In SPE Formation Damage Control Symposium. Society of Petroleum Engineers.

Kasiralvalad, E. (2014). The great potential of nanomaterials in drilling & drilling fluid applications. International Journal of Nano Dimension, 5(5), 463.

Kulkarni, S. D., Teke, K., & Savari, S. (2014, April). Modeling Suspension of Lost Circulation Materials in a Drilling Fluid. In Oral presentation of paper AADE-14-FTCE-24 given at the AADE Fluids Technical Conference and Exhibition, Houston (pp. 15-16).

Kumar, A., Savari, S., Whitfill, D., & Jamison, D. (2011, April). Application of fiber laden pill for controlling lost circulation in natural fractures. In AADE national technical conference and exhibition, Houston, Texas, USA (pp. 12-14).

Kumar, A., & Savari, S. (2011, April). Lost circulation control and wellbore strengthening: looking beyond particle size distribution. In AADE national technical conference and exhibition, Houston, Texas, USA (pp. 12-14).

Lavrov, Alexandre, Chapter 1 - The Challenge of Lost Circulation, In Lost Circulation, Gulf Professional Publishing, Boston, 2016, Pages 1-11, ISBN 9780128039168, https://doi.org/10.1016/B978-0-12-803916-8.00001-7. (http://www.sciencedirect.com/science/article/pii/B9780128039168000017)

Lecolier, E., Herzhaft, B., Rousseau, L., Neau, L., Quillien, B., & Kieffer, J. (2005, January). Development of a nanocomposite gel for lost circulation treatment. In SPE European Formation Damage Conference. Society of Petroleum Engineers.

Loggins, S. M. J., Cunningham, C., Akhtarmanesh, S., Gunter, B., & Hareland, G. (2017, August). The Effect of Mechanically and Chemically Generated Barite Nanoparticles on

the Reduction of Fluid Filtrate. In 51st US Rock Mechanics/Geomechanics Symposium. American Rock Mechanics Association.

Mostafavi, V., Hareland, G., Belayneh, M., & Aadnoy, B. S. (2011, January). Experimental and mechanistic modeling of fracture sealing resistance with respect to fluid and fracture properties. In 45th US Rock Mechanics/Geomechanics Symposium. American Rock Mechanics Association.

Morita, N., Black, A. D., & Guh, G. F. (1990, January). Theory of lost circulation pressure. In SPE Annual Technical Conference and Exhibition. Society of Petroleum Engineers.

Nygaard, R., & Salehi, S. A. (2011, April). Critical Review of Wellbore Strengthening: Physical Model and Field Deployment. In AADE National Technical Conference and Exhibition, Houston, No. AADE-11-NTCE-24.

Savari, S., Whitfill, D. L., & Kumar, A. (2012, January). Resilient lost circulation material (LCM): A significant factor in effective wellbore strengthening. In SPE Deepwater Drilling and Completions Conference. Society of Petroleum Engineers.

Savari, S., Whiftill, D. L., Jamison, D. E., & Kumar, A. (2014). A Method To Evaluate Lost-Circulation Materials-Investigation of Effective Wellbore-Strengthening Applications. SPE Drilling & Completion, 29(03), 329-333.

Sensoy, T., Chenevert, M. E., & Sharma, M. M. (2009, January). Minimizing water invasion in shales using nanoparticles. In SPE Annual Technical Conference and Exhibition. Society of Petroleum Engineers.

Srivatsa, J. T., & Ziaja, M. B. (2011, January). An experimental investigation on use of nanoparticles as fluid loss additives in a surfactant-polymer based drilling fluids. In International Petroleum Technology Conference. International Petroleum Technology Conference.

Sweatman, R. E., Kessler, C. W., & Hillier, J. M. (1997, January). New solutions to remedy lost circulation, crossflows, and underground blowouts. In SPE/IADC drilling conference. Society of Petroleum Engineers.

U.S. Department of Energy. Energy Information Administration. (March 2016). Independent Statistics and Analysis: Trends in U.S. Oil and Natural Gas Upstream Costs, Washington DC

Van Oort, E., Browning, T., Butler, F., Lee, J., & Friedheim, J. (2007, April). Enhanced lost circulation control through continuous graphite recovery. In Proceedings of the AADE National Technical Conference. Houston (pp. 10-12).

Van Oort, E., Friedheim, J. E., Pierce, T., & Lee, J. (2011). Avoiding losses in depleted and weak zones by constantly strengthening wellbores. SPE Drilling & Completion, 26(04), 519-530.

Vidick, B., Yearwood, J. A., & Perthuis, H. (1988, January). How to solve lost circulation problems. In International Meeting on Petroleum Engineering. Society of Petroleum Engineers.

Whitfill, D. L., & Hemphill, T. (2003, January). All lost-circulation materials and systems are not created equal. In SPE Annual Technical Conference and Exhibition. Society of Petroleum Engineers.

Whitfill, D. L., & Hemphill, T. (2004). Pre-treating fluids with lost circulation materials. Drilling contractor, 60(3), 54-57.

Zakaria, M., Husein, M. M., & Harland, G. (2012, January). Novel nanoparticle-based drilling fluid with improved characteristics. In SPE International Oilfield Nanotechnology Conference and Exhibition. Society of Petroleum Engineers.

APPENDICES

Standard Operating Procedure for High Pressure Testing:

Procedure Title: High Pressure Lost Circulation/Nanoparticle Testing

PI/Supervisor: Seth Loggins and/or current lab contact

Department: Petroleum Engineering Building/Room: ATRC 133

Engineering Controls & Personal Protective Equipment:

- Chemical fume hood (if needed)
- Nitrile gloves
- Safety glasses
- Lab coat
- Closed-toe shoes

Procedure
Provide specific experimental steps:

1. Ensure nitrogen tank is properly secured and connected to pump, then open the nitrogen tank all the way to ensure proper delivery of gas to the pump. Set regulator output pressure at 75psi.
2. Turn on the pump 15 minutes prior to testing to ensure all transducers are warmed up. Open VINDUM computer application and establish communication the pump. Set pump delivery mode on "Dual Rate Specific Delivery" and set the safety pressure at 20psi. Turn on the mass scale and zero the scale after placing the fluid catch on top of the mass scale. Open OHAUS computer application and run program to establish communication to the scale.
3. Inspect all pieces of equipment (O-rings, threads, fittings, gauges and flow ports) and ensure they are lubricated (O-rings) and secure prior to testing. Replace parts as needed. Do not test with malfunctioning equipment.
4. Ensure O-rings on piston are lubricated and that the bleed port is opened 1.5 turns. Place piston in testing cell using the T-handle. Attach the flow valve to the bottom of the testing cell. Connect flow manifold to the bottom of the flow valve. Ensure all equipment is secure.

5. Operate the pump at 25cc/min and ensure flow is coming through the bleed port on the piston. This ensures all air is out of the system. Using the T-handle and a paper towel, soak up pumped water that is on top of the piston. Close bleed port on the piston using the hexagonal T-handle.
6. Operate pump at 25cc/min until a cumulative volume of 42mL is pumped. Stop pump at this time. During this time make sure no fluid is bypassing the piston. (Replace O-rings if fluid is bypassing the piston)
7. Place the O-ring and spacer ring inside the top portion of the testing cell.
8. Prepare 350mL of desired mud sample per laboratory procedures. Weigh desired amount of LCM and nanoparticle material for test sample. Use the fume hood if dealing with nanoparticles. Be sure the mud is properly hydrated prior to testing.
9. Take the 350mL mud sample and LCM/nanoparticles and combine them under the fume hood. Mix the sample containing the particles under the fume hood for 2 minutes.
10. Take the sample and pour it into the testing cell until the fluid level is just below the top portion of the spacer ring.
11. Placed the desired slotted or tapered disc on top of the spacer ring.
12. Secure the top portion of the testing cell with the end cap using the tightening handle.
13. Attach the flow out tubing to the top of the end cap and ensure direction of flow is towards the fluid catch located on top of the mass scale. At this point testing is ready to begin.
14. Prior to pumping, ensure the desired rate (25cc/min) and safety pressure (1,200psi) are established. Zero the cumulative volume meter. Open the desired real-time pumping graph for monitoring purposes. Hit the record button to ensure data is being transferred to the appropriate file and start the pump.
15. The following pumping schedule should be followed accordingly:
    a. Pump at a constant rate of 25cc/min until the safety pressure is reached.
        i. Once the safety pressure is met, the pump will shut-off and only pressure leakage through the seal will be realized. Do not allow more than 300mL of volume to be pumped during this time. In this case, shut off the pump and bleed off pressure per guidelines.
    b. Monitor the pressure leak-off for 5-minutes
        i. During this time switch the pump delivery from constant rate to “Dual Pressure Specific Delivery”. Set the safety pressure to 1,400psi. Set the “set pressure” to 100psi above last encountered pressure prior to the end of the 5-minute leak off duration.
    c. Start the pump using constant pressure conditions until 1,200psi is reached. Maintain 1,200psi constant pressure delivery for 5-minutes
        i. The “set pressure” will be manually inputted in 100psi intervals until 1,200psi is achieved.
    d. Stop the pump after the 5-minute constant pressure interval and monitor pressure for 5-minutes.
        i. Once the pump is shut off, only pressure leakage through the seal will be recognized.
    e. After the 5-minute interval of monitoring pressure the test is complete
        i. Bleed off pressure by opening the flow-out valve. Stop recording the pumping data and ensure pressure bleed-off has occurred via gages on CPU and apparatus.

16. Remove the flow-out tubing, end cap and fluid catch and rinse and dispose of materials in waste disposal bucket.
17. Remove the fracture disc, spacer ring, and O-ring from top of testing cell and rinse and dispose of in disposal bucket.
18. Detach flow manifold and back out flow valve one quarter turn.
19. Lift testing cell using the bottom flow valve and push-in the red knobbed testing cell pin to ensure cell is lifted off the bottom of the apparatus housing.
20. Remove the bottom flow valve.
21. Lift the testing cell out of the housing and dispose of testing mud in disposal bucket.
22. Open bleed port of piston one quarter turn using hexagonal T-handle.
23. Remove the piston from the testing cell using the T-handle. (Be sure to gently pull on piston)
24. Wash testing cell and piston. Inspect equipment prior to re-assembly.
    i. If re-test desired, start at step #3 in SOP. If not, follow step #25.
25. Save mass scale and pumping data.
26. Turn off pump and mass scale.
27. Close valve on the nitrogen tank.

Pressure Variances Due To Rheology Influence:

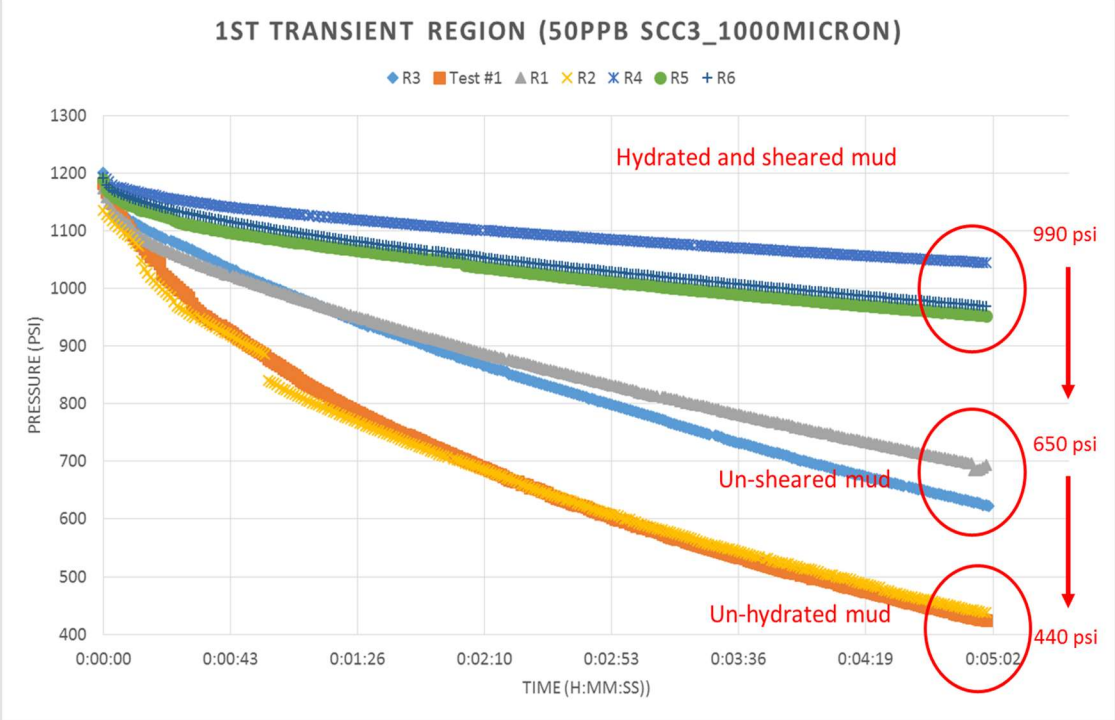

Figure A-1: Rheology variance for 1st transient region for 50 ppb SCC3_1000 micron

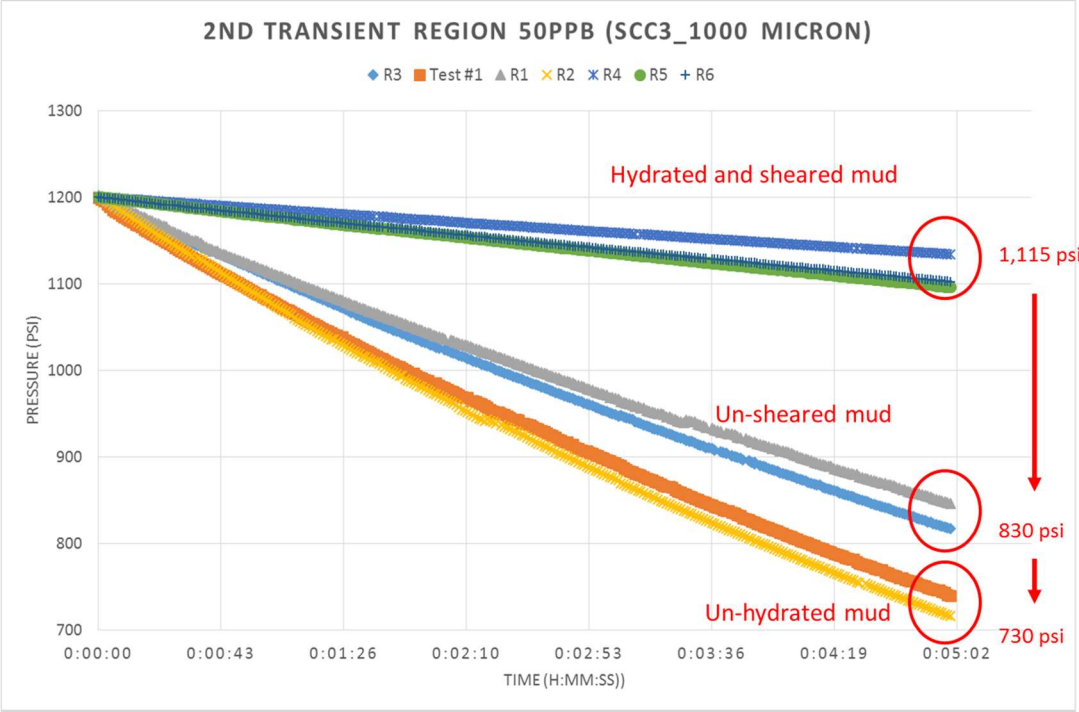

Figure A-2: Rheology variance for 2nd transient region for 50 ppb SCC3_1000 micron

All LCM Pressure Tests Including Repeatability:

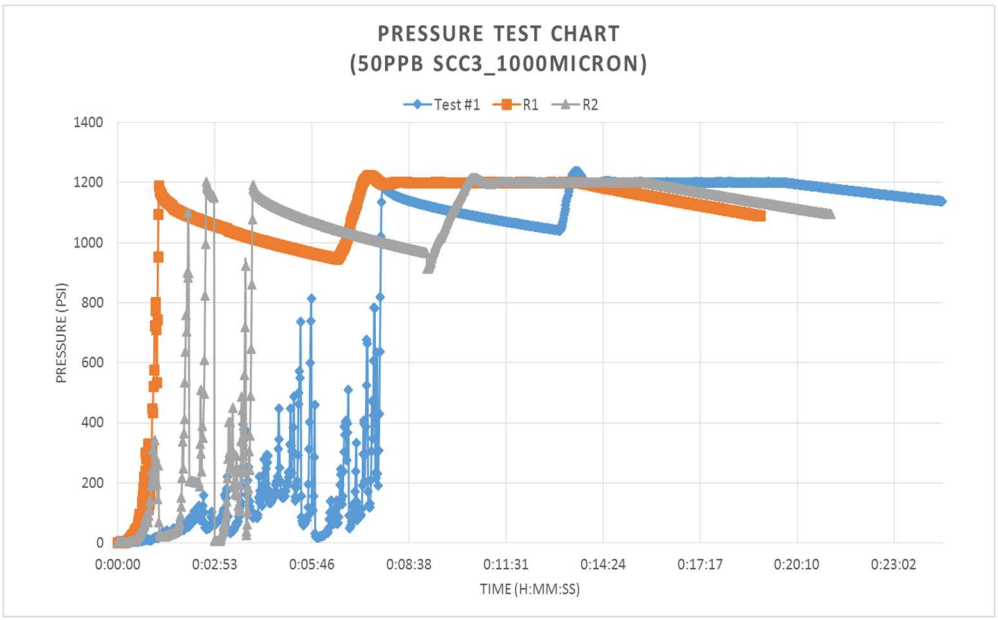

Figure A-3: 1000 micron_50 ppb sized calcium carbonate tests

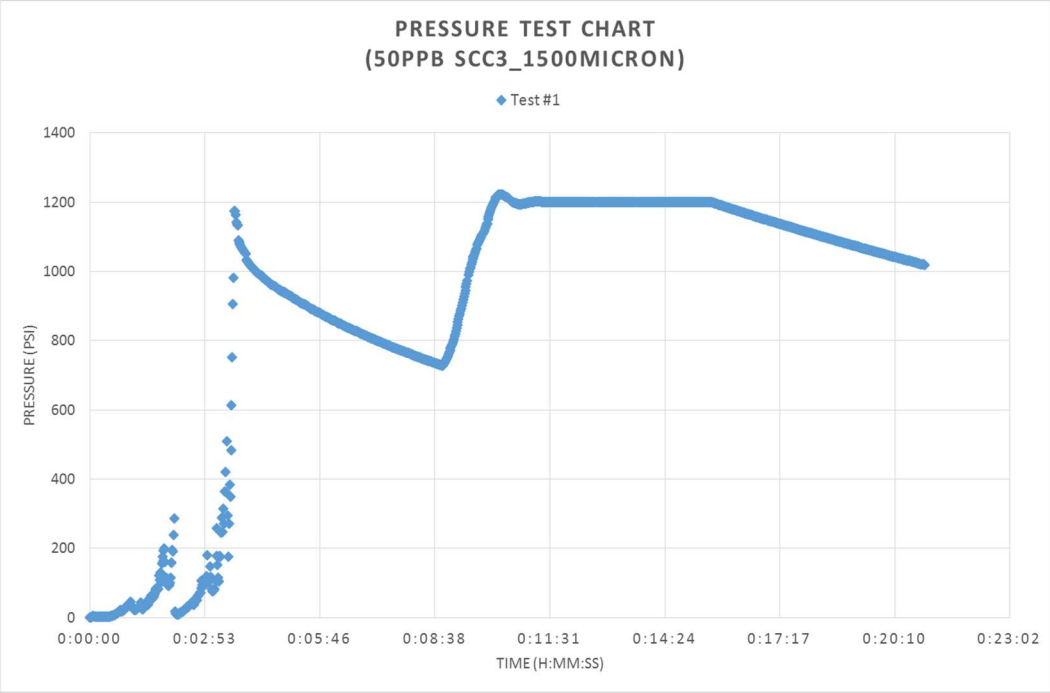

Figure A-4: 1500 micron_50 ppb sized calcium carbonate test

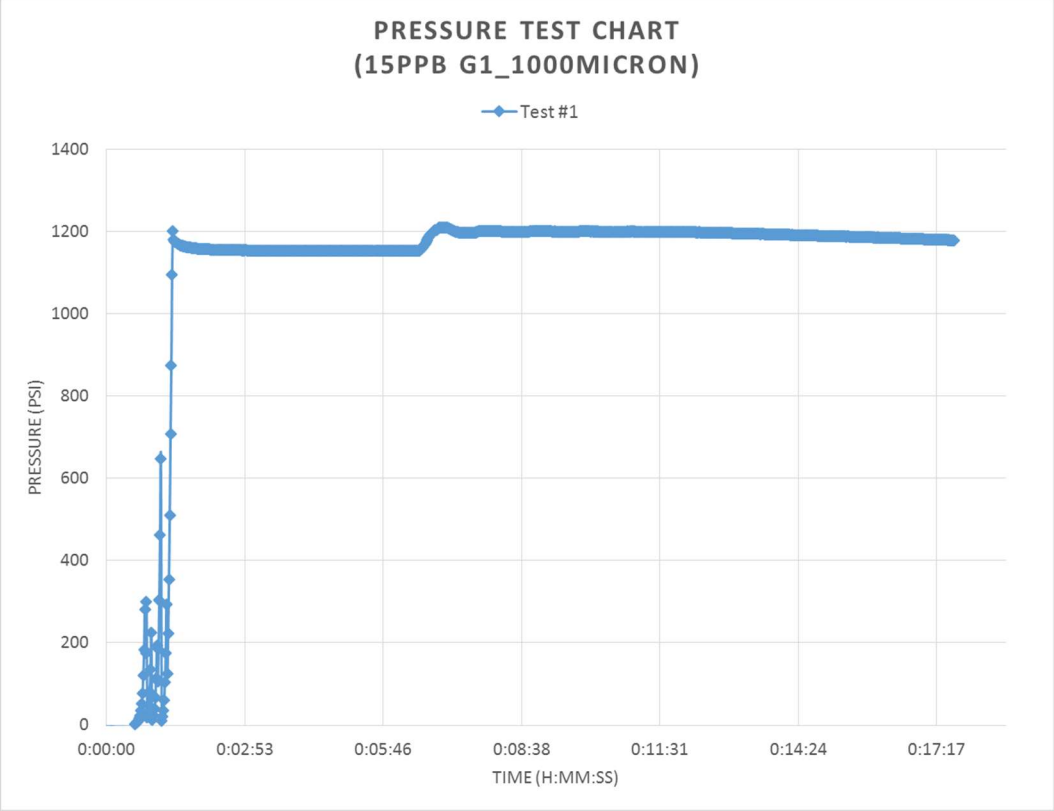

Figure A-5: 1000 micron_15 ppb graphite test

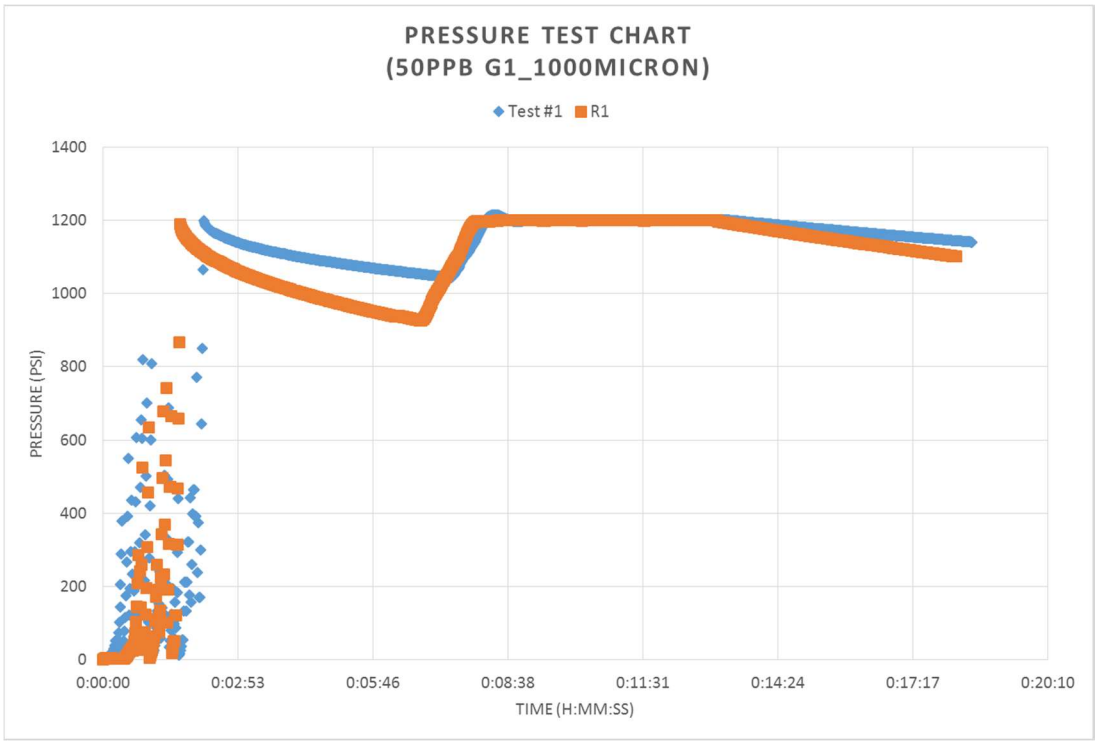

Figure A-6: 1000 micron_50 ppb graphite tests

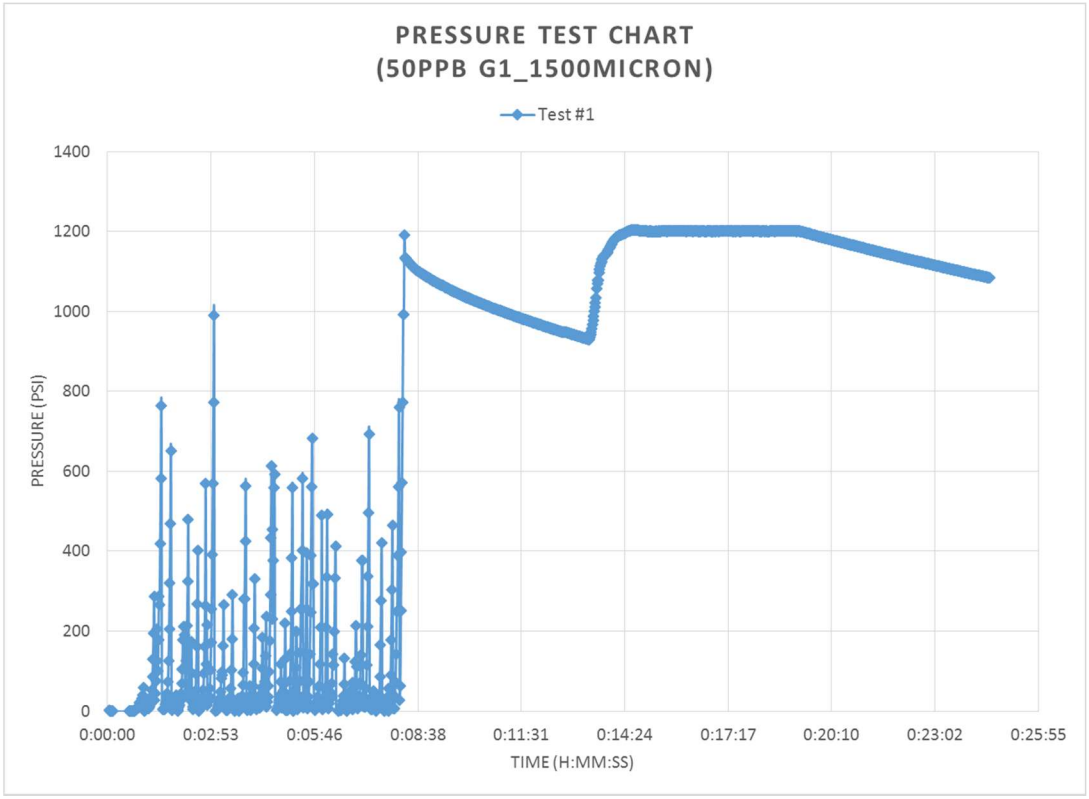

Figure A-7: 1500 micron_50 ppb graphite test

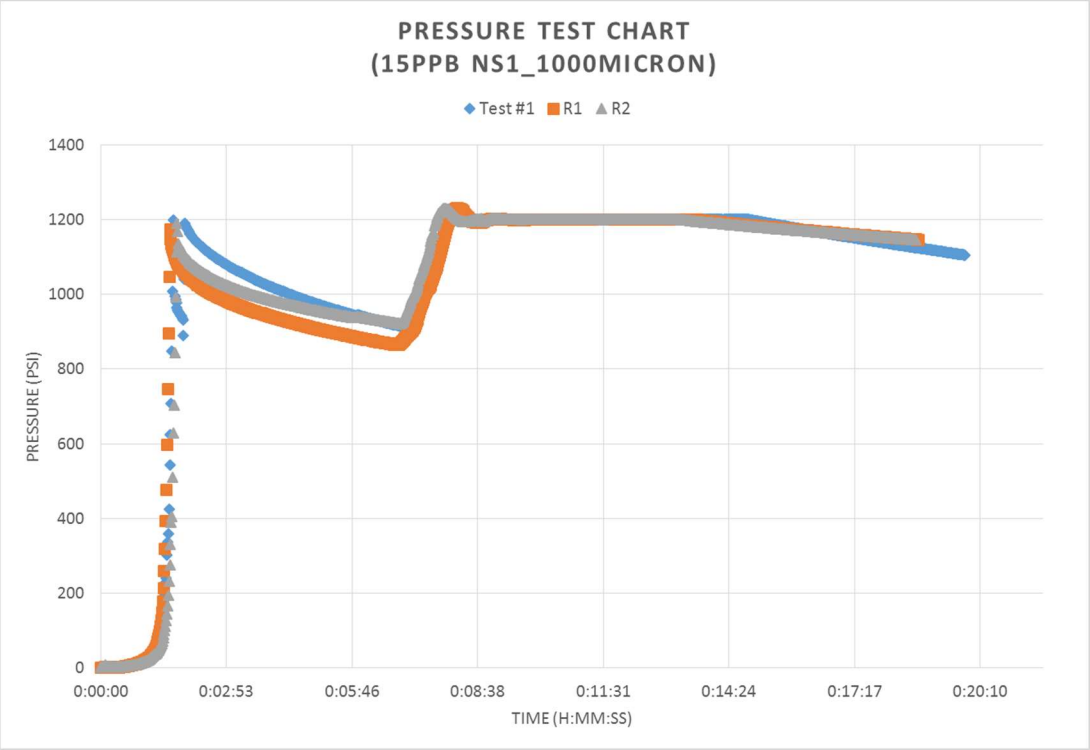

Figure A-8: 1000 micron_15 ppb nut shell tests

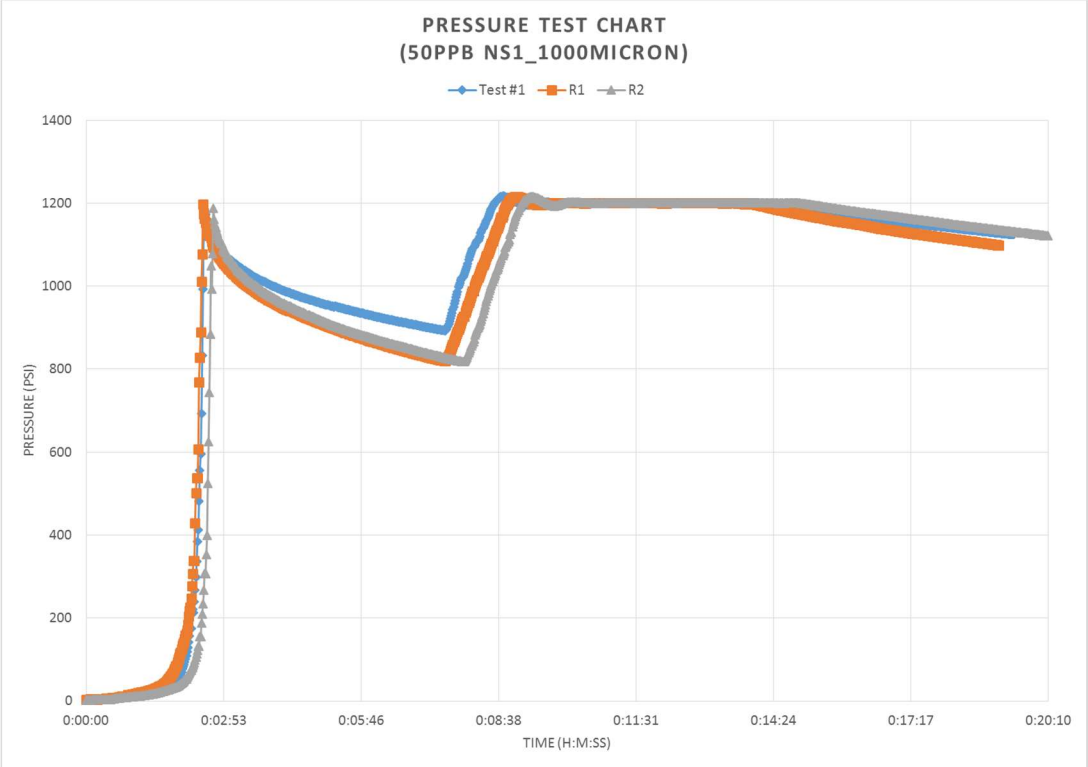

Figure A-9: 1000 micron_50 ppb nut shell tests

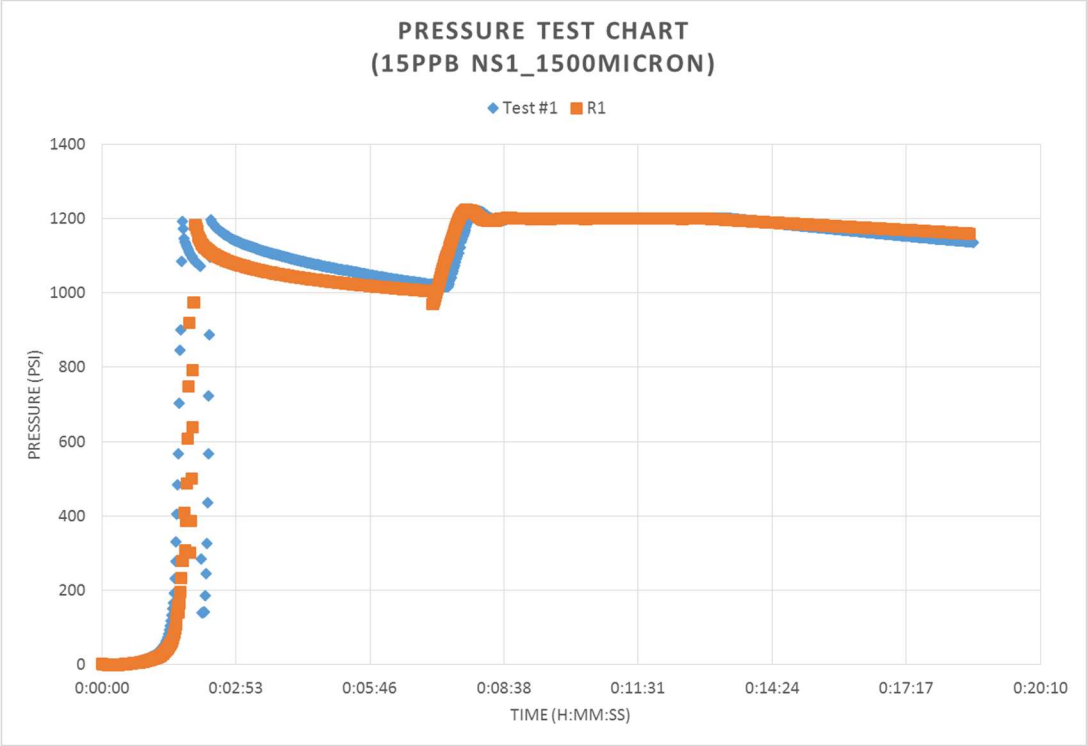

Figure A-10: 1500 micron_15 ppb nut shell tests

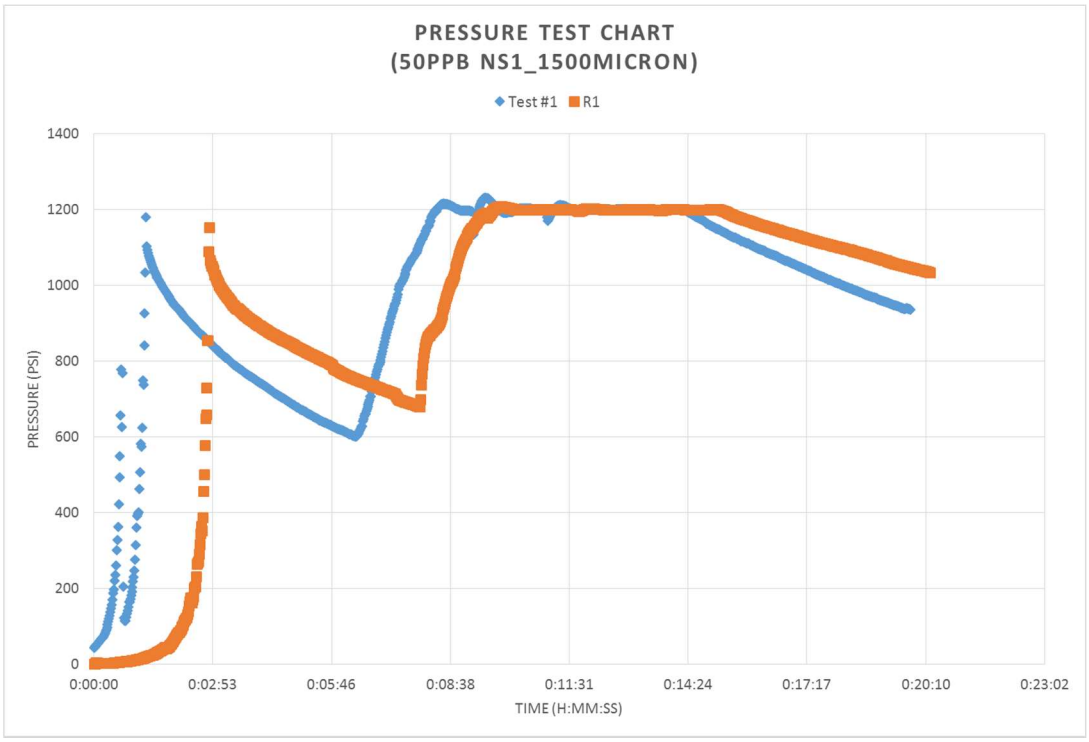

Figure A-11: 1500 micron_50 ppb nut shell tests

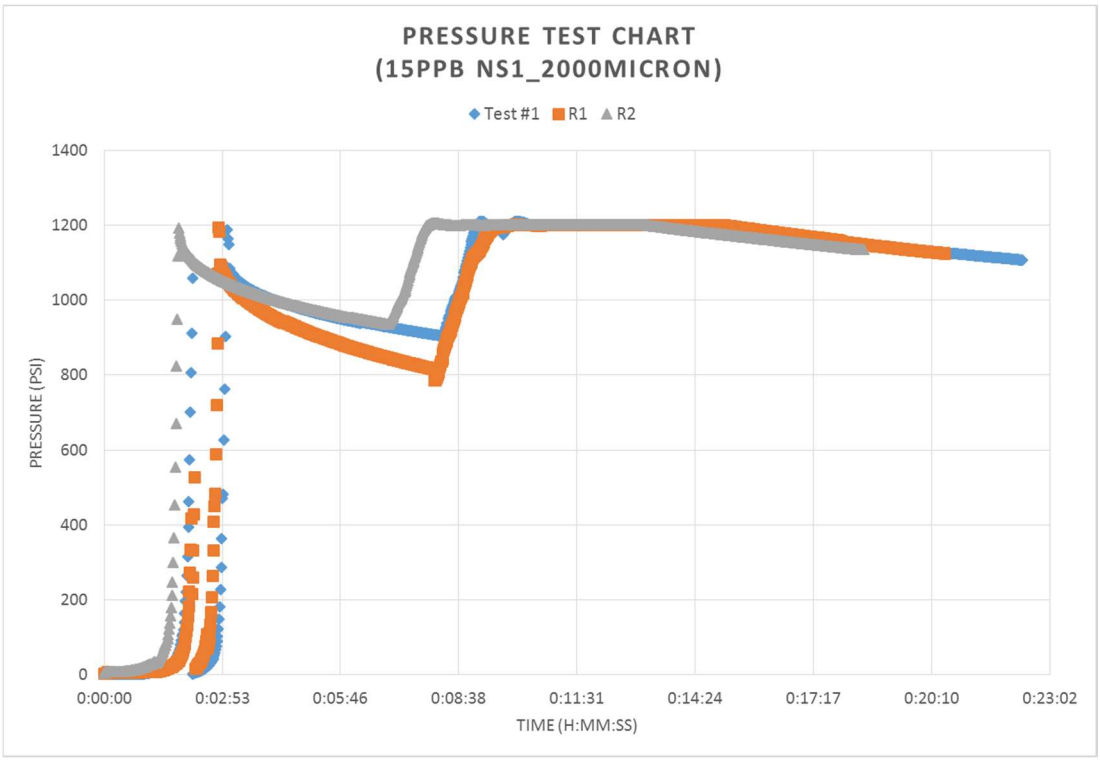

Figure A-12: 2000 micron_15 ppb nut shell tests

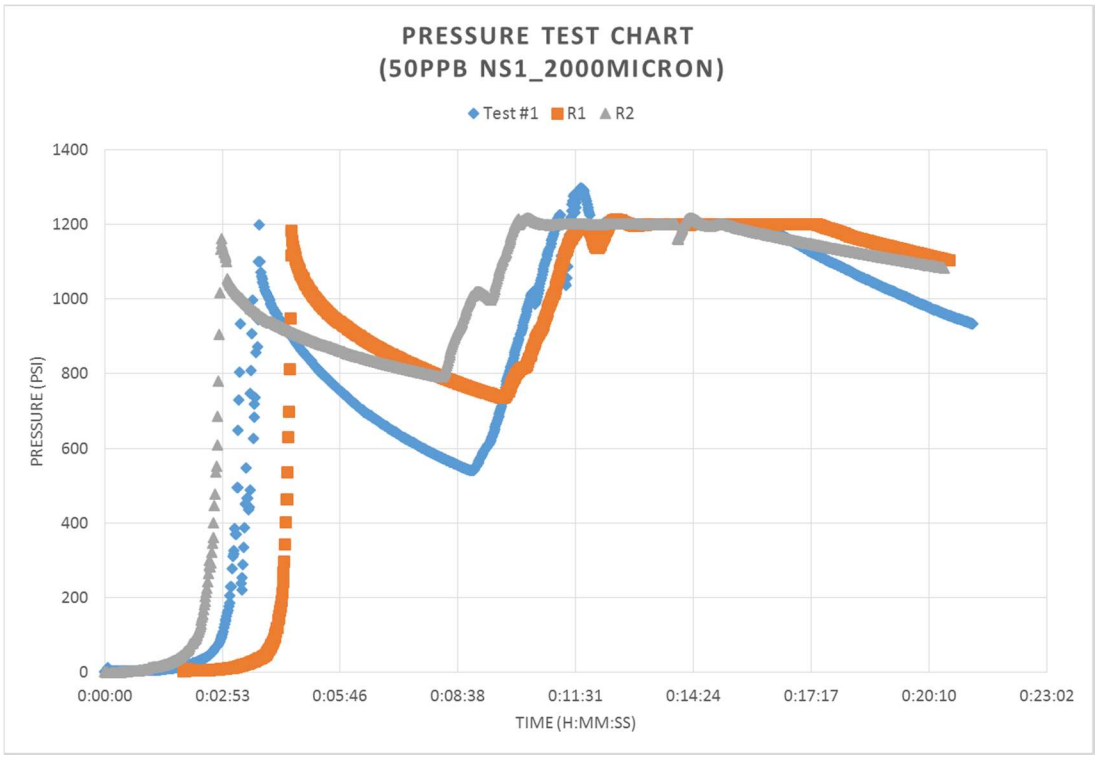

Figure A-13: 2000 micron_50 ppb nut shell tests

All Transient Comparisons for LCM Pressure Tests Including Repeatability:

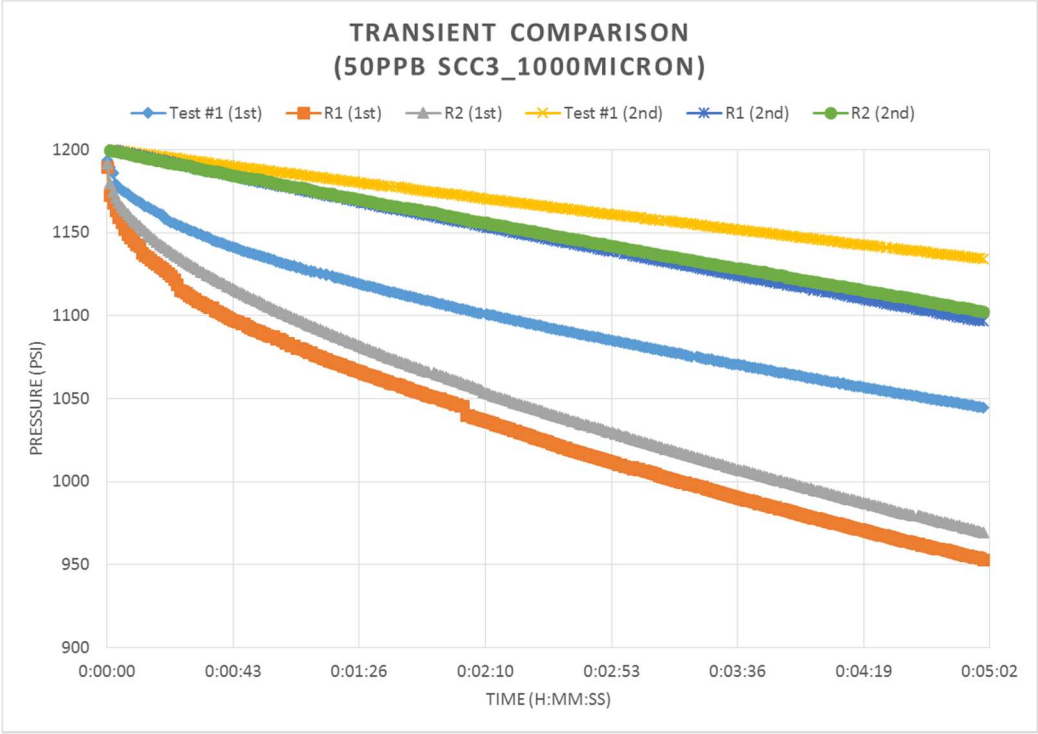

Figure A-14: Transient comparison for 1000 micron_50 ppb sized calcium carbonate tests

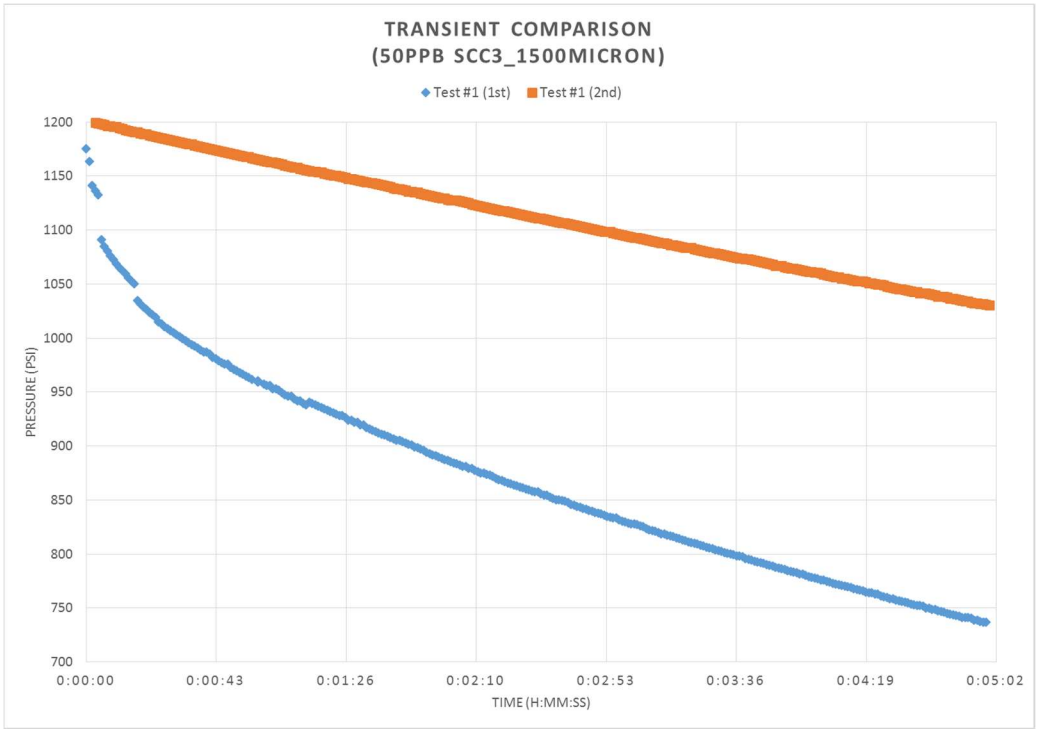

Figure A-15: Transient comparison for 1500 micron_50 ppb sized calcium carbonate test

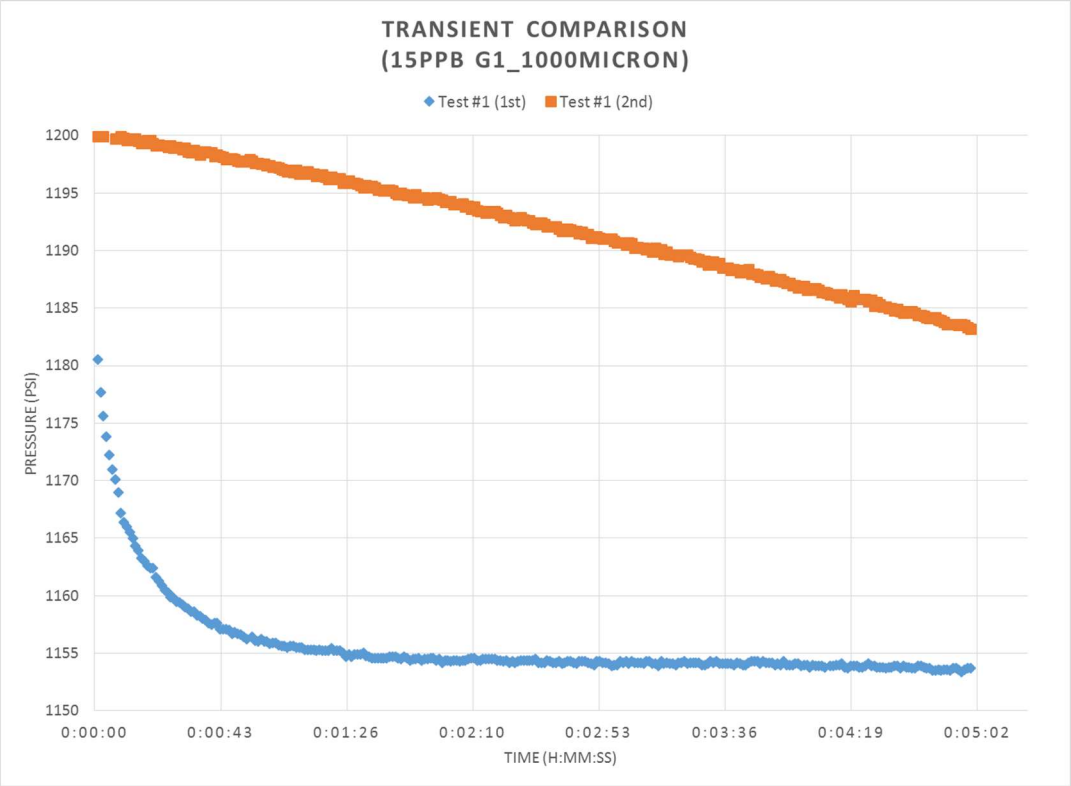

Figure A-16: Transient comparison for 1000 micron_15 ppb graphite test

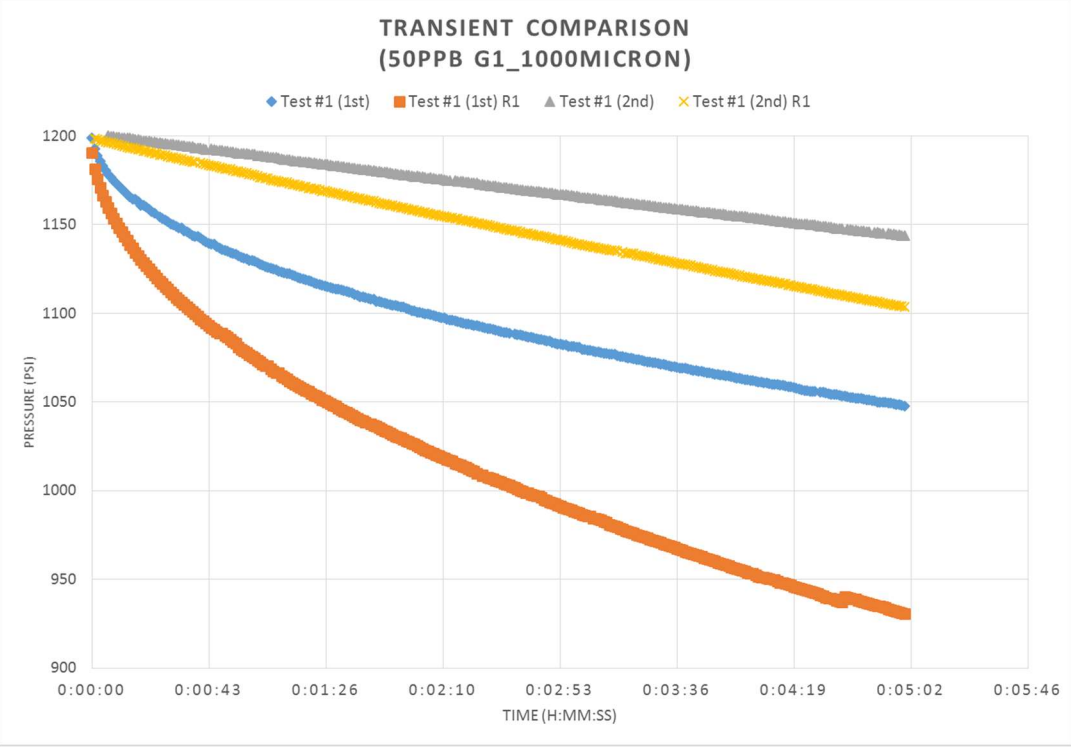

Figure A-17: Transient comparison for 1000 micron_50 ppb graphite tests

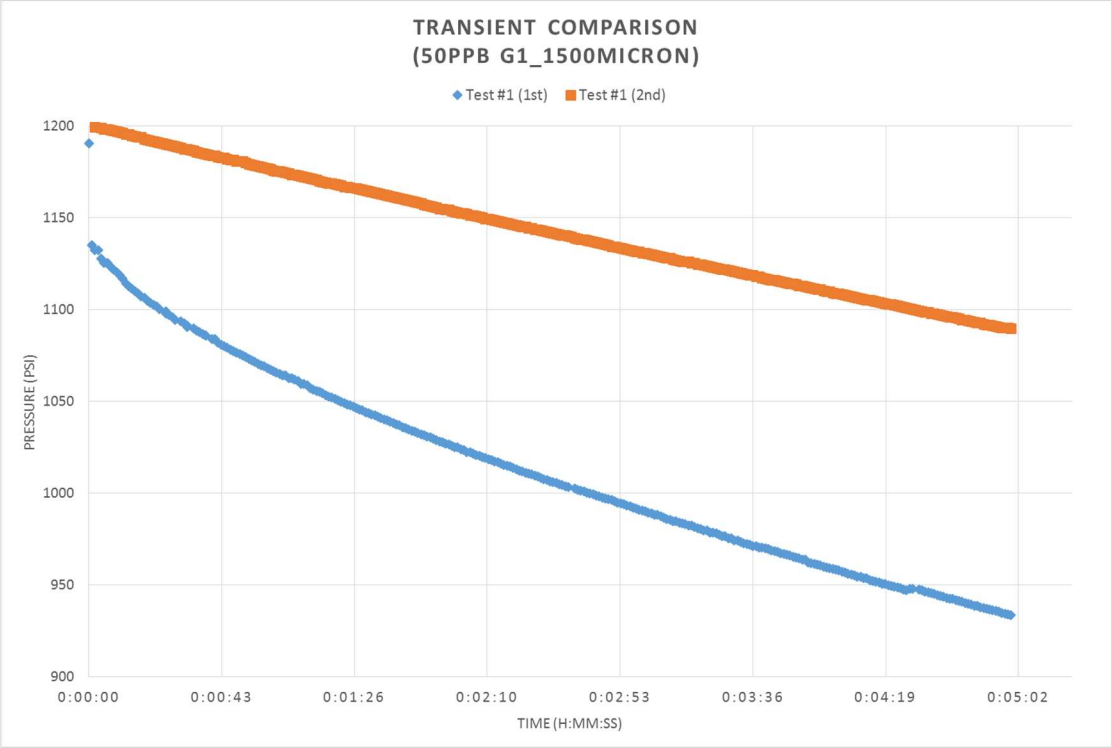

Figure A-18: Transient comparison for 1500 micron_50 ppb graphite test

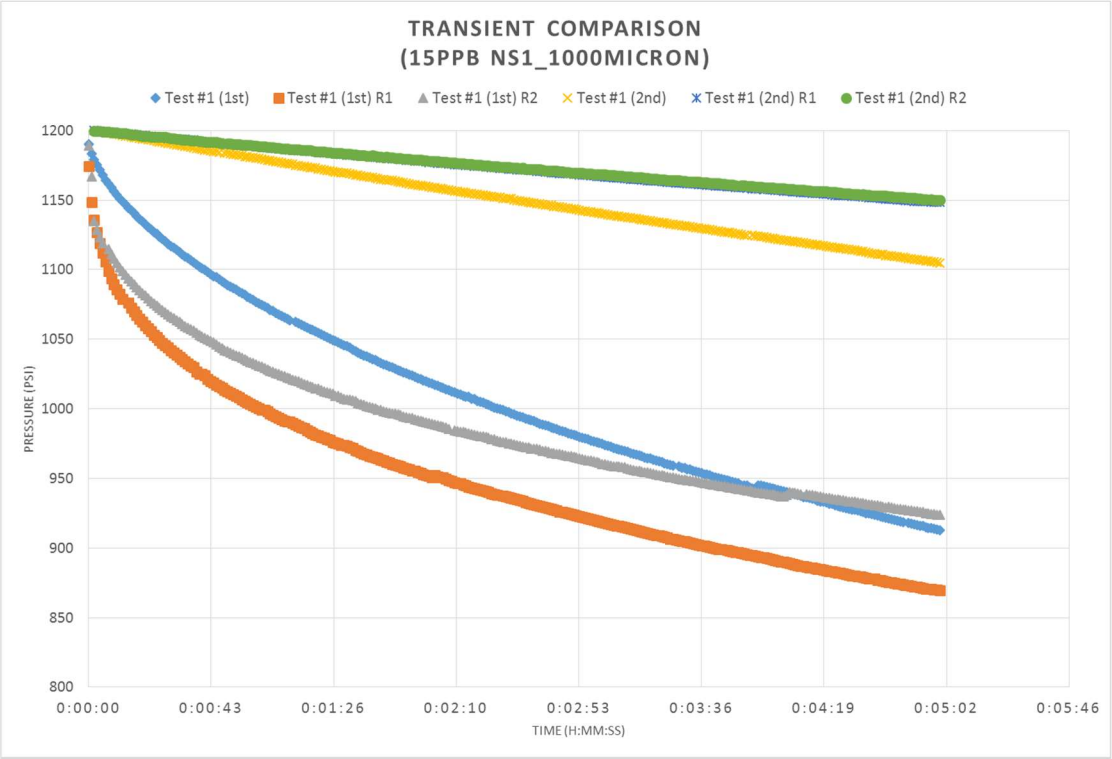

Figure A-19: Transient comparison for 1000 micron_15 ppb nut shell tests

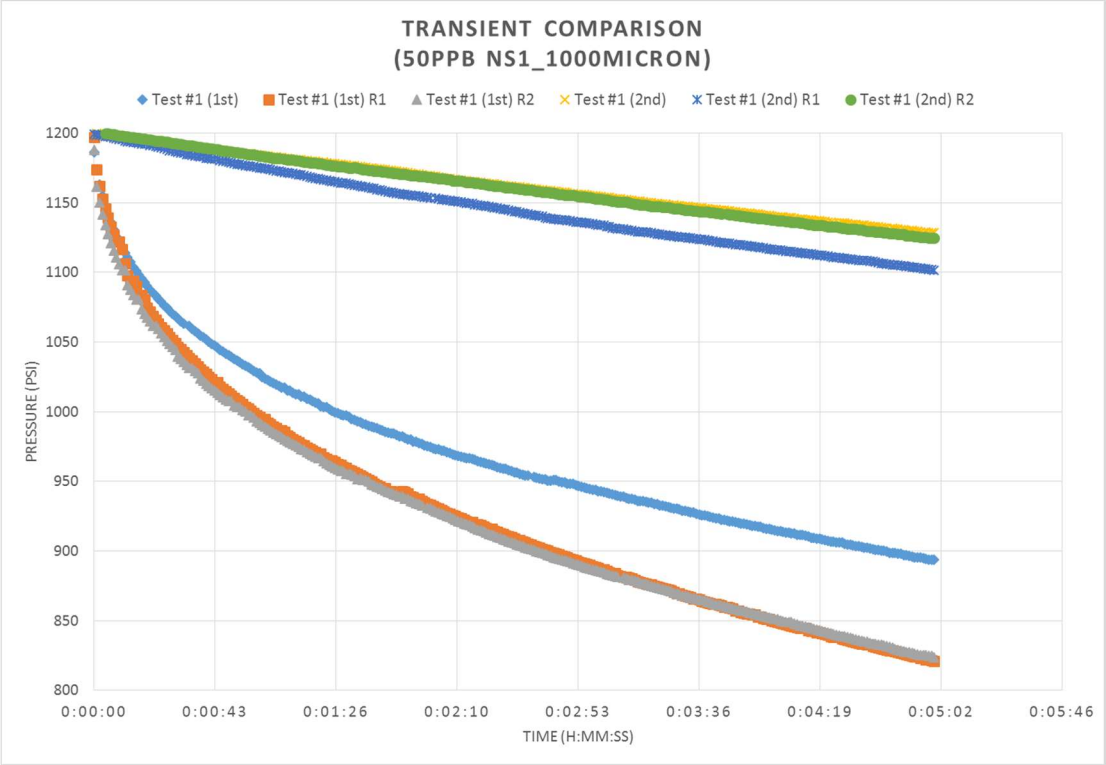

Figure A-20: Transient comparison for 1000 micron_50 ppb nut shell tests

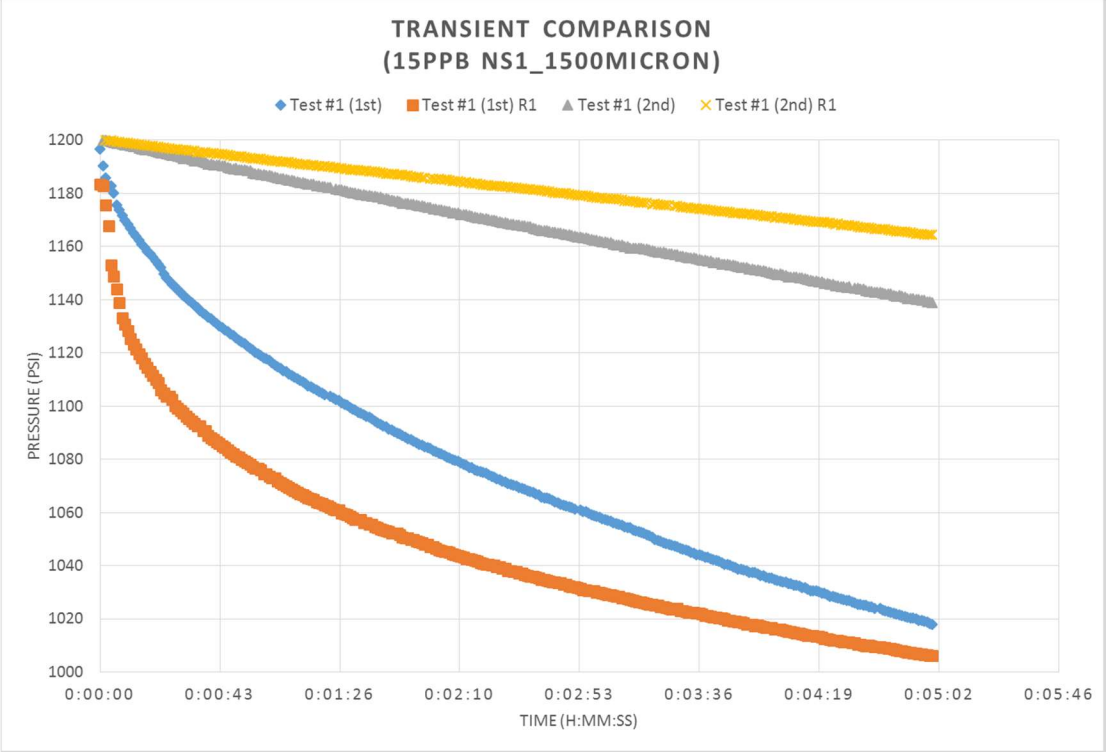

Figure A-21: Transient comparison for 1500 micron_15 ppb nut shell tests

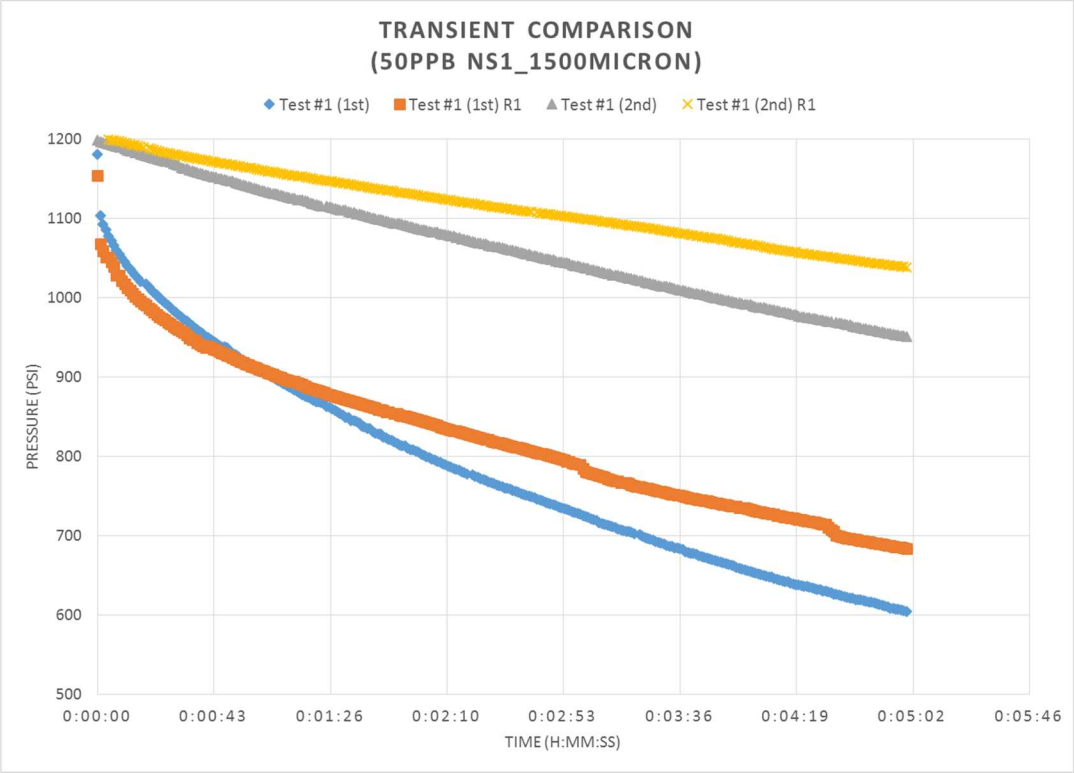

Figure A-22: Transient comparison for 1500 micron_50 ppb nut shell tests

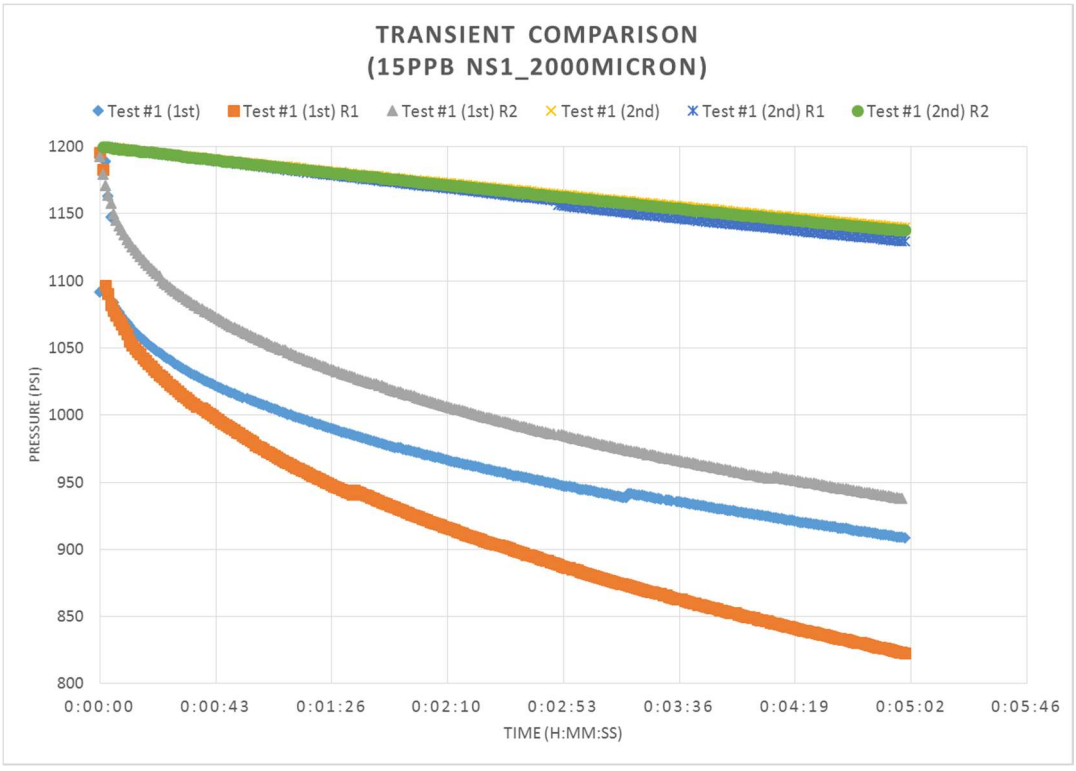

Figure A-23: Transient comparison for 2000 micron_15 ppb nut shell tests

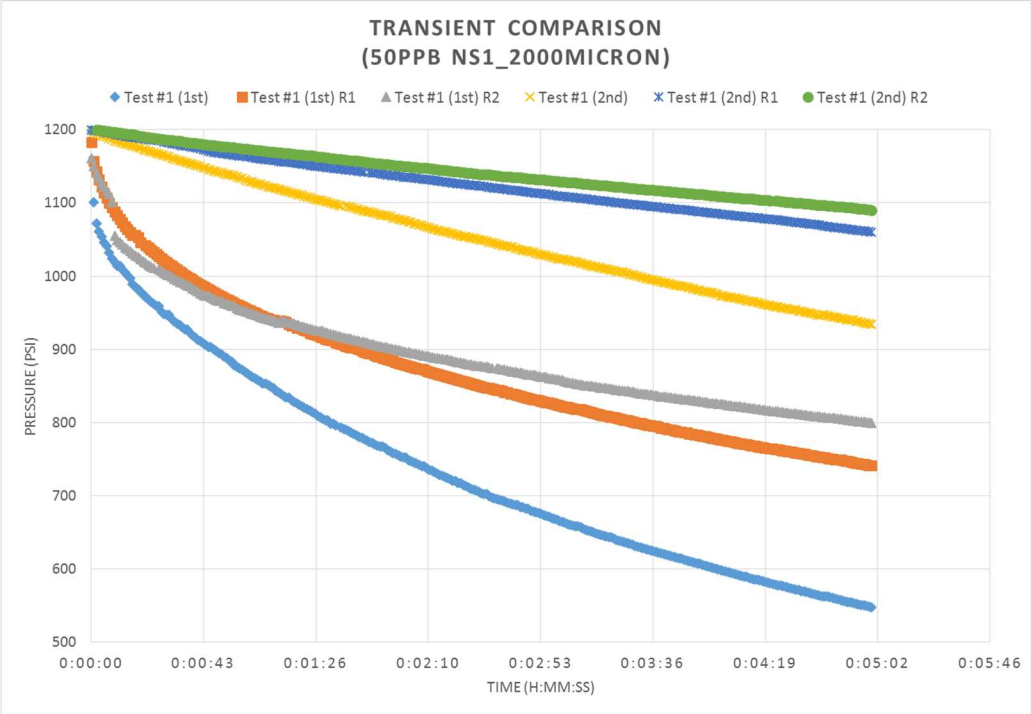

Figure A-24: Transient comparison for 2000 micron_50 ppb nut shell tests

All Nanoparticle Pressure Tests Including Repeatability:

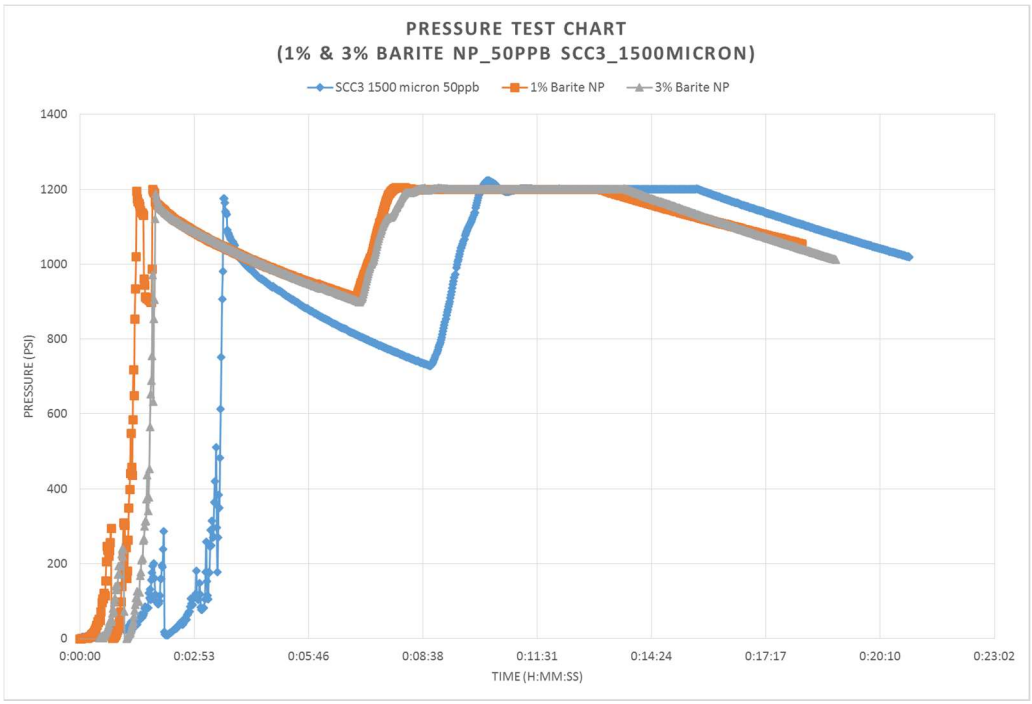

Figure A-25: 1500 micron_50 ppb sized calcium carbonate tests with 1% and 3% barite NP

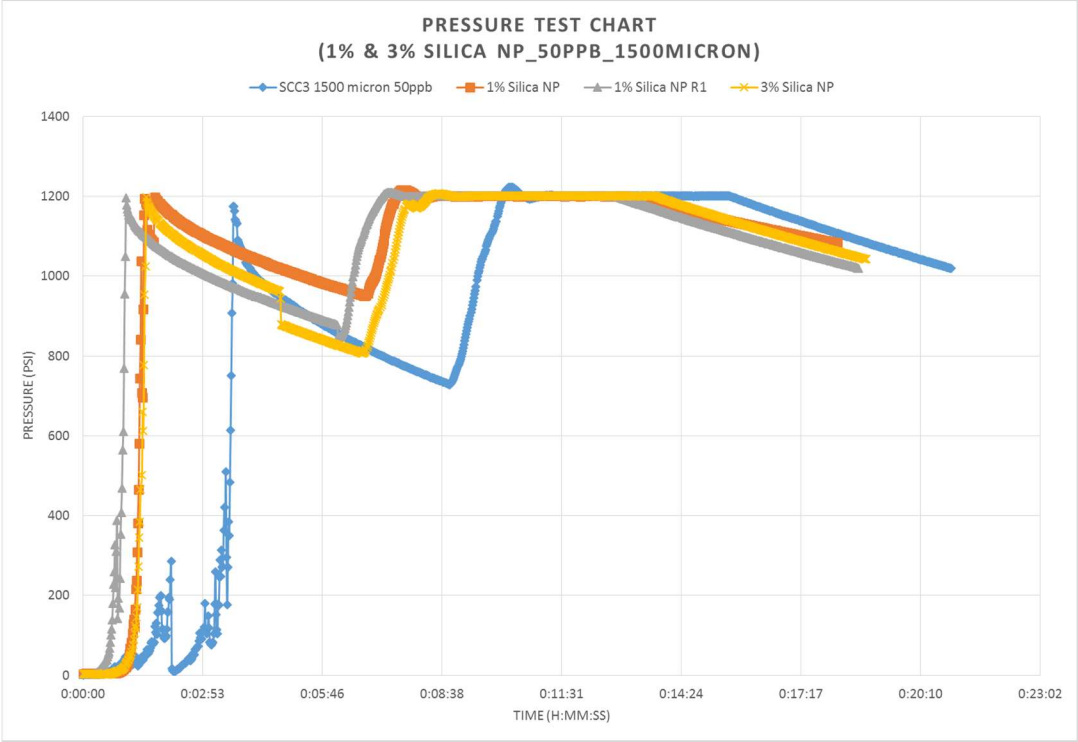

Figure A-26: 1500 micron_50 ppb sized calcium carbonate tests with 1% and 3% silica NP

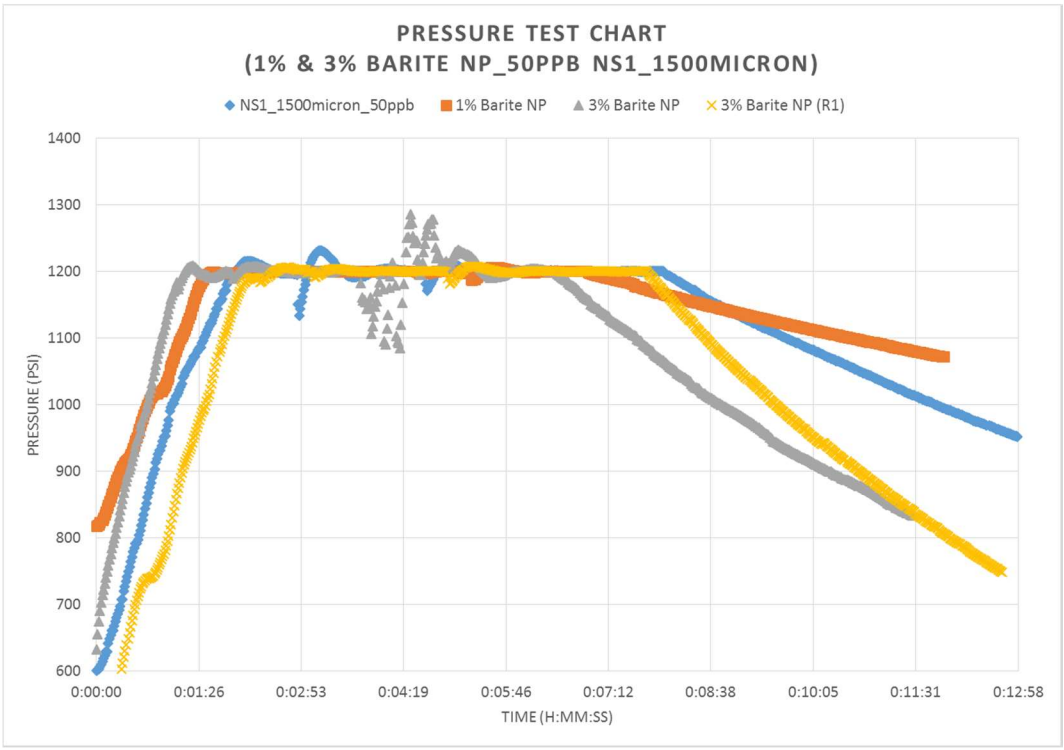

Figure A-27: 1500 micron_50 ppb nut shell tests with 1% and 3% barite NP

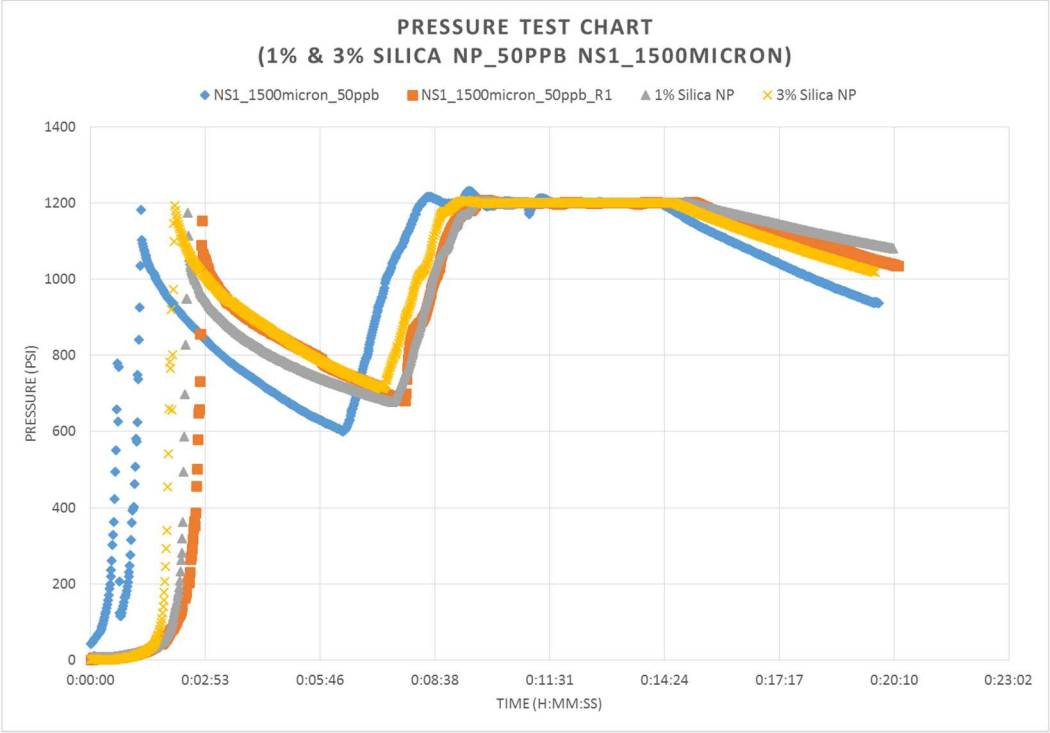

Figure A-28: 1500 micron_50 ppb nut shell tests with 1% and 3% silica NP

All Transient Comparisons for Nanoparticle Pressure Tests Including Repeatability:

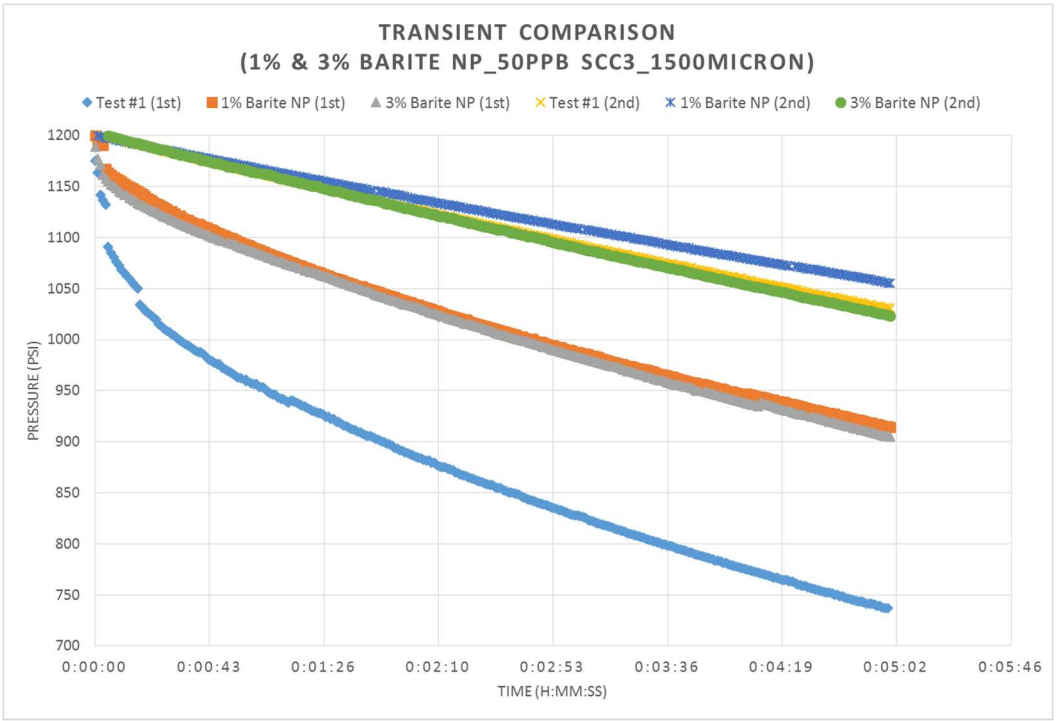

Figure A-29: Transient comparison for sized calcium carbonate tests with 1% and 3% barite NP

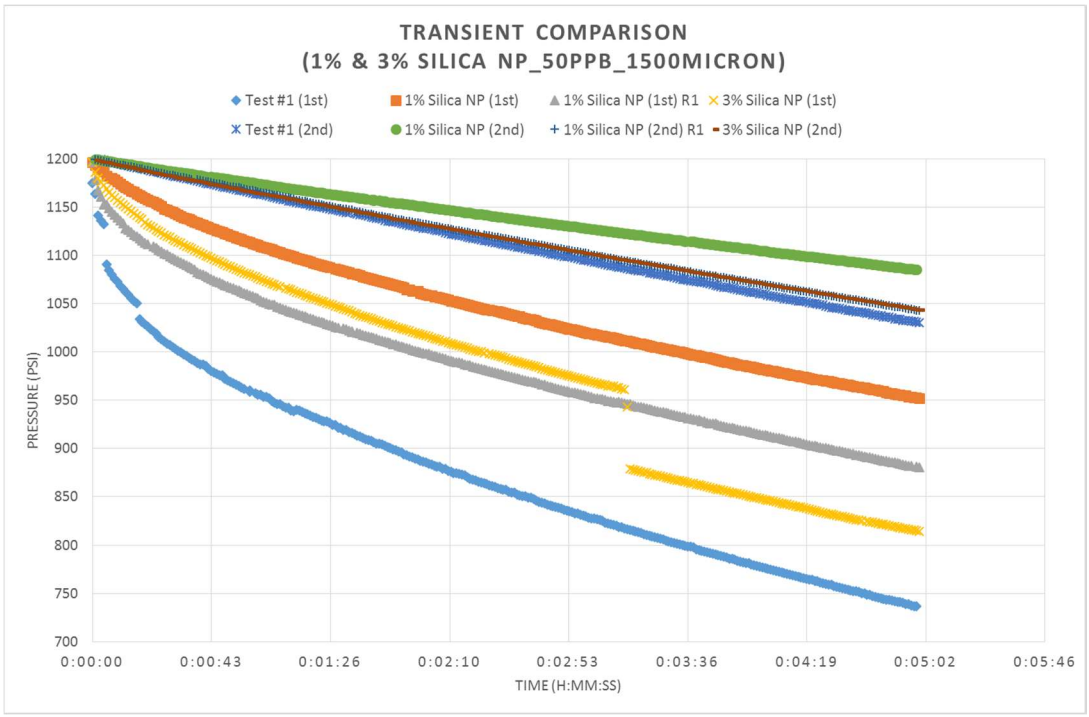

Figure A-30: Transient comparison for sized calcium carbonate tests with 1% and 3% silica NP

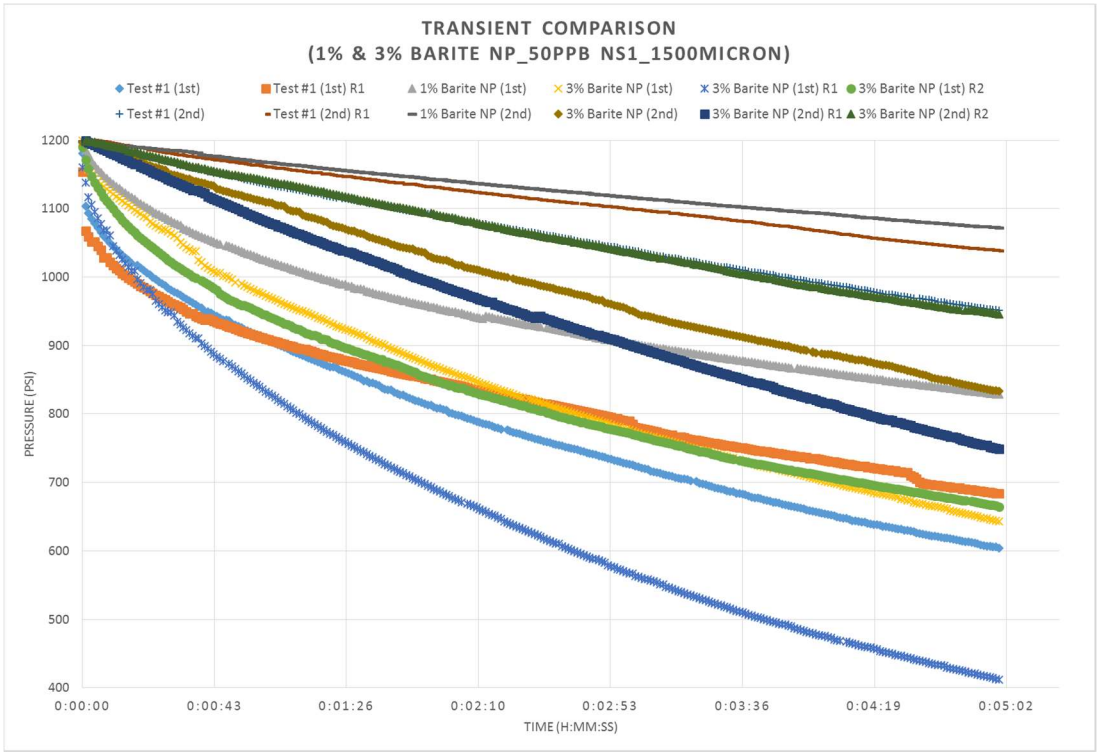

Figure A-31: Transient comparison for nut shell tests with 1% and 3% barite NP

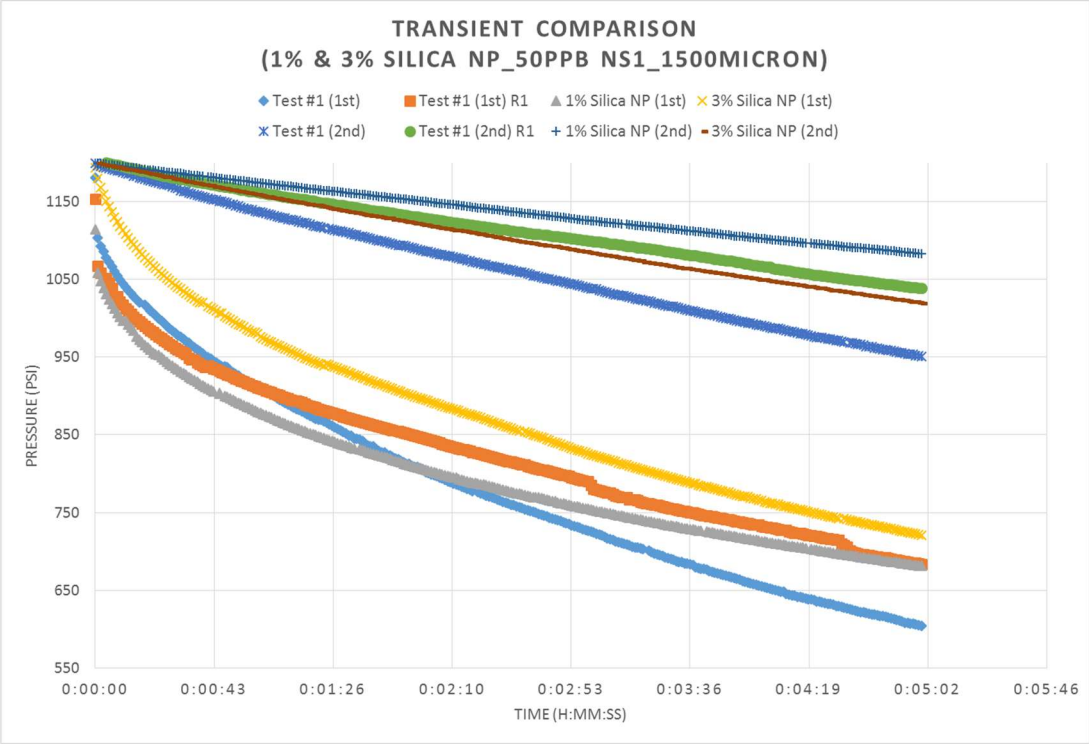

Figure A-32: Transient comparison for nut shell tests with 1% and 3% silica NP

VITA

Seth Michael James Loggins

Candidate for the Degree of

Master of Science

Thesis: A MODIFIED HIGH PRESSURE APPROACH TO INVESTIGATE THE SEALING INTEGRITY OF LOST CIRCULATION MATERIALS IN COMBINATION WITH NANOPARTICLES

Major Field: Petroleum Engineering

Biographical:

Education:

Completed the requirements for the Master of Science in Petroleum Engineering at Oklahoma State University, Stillwater, Oklahoma in December 2017.

Completed the requirements for the Bachelor of Science in Petroleum Engineering at New Mexico Institute of Mining and Technology, Socorro, New Mexico in 2014.

Experience:

Diverse set of experience in various oil and gas plays comprising of production optimization & strategic business development in the San Juan Basin located in Northwestern New Mexico. Gained fundamental drilling experience in the Niobrara located in Colorado and reservoir evaluation experience of the Utica shale play located in Ohio. Obtained full time drilling engineering experience in the Eagle Ford play located in South Texas.

Professional Memberships:

Society of Petroleum Engineers (Oklahoma State Chapter)
American Association of Drilling Engineers (Oklahoma State Chapter)